

**Regulation of membrane biogenesis and lipid homeostasis in
Tetrahymena thermophila - Role of Phosphatidic Acid
phosphoHydrolase (PAH)**

By

Anoop.N

LIFE 11201004008

National Institute of Science Education and Research, Bhubaneswar

A thesis submitted to the

Board of Studies in Life Sciences

In partial fulfillment of requirements

for the Degree of

DOCTOR OF PHILOSOPHY

of

HOMI BHABHA NATIONAL INSTITUTE



November, 2018

Homi Bhabha National Institute¹

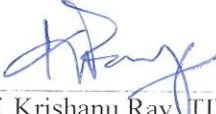
Recommendations of the Viva Voce Committee

As members of the Viva Voce Committee, we certify that we have read the dissertation prepared by Anoop.N entitled "Regulation of membrane biogenesis and lipid homeostasis in *Tetrahymena thermophila* - Role of Phosphatidic Acid phosphoHydrolase (PAH)" and recommend that it may be accepted as fulfilling the thesis requirement for the award of Degree of Doctor of Philosophy.


Chairman – Dr. Molov Sarkar, NISER, Bhubaneswar Date: 22-11-18


Guide / Convener – Dr. Abdur Rahaman, NISER, Bhubaneswar Date: 22/11/18

Co-guide- None Date:


Examiner – Prof. Krishanu Ray, TIFR, Mumbai Date: 22/11/18


Member 1- Dr. Praful Singru, NISER, Bhubaneswar Date: 22.11.18


Member 2- Dr. Renjith Mathew, NISER, Bhubaneswar Date: 22/11/18


External member – Dr. Chinmay Pradhan,
Utkal University, Bhubaneswar Date: 22/11/18

Final approval and acceptance of this thesis is contingent upon the candidate's submission of the final copies of the thesis to HBNI.

I/We hereby certify that I/we have read this thesis prepared under my/our direction and recommend that it may be accepted as fulfilling the thesis requirement.

Date: 22/11/18

Place: NISER, Bhubaneswar



Dr. Abdur Rahaman

Co-guide (if applicable)

Guide

¹ This page is to be included only for final submission after successful completion of viva voce.

STATEMENT BY AUTHOR

This dissertation has been submitted in partial fulfillment of requirements for an advanced degree at Homi Bhabha National Institute (HBNI) and is deposited in the Library to be made available to borrowers under rules of the HBNI.

Brief quotations from this dissertation are allowable without special permission, provided that accurate acknowledgement of source is made. Requests for permission for extended quotation from or reproduction of this manuscript in whole or in part may be granted by the Competent Authority of HBNI when in his or her judgment the proposed use of the material is in the interests of scholarship. In all other instances, however, permission must be obtained from the author.

A handwritten signature in black ink, appearing to read 'Anoop.N', written over a horizontal line.

Anoop.N

DECLARATION

I, hereby declare that the investigation presented in the thesis has been carried out by me. The work is original and has not been submitted earlier as a whole or in part for a degree / diploma at this or any other Institution / University.

A handwritten signature in black ink, appearing to read 'Anoop.N', written over a horizontal line.

Anoop.N

List of Publications arising from the thesis

Journal

- 1) **Anoop Narayana Pillai**, Sushmita Shukla, and Abdur Rahaman. 2017. An evolutionarily conserved phosphatidate phosphatase maintains lipid droplet number and ER morphology but not nuclear morphology. *Biology Open*, **6**, 1629-1643, doi: 10.1242/bio.028233.
- 2) **Anoop Narayana Pillai***, Sushmita Shukla*, Sudhanshu Gautam* and Abdur Rahaman. 2017. Small phosphatidate phosphatase (TtPAH2) of *Tetrahymena* complements respiratory function and not membrane biogenesis function of yeast PAH1. *Journal of Bioscience*, **42**,613-621, doi: 10.1007/s12038-017-9712-7. (* = Equal contribution).

Chapters in books and lectures notes

Not Applicable

Conferences

- 1) **Anoop.N** and Abdur Rahaman. Regulation of nuclear expansion in *Tetrahymena* thermophila. 36th All India Cell Biology Conference and International Symposium on "Stress Adaptive Response and Genome Integrity" Oct. 17- 19, 2012. BARC, Mumbai.
- 2) **Anoop.N**, Sushmita Shukla, Sudhanshu Gautam and Abdur Rahaman. Evolutionary conserved cascade for cell cycle regulation of nuclear expansion: Role of Phosphatidate Phosphatase1 (PAH1), 83rd Annual meeting of Society of Biological Chemists (India) and symposium on 'Evolution: Molecules to Life', Dec. 18 - 21, 2014. Bhubaneswar.
- 3) **Anoop.N**, Sushmita Shukla and Abdur Rahaman. An evolutionary conserved phosphatase cascade for cell cycle regulated membrane biogenesis and lipid homeostasis: Role of *Tetrahymena* Phosphatidate Phosphatase1, EMBO Conference 'Europhosphatase 2017: Phosphatases in cell fates and decisions', July 23 – 28, 2017. Paris, France.

Workshop

- 1) Science Communication Workshop organized by The Wellcome Trust/DBT India Alliance held on 11th September 2014 at ILS, Bhubaneswar.
- 2) Bangalore Microscopy Course (BMC-2015), Sept 20-27, 2015, NCBS, Bangalore, India

Other Publications

- 1) Sushmita Shukla, **Anoop Narayana Pillai**, Abdur Rahaman. 2018. A Putative *NEMI* Homolog Regulates Lipid Droplet Biogenesis via *PAH1* in *Tetrahymena thermophila*". *Journal of Bioscience*, **43**, 693-706.
- 2) Gaurav Jha, Subhasis Roy, Prabhat Kumar Sahu, Somnath Banerjee, **N. Anoop**, Abdur Rahaman, Moloy Sarkar. 2018 Free-radical Sensing in Aqueous Medium by using Hydrazino-Naphthalimide Anchored Mesoporous Silica (MCM-41) Nanoparticles: A Combined Fluorescence and Cellular Imaging Study. *Chemical Physics Letters*, **692**, 324–332.
- 3) Jha, G, **Anoop N**, Rahaman, A, Sarkar. 2015. Fluoride ion sensing in aqueous medium by employing nitrobenzoxadiazole-postgrafted mesoporous silica nanoparticles (MCM-41). *M. Phys. Chem. Chem. Phys*, **17**, 3525-3533.
- 4) Abhas Kumar Bhoi, Sudhir Kumar Das, Debashis Majhi, Prabhat Kumar Sahu, A. Nijamudheen, **Anoop N**, Abdur Rahaman, and Moloy Sarkar. 2014. Analyte Interactions with a New Ditopic Dansylamide-Nitrobenzoxadiazole Dyad: A Combined Photophysical, NMR, and Theoretical (DFT) Study. *J. Phys. Chem. B*, **118**, 9926–9937.



Anoop.N

ACKNOWLEDGEMENTS

I would like to convey my heartiest regards to all those who have contributed, supported and guided me throughout the entire duration of my Ph.D. research.

First and foremost, I am grateful to my thesis supervisor Dr. Abdur Rahaman for his continuous support and guidance throughout my tenure as a Ph.D. student. I thank him for his scientific input, unwavering support, and enthusiasm towards the work done and his excellent guidance, and patience during my stay in his lab. Thank you so much for the rapid thesis editing. I would also like to extend my thanks to my doctoral committee members Dr. Moley Sarkar, Dr. Praful Singru, Dr. Chandan Goswami, Dr. Renjith Mathew, and Dr. Chinmay Pradhan for expressing interest in my project, their helpful comments and suggestions. I want to specially thank Dr. Ramanajum Srinivasan for his suggestions and help in image analysis.

I acknowledge CSIR, India for my PhD fellowship. I am thankful to HBNI for supporting me for the international travel to present my work and also for supporting me with stipend during extension tenure. I would like to thank Dr. Symeon Siniossoglou at the University of Cambridge Dr. Laurie K. Read at SUNY, Buffalo and Dr. Roop Mallik for providing resources needed to perform this work. I would like to express my heartiest thanks to all the present and past members of AR lab. Special thanks to Usha for all her help especially in the initial years at lab when we together learned and taught each other. Sushmita needs special thanks for all her support in the manuscript writing and yeast work. I would like to thank Himani for all the support and help, provided by her since she joined our lab. I want to specially thank Sudhanshu who worked with me for his Masters project and has always been there to assist me in any work whenever I needed his help. I am also extremely grateful to Ahamed, Manish, Shreyasi, and Alokonanda, for their constant support and help during their stay at our lab. I have learned a lot while working with you all. Thank you so much. I would like to thank all the labs of NISER SBS, which helped me in many different aspects in the completion of my work. I want to specially thank lab members of Dr. Singru, Dr. Panigrahi, and Dr. Debasmita for all the help and fun time provided by you people. I am deeply thankful to Adinarayan and Prabhat for all the help extended towards me to work at department of Chemical Sciences.

I would like to thank those people at NISER SBS – Ashutosh, Santosh, Tapan, Bibek, Bushra, Sony, Manoj, Subhranshu and Ankit for the wonderful moments we spent together. I would like to thank Biswaranjan for helping me in statistical analysis and Santosh bhaiya for final

formatting of my thesis. I had a great time in the final year at campus with people like Anoop VP, Sujith, Jyothis and Jobin – they kept me happy during the stressful time. I thank Ajesh and his wife Gowri for all the good time we had. I know I have got some friends for life long. I would like to express my warm regards to Anil sir, Sree Chechi and their kids Sidhu and Rishi for the love and care they gave me. I want to express my heartiest thanks and warm regards to my fabulous batch mates Uday and Charles. Uday, I really value the help and support you have showered on me and will always treasure our friendship. I would like to specially thank Sushmita for her immense support throughout my PhD tenure.

I would like to thank Rahul who was always with me in all my joys and sorrows and will always value and cherish his company. I thank all my family members for their love, care, and support throughout these long years. Amma and Kochechi - you people are like pillars supporting my life. It is all because of your blessings and prayers I am able to complete my Ph.D. work.

Thank you all for being in my life.

Thank you all...

Anoop.

CONTENTS

Synopsis		i
List of Figures		xiii
List of Tables		xv
List of Abbreviations		xvi
CHAPTER 1	Introduction and Review of Literature	1
	1.1 Membrane biogenesis and lipid homeostasis	2
	1.2 Phospholipid Biosynthesis	5
	1.3 Phosphatidate phosphatases	7
	1.3.1 Magnesium dependent (PAP1) and Magnesium independent (PAP2) enzymes	8
	1.4 Phosphatidic acid phosphohydrolase (PAH1) regulate lipid biosynthesis and lipid droplet biogenesis	12
	1.5 Regulation of yeast PAH1 by phosphorylation and dephosphorylation	17
	1.6 Lipins - the metazoan PAH1 homolog	20
	1.6.1 Lipin transcriptional co-regulator activity	23
	1.6.2 Lipin regulation by phosphorylation	24
	1.6.3 Lipin gene mutations and disease	26
	1.7 Phosphatidic acid phosphohydrolase (PAH) in the phylogeny	26
CHAPTER 2	Elucidation of the role of <i>Tetrahymena</i> PAH1 in membrane biogenesis and lipid homeostasis	29
	2.1. Introduction	32
	2.2. Materials	34
	2.3. Methods	34
	2.4. Results	47
	2.5. Discussion	62
CHAPTER 3	Investigation of the role of <i>Tetrahymena</i> PAH1 in mediating cell cycle regulation of nuclear expansion	67
	3.1. Introduction	68
	3.2. Materials	69

	3.3. Methods	70
	3.4. Results	78
	3.5. Discussion	83
CHAPTER 4	Analysis of conservation of <i>PAH</i> functions across eukaryotic clades	85
	4.1. Introduction	86
	4.2. Materials	86
	4.3. Methods	87
	4.4. Results	90
	4.5. Discussion	93
CHAPTER 5	Functional characterisation of <i>Tetrahymena PAH2</i>	95
	5.1. Introduction	96
	5.2. Materials	97
	5.3. Methods	97
	5.4. Results	100
	5.5. Discussion	105
Summary and Conclusion		106
	Summary	107
	Conclusion	109
Bibliography		110
	References	111



Homi Bhabha National Institute

SYNOPSIS OF Ph. D. THESIS

- 1. Name of the Student:** Anoop.N
- 2. Name of the Constituent Institution:** National Institute of Science Education and Research
- 3. Enrolment No. :** LIFE 11201004008
- 4. Title of the Thesis:** Regulation of membrane biogenesis and lipid homeostasis in *Tetrahymena thermophila* - Role of Phosphatidic Acid phosphoHydrolase (PAH)
- 5. Board of Studies:** Life Sciences

SYNOPSIS

Introduction

Phospholipids constitute the principal structural components of lipid bilayers and play a key role in membrane biogenesis, lipid metabolism, and signaling (Van Meer et al., 2008). The lipid composition of the membrane is pivotal in maintaining shape, size, and the number of organelles, and is achieved through the synthesis, transport, and alteration of phospholipids and membrane proteins (McMahon and Gallop, 2005). The regulation of lipid synthesis and storage is critical for maintaining lipid homeostasis since both excess and defect in fat storage results in various lipid-associated disorders (Harris and Finck, 2011).

The shape and size of organelles are maintained depending on the metabolic requirements of the cell. The molecular mechanisms that link lipid production to organelle morphology and number are not known. Phosphatidate phosphatase (PAP) enzymes are

involved in lipid synthesis, signaling, and also act as a key regulator of lipid metabolism and cell physiology. There are two distinct families of PAP enzymes, Mg^{2+} -dependent (PAP1) and Mg^{2+} -independent (PAP2), that serve different physiological functions in lipid metabolism (Sciorra and Morris, 2002; Reue and Brindley, 2008). The PAP1 enzyme is encoded by *PAH1* in yeast and by *LIPIN* in mammals. PAP1 regulates lipid homeostasis by dephosphorylation of phosphatidic acid (PA) to generate diacylglycerol (DAG) (Lin and Carman, 1989), thus controlling the balance between phospholipids and storage lipids. Studies of PAP1 have focused only on Opisthokonta (fungi, nematode, flies, and animals) (Harris and Finck, 2011; Ugrankar et al., 2011) and Plantae clades (Nakamura et al., 2009). PAP1 enzymes and the regulatory cascades in which they participate are not reported in organisms belonging to Amoebozoa, Alveolata, and Excavata clades. *Tetrahymena thermophila* belongs to the Alveolata, a major evolutionary branch of eukaryotic protist and display functional complexity equivalent to the metazoan cells. We identified two homologs of phosphatidic acid phosphatase (*PAH1/LIPIN*) from Tetrahymena Genome Database and designated them as *TtPAH1* (TTHERM_00189270) and *TtPAH2* (TTHERM_00215970).

With this background, we framed our objectives as

- 1) Elucidation of the role of *Tetrahymena PAH1* in membrane biogenesis and lipid homeostasis.
- 2) Investigation of the role of *Tetrahymena PAH1* in mediating cell cycle regulation of nuclear expansion.
- 3) Analysis of conservation of *PAH* functions across eukaryotic clades.
- 4) Functional characterisation of *Tetrahymena PAH2*.

Chapter 1: Introduction and Review of Literature

Lipin/PAH proteins are Mg^{2+} -dependent phosphatidic acid phosphatases and perform dephosphorylation of phosphatidic acid (PA) to generate diacylglycerol (DAG) (Lin and

Carman, 1989; Han et al., 2006). DAG is acylated to form triacylglycerol (TAG) (Han et al., 2006), an essential storage form of energy which gets deposited in lipid droplets. TAG acts as a reservoir of cellular energy and also as a precursor for membrane phospholipids making it a key player in lipid homeostasis. Phosphatidic acid (PA) and diacylglycerol (DAG) are the central precursors which control the levels of phospholipids and the storage lipid. In yeast, phospholipid level and lipid storage are controlled through two independent pathways; the cytidine diphosphate diacylglycerol (CDP-DAG) pathway (*de novo*) and Kennedy pathway (salvage) (Carman and Zeimet, 1996; Carman and Henry, 1999). In metazoans, the CDP-DAG pathway that converts CDP-DAG to phospholipids does not exist and phospholipids are synthesized only through Kennedy pathway (Fagone and Jackowski, 2009).

The first lipin protein shown to function as a Mg^{2+} -dependent phosphatidic acid phosphatase was *S. cerevisiae* Pah1 (Han et al., 2006). *Saccharomyces cerevisiae* express a single lipin homolog *PAH1*, while mammals express three lipin paralogs: *LIPIN1*, *LIPIN2*, and *LIPIN3* (Harris and Finck, 2011). Lipins are relatively large proteins and contains a carboxy-terminal region (C-LIP) with a haloacid dehalogenase-like (HAD) domain possessing the DXDXT/V catalytic motif, and an amino-terminal domain (N-LIP) (Siniossoglou, 2009). Lipins/PAHs localize to the cytoplasm and translocate to membranes in order to dephosphorylate PA. Phosphorylation and dephosphorylation at multiple sites regulate the activity and subcellular localization of PAH proteins (Siniossoglou, 2009; Harris and Finck, 2011). PAH1 is phosphorylated by protein kinases such as CDC28/CDK1 and PHO85 rendering it catalytically inactive (Siniossoglou, 2009; Pascual and Carman, 2013). Dephosphorylation of Pah1 by a nuclear/ER membrane complex consisting of a catalytic phosphatase subunit Nem1, and its regulatory subunit, Spo7, activates its catalytic function and recruit it to the membrane (Siniossoglou, 2009).

Lipin 1 was initially identified as the gene mutated in the fatty liver dystrophy (*fld*) mouse (Péterfy et al., 2001). In mammals, defects in lipins lead to various metabolic disorders including lipodystrophy and insulin resistance, rhabdomyolysis, peripheral neuropathy, and inflammation (Harris and Finck, 2011; Csaki et al., 2013). Apart from enzymatic function, mammalian lipins regulate gene expression as transcriptional regulators by modulating the activity of key transcription factors (Harris and Finck, 2011). In *C. elegans*, down-regulation of lipin affects ER organization and nuclear envelope dynamics (Golden et al., 2009a). Deletion of yeast *PAH1* causes aberrant expansion of nuclear/ER membrane, fatty acid toxicity, increased phospholipid synthesis, decreased TAG level and lipid droplet number, and slow growth and temperature sensitivity (Siniossoglou, 2009; Adeyo et al., 2011). Yeast PAH1 translocates to the nucleus where it interacts with the promoter of phospholipid synthesis genes (Santos-Rosa et al., 2005). Thus phosphatidic acid phosphohydrolase (PAH) acts as a major regulator of lipid metabolism by controlling the levels of lipids.

Chapter 2: Elucidation of the role of *Tetrahymena PAH1 (TtPAH1)* in membrane biogenesis and lipid homeostasis.

Analysis of the amino acid sequence by Interpro revealed that TtPAH1, like other Mg^{2+} dependent phosphatidic acid phosphatases, contains an essential catalytic motif, DXDXT/V in the HAD-like domain of the C-LIP region, and a conserved glycine residue (G75) in N-LIP region critical for PAP function, suggesting it is a Mg^{2+} -dependent phosphatidate phosphatases. This was further confirmed by *in vitro* colorimetric assay using phosphatidic acid as the substrate. Subcellular localization of TtPAH1 by overexpressing *TtPAH1* bearing GFP fusion tag showed both cytoplasmic as well as membrane localization. Co-localization of TtPAH1-GFP with ER-Tracker Red revealed that TtPAH1-GFP is localized in the ER membrane. To evaluate the role of *TtPAH1*, the knockout strain ($\Delta Ttpah1$) was generated by removing all the 45 copies of *TtPAH1* from the macronucleus of

wild-type *Tetrahymena* using homologous recombination. The loss of *PAH1* in *Tetrahymena* did not result in any growth defect. Moreover, the expression of another *PAH* homolog (*TtPAH2*) was not enhanced in $\Delta Ttpah1$ cells. These results suggest that *TtPAH1* is dispensable for normal growth of *Tetrahymena*.

Since PAH proteins are required for the synthesis of triacylglycerol (the main constituent of lipid droplets) through diacylglycerol, the lipid droplet number of $\Delta Ttpah1$ was compared with that of wild-type cells. Lipid droplets were visualized by staining with Oil Red O dye. $\Delta Ttpah1$ cells showed ~60% reduction in lipid droplet number compared to the wild-type in both growing and starved conditions. Overexpression of *TtPAH1* resulted in ~20% increase in lipid droplet number compared to the wild-type, further confirming that *TtPAH1* regulates the lipid droplet biogenesis in *Tetrahymena*.

Endoplasmic reticulum, a complex network consisting of flat sheets and highly curved tubules, serves as the primary site for *de novo* lipid biosynthesis. To understand whether *TtPAH1* is important in maintaining ER morphology, both $\Delta Ttpah1$ and wild-type cells were stained with ER-Tracker dye, and ER morphology and content were evaluated. Deletion of macronuclear copies of *TtPAH1* in *Tetrahymena* alters ER morphology resulting in an increased proportion of sheet to tubule structure. The ER content also increased significantly in the cells lacking *TtPAH1* suggesting that *TtPAH1* is required for creating and/or maintaining the ER structure.

Tetrahymena harbors one polyploid, macronucleus (MAC) and a diploid micronucleus (MIC). Since the outer membrane of the nucleus is continuous with the endoplasmic reticulum, defect in ER is generally reflected in nuclear morphology. To see if the *TtPAH1* is necessary to maintain normal nuclear envelope (NE) morphology, *NUP3-GFP* (a nuclear pore component marker specifically localizing to macronucleus) was expressed in both $\Delta Ttpah1$ cells and wild-type cells to visualize the NE. The result showed that loss of

TtPAH1 did not cause any visible defect in nuclear morphology suggesting that unlike yeast, *PAH1* is not essential for maintaining normal nuclear morphology in *Tetrahymena*. The result was further confirmed by staining isolated nucleus of $\Delta Ttpah1$ cells and wild-type cells with a lipophilic dye DiOC6(3).

Chapter 3: Investigation of the role of *Tetrahymena PAH1* in mediating cell cycle regulation of nuclear expansion in yeast.

Loss of *PAH1* in yeast results in abnormal nuclear expansion. However *TtPAH1* did not regulate nuclear expansion in *Tetrahymena*. To explore whether *TtPAH1*, can rescue the abnormal nuclear expansion of $\Delta pah1$ yeast, *TtPAH1* was introduced into these cells and nuclear morphology was evaluated. To assess nuclear morphology, a nucleoplasmic protein, PUS was expressed as a GFP-fusion protein and analysed by confocal microscopy. $\Delta pah1$ yeast cells show abnormal expansion of nuclear envelope that appears as nuclear membrane projections. In contrast, *pah1* Δ cells expressing *TtPAH1* showed normal round nuclear morphology. Deletion of *PAH1* induces the expression of *INO1*, *INO2*, and *OPI3* involved in lipid synthesis of the ER/nuclear membrane. In addition to the rescue of abnormal nuclear expansion, *TtPAH1* was able to repress expression of these genes, suggesting that *TtPAH1* could replace yeast *PAH1* in regulating expression of phospholipid biosynthesis genes. *pah1* Δ cells also exhibit slow growth at 30°C, temperature sensitive growth at 37°C and respiratory deficiency. Expression of *TtPAH1* restored normal growth at 30°C, temperature sensitivity and respiratory deficiency. Analysis of total lipids from *pah1* Δ cells complemented with *TtPAH1* showed an increase in TAG levels as compared to *pah1* Δ yeast cells. Taken together, these results suggest that *TtPAH1* retains all the known functions of yeast *PAH1*, and hence is functionally conserved between yeast and *Tetrahymena*.

To evaluate whether the catalytic motif DXDXT/V of *TtPAH1* is essential for rescuing these phenotypes, two aspartate residues (D666 & D668) of DXDXT/V motif in

TtPAH1 were mutated to glutamate residues and the mutant *TtPAH1*(*TtPAH1_{mut}*) was used for complementation of *pah1Δ* yeast cells. As expected, the mutant protein was unable to rescue aberrant nuclear morphology, slow growth at 30°C, and the respiratory defect, suggesting that the catalytic activity of TtPAH1 is important for its function.

Chapter 4: Analysis of conservation of PAH functions across eukaryotic clades.

Lipid homeostasis and membrane biogenesis are fundamental to all eukaryotes and expected to be conserved across eukaryotic lineages. The role of *PAH* in these processes is focused mainly on the Opisthokont and Archaeplastid clades. The cellular function of *PAH* is not known in organisms belonging to Amoebozoa, Excavata, Rhizaria and Alveolata clades. In this study, the presence of such a cascade along with their evolutionary relatedness is analysed in these lower eukaryotic clades. The sequence analysis of *PAH* homologs from organisms belonging to different clades suggests that it is conserved across eukaryotic lineage. The present study established that *PAH* is conserved between yeast and *Tetrahymena*. Therefore, to evaluate if it is also conserved in other clades, putative *PAH* homologs from organisms representing Amoebozoa (*Dictyostelium discoideum*) and Excavata (*Trypanosoma brucei*) and *Arabidopsis thaliana* (representing Plantae) were analysed in a complementation study using *pah1Δ* yeast cells. *PAH* homologs from organisms representing Opisthokont clades were not included in this study since these are known to exhibit phosphatidic acid phosphatase activity and to complement yeast *PAH1*. Though *Arabidopsis PAH* (*AtPAH2*) homolog rescues growth and respiratory phenotypes of *pah1Δ* yeast cells (Nakamura et al., 2009), it is not known if it also rescues the nuclear defect phenotype as well. Therefore, *AtPAH2* was also included for complementation assay. This selection covered all the major eukaryotic clades except Rhizaria, for which sequence information was not available. Complementation of *pah1Δ* yeast cells with *Trypanosoma PAH1* (*TbPAH1*), *Arabidopsis PAH2* (*AtPAH2*) and *Dictyostelium discoideum* (*DdPAH1*) showed that the conservation

extends to distantly related clades. While *TbPAH1* rescued all the known defects of *pah1Δ* yeast cells, *DdPAH2* did not rescue growth phenotype but rescued the nuclear defect partially. As reported earlier, *AtPAH2* rescued the slow growth phenotype of *pah1Δ* yeast cells. It also rescued the aberrant nuclear morphology of *pah1Δ* yeast cells. These results along with results from earlier reports suggest that the PAH phosphatase cascade is functionally conserved across eukaryotic lineages, indicating that it originated before the lineages diverged very early in eukaryotic evolution.

Chapter 5: Functional characterisation of *Tetrahymena PAH2*.

Unlike other Pah proteins which are close to 100 kDa, TtPAH2 is a low molecular-weight phosphatidate phosphatase protein of 37 kDa. TtPAH2 harbors two conserved regions, N-LIP and C-LIP present in all known PAP1 proteins. Sequence analysis also revealed that TtPAH2 contains a conserved catalytic motif (DXDXT) in C-LIP found in the members of the Mg²⁺-dependent phosphatase superfamily. To determine whether TtPAH2 is a Mg²⁺-dependent (PAP1) or Mg²⁺-independent (PAP2) phosphatidic acid phosphatase, the enzymatic activity of recombinant TtPAH2 was examined using PA as substrate. The recombinant TtPAH2 dephosphorylated PA in a concentration and time-dependent manner. There was no detectable phosphatase activity in the absence of magnesium ions suggesting that TtPAH2 is a Mg²⁺-dependent phosphatidic acid phosphatase belonging to the PAP1 family of phosphatase. Analysis of sub-cellular localization of *TtPAH2-GFP* in the wild-type *Tetrahymena* cells by confocal microscopy showed that the TtPAH2-GFP is distributed throughout the cell both in cytoplasm and membranes. It was further confirmed by western blot analysis of both the membrane fraction and the cytosolic fraction of the total lysate of cells expressing *TtPAH2-GFP*.

To assess whether *TtPAH2* has a direct role in ER morphology, both $\Delta Ttpah2$ and the wild-type cells were stained with ER Tracker Green and imaged under a confocal

microscope. The results showed that there was no significant difference in ER morphology and total ER content between $\Delta Ttpah2$ and the wild-type cells. These results suggest that unlike other known *PAH* homologs, *TtPAH2* do not regulate endoplasmic reticulum morphology in *Tetrahymena*.

Summary

- *Tetrahymena* possesses two *PAH* homologs, *TtPAH1* and *TtPAH2*.
- *TtPAH1* and *TtPAH2* localize to both membranes and cytoplasm, and are not required for normal growth of *Tetrahymena*.
- *TtPAH1* is a magnesium dependent phosphatidic acid phosphatase required for lipid droplet biogenesis and maintaining tubular endoplasmic reticulum morphology in *Tetrahymena*.
- *TtPAH1* does not regulate nuclear membrane expansion in *Tetrahymena*
- *TtPAH1* restores a normal nuclear morphology, suppresses slow growth, temperature-sensitive growth and respiratory deficiency of *pah1* Δ yeast cells
- *TtPAH1* suppresses the expression of phospholipid biosynthetic genes in yeast and restores TAG levels of *pah1* Δ yeast cells.
- Catalytic motif (DXDGT) of *TtPAH1* is essential for rescuing all the defects of *pah1* Δ yeast cells.
- *PAH* is functionally conserved across eukaryotic evolutionary tree.
- *TtPAH2* belongs to magnesium dependent phosphatidic acid phosphatase family and does not regulate ER content and morphology in *Tetrahymena*.

Conclusion

The two homologs of phosphatidic acid phosphohydrolase gene (*TtPAH1* and *TtPAH2*) present in the genome database of *Tetrahymena thermophila* encoded for Mg^{2+} -dependent phosphatidate phosphatase. Even though the loss of *TtPAH1* increased the ER sheet structure and altered ER morphology it did not result in any defect in the nuclear envelope

morphology. We conclude that defects in ER morphology in *Tetrahymena* did not necessarily affect nuclear morphology in *Tetrahymena*. It suggests that in *Tetrahymena*, unlike other organisms, ER content and structure are functionally isolated from mechanisms underlying nuclear expansion. From complementation studies with *PAH1* homolog from organisms representing all major eukaryotic lineages we conclude that *PAH* is functionally conserved across all eukaryotic lineages. TtPAH2, even though catalytically active; did not regulate ER morphology in *Tetrahymena* which shows that catalytic activity alone is not sufficient for performing all the cellular functions.

References

- Adeyo, O., Horn, P.J., Lee, S., Binns, D.D., Chandrabhas, A., Chapman, K.D., and Goodman, J.M.** (2011). The yeast lipin orthologue Pah1p is important for biogenesis of lipid droplets. *J. Cell Biol.* *192*, 1043–1055.
- Carman, G.M., and Henry, S.A.** (1999). Phospholipid biosynthesis in the yeast *Saccharomyces cerevisiae* and interrelationship with other metabolic processes. *Prog. Lipid Res.* *38*, 361–399.
- Carman, G.M., and Zeimet, G.M.** (1996). Regulation of Phospholipid Biosynthesis in the Yeast *Saccharomyces cerevisiae*. *J. Biol. Chem.* *271*, 13293–13296.
- Csaki, L.S., Dwyer, J.R., Fong, L.G., Tontonoz, P., Young, S.G., and Reue, K.** (2013). Lipins, lipinopathies, and the modulation of cellular lipid storage and signaling. *Prog. Lipid Res.* *52*, 305–316.
- Fagone, P., and Jackowski, S.** (2009). Membrane phospholipid synthesis and endoplasmic reticulum function. *J. Lipid Res.* *50*, S311–S316.
- Golden, A., Liu, J., and Cohen-Fix, O.** (2009). Inactivation of the *C. elegans* lipin homolog leads to ER disorganization and to defects in the breakdown and reassembly of the nuclear

envelope. *J. Cell Sci.* 122, 1970–1978.

Han, G.S., Wu, W.I., and Carman, G.M. (2006). The *Saccharomyces cerevisiae* lipin homolog is a Mg²⁺-dependent phosphatidate phosphatase enzyme. *J. Biol. Chem.* 281, 9210–9218.

Harris, T.E., and Finck, B.N. (2011). Dual function lipin proteins and glycerolipid metabolism. *Trends Endocrinol. Metab.* 22, 226–233.

Lin, Y., and Carman, G.M. (1989). Purification and Characterization of Phosphatidate Phosphatase from *Saccharomyces cerevisiae*. 264, 8641–8645.

McMahon, H.T., and Gallop, J.L. (2005). Membrane curvature and mechanisms of dynamic cell membrane remodelling. *Nature* 438, 590–596.

Mietkiewska, E., Siloto, R.M.P., Dewald, J., Shah, S., Brindley, D.N., and Weselake, R.J. (2011). Lipins from plants are phosphatidate phosphatases that restore lipid synthesis in a *pah1* Δ mutant strain of *Saccharomyces cerevisiae*. 278, 764–775.

Nakamura, Y., Koizumi, R., Shui, G., Shimojima, M., Wenk, M.R., and Ito, T. (2009). Arabidopsis lipins mediate eukaryotic pathway of lipid metabolism and cope critically.

Pascual, F., and Carman, G.M. (2013). Phosphatidate phosphatase, a key regulator of lipid homeostasis. *Biochim. Biophys. Acta - Mol. Cell Biol. Lipids* 1831, 514–522.

Péterfy, M., Phan, J., Xu, P., and Reue, K. (2001). Lipodystrophy in the fld mouse results from mutation of a new gene encoding a nuclear protein, lipin. 27, 121–124.

Reue, K., and Brindley, D.N. (2008). Multiple roles for lipins / phosphatidate phosphatase enzymes in lipid metabolism. 49, 2493–2503.

Santos-Rosa, H., Leung, J., Grimsey, N., Peak-Chew, S., and Siniosoglou, S. (2005). The yeast lipin Smp2 couples phospholipid biosynthesis to nuclear membrane growth. *EMBO J.* 24, 1931–1941.

Sciorra, V.A., and Morris, A.J. (2002). Roles for lipid phosphate phosphatases in regulation

of cellular signaling. *1582*, 45–51.

Siniosoglou, S. (2009). Lipins, lipids and nuclear envelope structure. *Traffic 10*, 1181–1187.

Ugrankar, R., Liu, Y., Provaznik, J., Schmitt, S., and Lehmann, M. (2011). Lipin Is a Central Regulator of Adipose Tissue Development and Function in *Drosophila melanogaster*. *31*, 1646–1656.

Van Meer, G., Voelker, D.R., and Feigenson, G.W. (2008). Membrane lipids: where they are and how they behave. *Nat. Rev. Mol. Cell Biol.* *9*, 112–124.

List of figures

- Figure 1.1: Overview of lipid biosynthetic pathways.
- Figure 1.2: The domain organization of PAP1 and PAP2 enzymes
- Figure 1.3: Schematic showing mechanisms of regulation of PA phosphatase Pah1 and its function
- Figure 1.4: Major phenotypes shown by yeast *pah1* Δ strains
- Figure 1.5: The *Tetrahymena* life cycle
- Figure 2.1: Domain Organization of TtPAH1 and Multiple sequence alignment showing partial sequences of N-LIP and C-LIP of PAH1 proteins
- Figure 2.2: TtPah1 displays magnesium dependent phosphatidate phosphatase activity.
- Figure 2.3: TtPah1 is distributed both in cytosol and in membranes.
- Figure 2.4: TtPah1 localizes to ER.
- Figure 2.5: Generation of *TtPAH1* knockouts (Δ *TtPah1*)
- Figure 2.6: Growth curve of *Tetrahymena* wild-type versus Δ *Ttpah1* cells.
- Figure 2.7: Lack of growth defect in Δ *Ttpah1* is not due to compensatory overexpression of the other homolog *TtPAH2*
- Figure 2.8: Deletion of *TtPAH1* reduces lipid droplet number in *Tetrahymena*.
- Figure 2.9: Deletion of *TtPAH1* showed reduced lipid droplet number in starved conditions.
- Figure 2.10: Overexpression of *TtPAH1* causes increase in lipid droplet number
- Figure 2.11: *TtPAH1* is needed for maintaining tubular ER and deletion of *TtPAH1* results in increased ER content.
- Figure 2.12: Loss of *TtPAH1* does not show visible nuclear envelope defect in *Tetrahymena*.
- Figure 2.13: Loss of *TtPAH1* does not show nuclear membrane expansion in *Tetrahymena*
- Figure 3.1: *TtPAH1* rescues the nuclear structure defect
- Figure 3.2: *TtPAH1* rescues the slow growth, temperature sensitivity and respiratory deficiency phenotypes of *pah1* Δ yeast cells.
- Figure 3.4: *TtPAH1* repress expression of genes involved in lipid biosynthesis
- Figure 3.5: Catalytic mutant of TtPAH1 could not rescue phenotypes of *pah1* Δ yeast cells.

- Figure 4.1: Phosphatidate phosphatase has similar domain organization across eukaryotic lineages
- Figure 4.2: Regulation of nuclear envelope expansion function of PAH proteins are conserved across eukaryotic lineages
- Figure 4.3: PAH proteins from Excavata and Plantae rescued growth phenotypes of yeast *pah1* Δ strains
- Figure 5.1: Domain organisation of Ttpah2
- Figure 5.2: Sequence analysis of Ttpah2
- Figure 5.3: TtPah2 encodes a magnesium dependent phosphatidate phosphatase
- Figure 5.4: TtPAH2 localizes to both cytosol and membranes
- Figure 5.5: *TtPAH2* does not regulate ER morphology

List of Tables

- Table 2.1: Oligonucleotides used chapter 2
- Table 2.2: PCR reaction components and conditions for amplification of *TtPAH1* using phusion Polymerase
- Table 2.3: PCR reaction components and conditions for amplification of alpha tubulin and *TtPAH1* using Taq polymerase for semiquantitative PCR
- Table 3.1: Amino acid composition for yeast in SD media
- Table 3.2: Oligonucleotides used in chapter 3
- Table 3.3: PCR reaction components and conditions used for amplification of commercially synthesized *TtPAH1* using phusion polymerase.
- Table 3.4: DNase treatment mixture for RNA isolated from yeast cells
- Table 4.1: Oligonucleotides used in chapter 4
- Table 4.2: PCR reaction components and conditions used for amplification of *TbPAH1*, *AtPAH2*, and *DdPAH1* using phusion polymerase
- Table 5.1: Oligonucleotides used in chapter 5
- Table 5.2: PCR reaction components and conditions used to amplify *TtPAH2* using phusion polymerase

ABBREVIATIONS

ATP	Adenosine Triphosphate
CTDNEP1	C-terminal domain nuclear envelope phosphatase 1
DAP1	4', 6-Diamidino-2-Phenylindole, Dihydrochloride
DEPC	Diethylpyrocarbonate
DiOC6(3)	3,3'-dihexyloxacarbocyanine iodide
DNA	Deoxyribonucleic acid
dNTP	Deoxy nucleotide phosphates
EDTA	Ethylenediaminetetraacetic acid
ER	Endoplasmic Reticulum
HAD	Haloacid Dehalogenase
HRP	Horse radish peroxidase
His	Histidine
INO1	Inositol-3-phosphate synthase
IPTG	Isopropyl beta-D-1thiogalactopyranoside
kDa	Kilo Dalton
KO	Knockout
LB	Luria Bertani
LD	Lipid droplet
MTT	Metallothionein
NE	Nuclear Envelope
NEM1	Nuclear Envelope Morphology protein 1
NEP1-R1	Nuclear envelope phosphatase 1-regulatory subunit 1
NUP	Nuclear pore

OPI3	Phosphatidyl-N-methylethanolamine N-methyltransferase
OD	Optical density
PAP	Phosphatidic Acid Phosphatase
PA	Phosphatidic acid
PAH	Phosphatidic Acid Hydrolase
PCR	Polymerase Chain Reaction
PC	Phosphatidylcholine
PE	Phosphatidylethanolamine
PS	Phosphatidylserine
rDNA	Ribosomal DNA
RPM	Rotations per minute
SD	Synthetic Complete Dextrose media
SPO7	Sporulation-specific protein 7
SDS-PAGE	Sodium Dodecyl Sulphate Poly Acrylamide Gel Electrophoresis
SPP	Super Proteose Peptone
TBST	Tris buffer saline tween
TAP	Tandem Affinity Purification
TAG	Triacylglycerol
WT	Wild type
YPD	Yeast Extract Peptone Dextrose

CHAPTER 1
Introduction and Review of Literature

1.1 Membrane biogenesis and lipid homeostasis

Membrane biogenesis involves the synthesis of cell membrane with the help of proteins and lipids. Membranes synthesised by this process of membrane biogenesis help in dividing the cell into structural and functional compartments. Membranes of the cell altogether are called as endomembrane system which includes different membranes suspended in the cytoplasm and the plasma membrane. Cell organelles like the nucleus, endoplasmic reticulum, vacuoles, lysosomes, Golgi apparatus and mitochondria are surrounded by membrane structure. The membranes of the different organelles vary in molecular composition to suit for the functions they perform (Mcmahon et al., 2015). Organelle membranes are important to several vital cell functions including protein synthesis, lipid production, and cellular respiration (Mcmahon et al., 2015; Lusk and King, 2017). It has now become evident, the pervasive importance of lipids in cell biology. From structural roles defining cellular compartments and surfaces with specific biological properties to functional roles in signal transduction and modulation of regulatory networks, the involvement of lipids in varied cellular functions is well established. Lipid homeostasis is maintained through a repertoire of proteins involved in synthesis, degradation, transport and sensing of lipids as well as the regulatory mechanisms that interconnect lipid metabolism with other cellular processes (Voeltz and Prinz, 2007). Lipid supply is fine-tuned through a multitude of negative feedback circuits initiated by both end products and intermediates of lipid synthesis pathways so as to retain the lipid homeostasis (Voeltz and Prinz, 2007). Also, there are evidences that the diversity of membrane lipids is maintained through cross-regulatory effects, whereby classes of lipids activate the activity of enzymes operating in another metabolic branch (Zhang, 2009; Lagace and Ridgway, 2013). A central yet unanswered question in cell biology concerns the amount of phospholipids or TAG that is required in a living cell. How lipid homeostasis is regulated in coordination with nutritional and environmental conditions is not known still a paradox. The cellular TAG

content in cells varies dramatically between different stages of growth and development which underscores its important metabolic role (Kohlwein, 2010). The key anabolic and catabolic enzymes involved in the TAG metabolism are conserved between yeast and mammals (Kurat et al., 2006; Nielsen, 2009; Kohlwein, 2010; Natter and Kohlwein, 2013). The specific requirements for storage (e.g.- TAG) and membrane lipids (phospholipids) oscillate as cells grow and divide or enter the non-replicative stationary (quiescent) phase (Kurat et al., 2006; Czabany et al., 2007; Nielsen, 2009). During these periods, it appears to be crucial to control the metabolic flux either into phospholipids (proliferative state) or into or out of TAG (stationary phase or nutrient limitation conditions) (Kohlwein, 2010).

Phospholipids constitute the major structural components of lipid bilayers and play a central role in membrane biogenesis, lipid metabolism, and signaling. Also the lipid composition of the membrane is critical for maintaining shape, size, and number of organelles, and is established through synthesis, transport, and modification of phospholipids (McMahon and Gallop, 2005). One of the defining organelle of eukaryotic cells is the nucleus that undergoes remarkable changes during the cell cycle and development (Webster et al., 2009; Schellhaus et al., 2016; Ungricht and Kutay, 2017). The intra-nuclear compartment is delimited by the nuclear envelope and consists of a double lipid bilayer, the outer and the inner nuclear membrane (King and Lusk, 2016; Ungricht and Kutay, 2017)). The outer nuclear membrane is physically and functionally linked to the endoplasmic reticulum (ER) (King and Lusk, 2016; Lusk and King, 2017), whereas the inner nuclear membrane faces the nucleoplasm. In metazoans nuclear membrane is covered by the nuclear lamina (Ungricht and Kutay, 2017). Dynamic changes in the structure of the nuclear envelope are essential for the proper execution of nuclear division in all eukaryotes (Webster et al., 2009; Imamoto and Funakoshi, 2012; Ungricht and Kutay, 2017). The surface area of a mother nucleus undergoing closed mitosis must increase to allow intra-nuclear mitotic spindle elongation and formation of the

daughter nuclei. The model yeasts *S. pombe* and *Saccharomyces cerevisiae* solve this problem through nuclear envelope (NE) expansion at mitotic entry. In *Saccharomyces cerevisiae*, and *S. pombe* the nuclear membrane does not breakdown during mitosis (Webster et al., 2009; Ebrahimi and Cooper, 2012; Sazer et al., 2014). In contrast, the fission yeast *S. japonicas* does not expand its NE and instead relies on NE breakdown during anaphase to allow chromosome segregation like metazoans (Sazer et al., 2014; Asakawa et al., 2016). In metazoan cells the nuclear envelope breaks down during mitosis which is called “open mitosis”(Webster et al., 2009; Schellhaus et al., 2016 Asakawa et al., 2016).

Maintenance of proper nuclear structure is important for cell physiology as highlighted by the identification of several diseases that are associated with changes in nuclear shape and are caused by mutations in nuclear envelope proteins (Broers, 2006; Worman et al., 2010; Katherine H.Schreiber and BrianK.Kennedy, 2013). Moreover, a number of specialized cell types undergo ‘nuclear differentiation’, like the mammalian blood cells where nuclei can be highly lobed and segmented or spermatocytes and myocytes where nuclei can become very elongated (Leitch, 2000). Recent studies in yeast and mammals have made clear that phospholipid metabolism is an important player in nuclear physiology including roles in nuclear function as dynamic building blocks of nuclear membrane, in communication between nucleus and other organelles (Santos-Rosa et al., 2005; Voeltz and Prinz, 2007; Siniosoglou, 2009). A significant number of phospholipid metabolic enzymes have been localized in the nucleus and phospholipids or their water-soluble metabolites can regulate gene expression, nucleocytoplasmic transport and nuclear organization. In addition, given the emerging view of the nuclear envelope as a master regulator of nuclear function, whether nuclear lipid metabolic enzymes have a role in growth and development by controlling nuclear architecture is still unanswered (Talamas and Capelson, 2015; Yang et al., 2017). The regulation of lipid synthesis and storage is critical for maintaining lipid homeostasis since

both excess and poor fat storage results in various lipid-associated disorders such as obesity, lipodystrophy, insulin resistance, diabetes, hypertension, cardiovascular disease, and cancer (Klingenspor et al., 1999; Reue et al., 2000; Péterfy et al., 2001; Prentki and Madiraju, 2008). However, the molecular mechanisms that link lipid production to organelle morphology is not clearly understood (Meer, 2009; Osellame et al., 2012; Schwarz and Blower, 2016). The lipid homeostasis and membrane biogenesis is interconnected and any perturbation in lipid biosynthetic pathways can reflect in organellar shape, size and lipid storage.

1.2 Phospholipid Biosynthesis

Phospholipids are key molecules that contribute to the structural definition of cells and that participate in the regulation of cellular processes (Van Meer et al., 2008). Phospholipid metabolism is a major activity that cells engage in throughout their growth. The yeast, *Saccharomyces cerevisiae*, served as a model system in which the regulation of phospholipid synthesis is studied (Carman and Henry, 1999; Kohlwein, 2010; Grillitsch et al., 2011). It has also played a foundational role in the field of molecular and cellular biology of lipids to show how lipid metabolism is linked with organelle dynamics. Its membranous organelles, the lipids that comprise these membranes and the phospholipid biosynthetic pathways that generate these membranes are similar in all eukaryotic cells. Many of the structural genes encoding for the phospholipid biosynthetic enzymes have been cloned and characterized, and a number of mutations in these genes have been isolated (Greenberg and Lopes, 1996; Griač, 1997; Wimalarathna et al., 2011). In addition, a number of phospholipid biosynthetic enzymes have been purified and studied. The characterization of the wild-type and mutant genes, as well as the gene products encoded by these alleles, has significantly advanced our understanding both of phospholipid biosynthesis and of its regulation (Greenberg and Lopes, 1996; Wimalarathna et al., 2011). Results from these genetic, molecular, and biochemical

studies have shown that the regulation of phospholipid synthesis is a complex, highly coordinated process (Greenberg and Lopes, 1996; Han, 2001).

The basic design of the phospholipid biosynthetic pathway is conserved from yeast to mammals (Nielsen, 2009; Natter and Kohlwein, 2013). The glycerol backbone of the central phospholipid precursor, phosphatidic acid (PA), partitions between the two major branches of the pathway in yeast (Figure 1.1). In one branch, PA is dephosphorylated to diacylglycerol (DAG) that is then used for the synthesis of the most abundant phospholipids phosphatidylethanolamine (PE) and phosphatidylcholine (PC), through the CDP-ethanolamine and the CDP-choline arms of the Kennedy pathway, respectively (Han, 2001; Carman and Han, 2009; Gibellini and Smith, 2010). In the other branch, PA is converted to CDP-DAG that gives rise to phosphatidylinositol (PI), phosphatidylglycerol and cardiolipin. Phospholipid biosynthesis is a complex process that contains a number of branch points. PS, PE, and PC are synthesized from PA by the CDP-DG pathway while PE and PC are also synthesized by the Kennedy (CDP-choline and CDP-ethanolamine) pathway (Figure 1.1) (Han, 2001; Greenberg and Lopes, 1996; Gibellini and Smith, 2010). CDP-DAG is also used for the synthesis of other phospholipids, including inositol-containing lipids (phosphoinositides and sphingolipids) and CL. The Kennedy pathway assumes a critical role in PC synthesis when the enzymes in the CDP-DG pathway are defective or repressed (Gibellini and Smith, 2010). In metazoans, the pathway that converts CDP-DAG to PC/PE do not exist and lipin is essential for PC/PE synthesis since they completely rely on Kennedy pathway for phospholipid synthesis (Fagone and Jackowski, 2009; Bahmanyar, 2015).

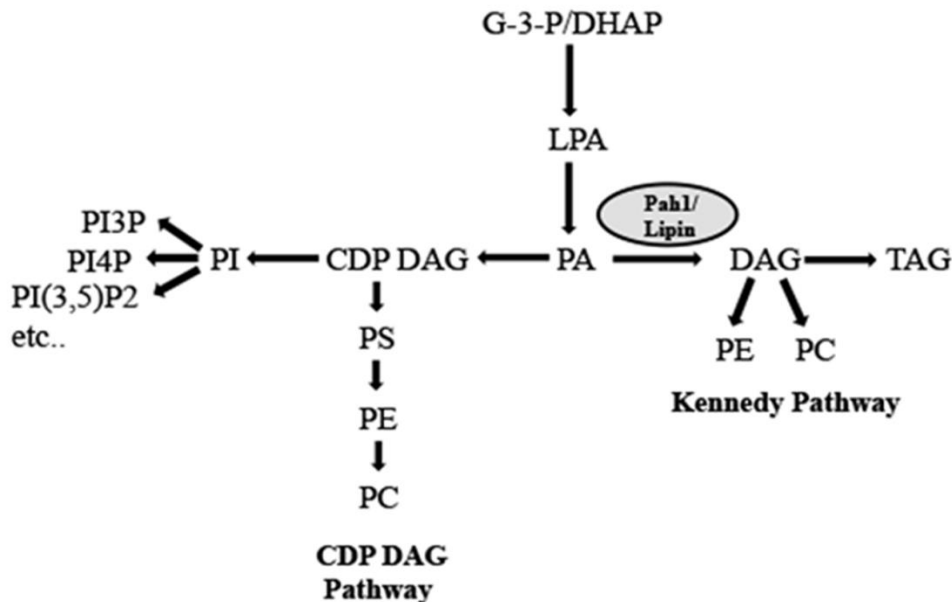


Figure 1.1: Overview of lipid biosynthetic pathways.

PA is a key precursor used for the synthesis of phosphatidylethanolamine (PE) and phosphatidylcholine (PC) through CDP-DAG pathway. In the presence of choline and ethanolamine, these phospholipids are synthesized through Kennedy pathway. In metazoans, the pathway that converts CDP-DAG (cytidine diphosphate diacylglycerol) to PC/PE (CDP-DAG pathway) does not exist whereas both the pathways are present in yeast. G-3-P- Glycerol-3-phosphate, LPA-Lysophosphatidate, PI3P-Phosphatidylinositol-3-phosphate, PI4P- Phosphatidylinositol-4-phosphate, PI (3, 5) P2- Phosphatidylinositol-3, 5-biphosphate, PS- Phosphatidylserine.

1.3 Phosphatidate phosphatases

Phosphatidate phosphatase (PAP, 3-sn-phosphatidate phosphohydrolase, EC 3.1.3.4) catalyzes the dephosphorylation of phosphatidate, yielding Diacylglycerol (DAG) and inorganic phosphate(Hoer and Oberdisse, 1994; Han et al., 2006; Carman and Han, 2006). PAP enzymes have roles in both the synthesis of lipids and the generation or degradation of lipid-signaling molecules in eukaryotic cells (Sciorra and Morris, 2002). They are classified as either Mg²⁺-dependent (referred to as PAP1 enzymes) or Mg²⁺- independent (referred to as PAP2) with respect to their cofactor requirement for catalytic activity. In both yeast and mammalian systems, PAP2 enzymes are known to be involved in lipid signaling (Sciorra and

Morris, 2002). In contrast the physiological roles of PAP1 enzymes have remained unclear for long time owing to a lack of molecular information.

1.3.1 Magnesium dependent (PAP1) and Magnesium independent (PAP2) enzymes

Since the initial characterization of the PAP reaction in 1957, both Mg^{2+} -dependent and -independent enzymes have been identified in yeast (Carman and Han, 2006; Pascual and Carman, 2013). Besides the difference in their cofactor requirement, these enzymes are distinguished by several other properties. PAP2 proteins such as Dpp1p and Lpp1p are relatively small integral membrane proteins confined to the vacuole and Golgi membranes, respectively (Toke et al., 1998; Faulkner et al., 1999; van Schooten et al., 2006; Pascual and Carman, 2013). Both proteins possess six transmembrane domains distributed over their polypeptide sequences. Dpp1p and Lpp1p do not require divalent cations for activity, while maximum activity of Pah1p (PAP1 protein) is dependent on Mg^{2+} ions (Toke et al., 1998; Pascual and Carman, 2013). This distinction in cofactor requirement can be explained by the differences in the catalytic motifs that govern the activity of each class of enzymes. The PAP activity of Pah1p is governed by a DXDX (T/V) motif (Figure 1.2) found in members of a superfamily of Mg^{2+} -dependent phosphatase enzymes (Han et al., 2007). The enzymatic activity of Mg^{2+} -independent PAP2 enzymes Dpp1p and Lpp1p is conferred by a three-domain lipid phosphatase motif composed of the consensus sequences KXXXXXXRP, PSGH and SRXXXXXHXXXD (Figure 1.2) (Stukey and Carman, 2008; Toke et al., 1999). PAP1 and PAP2 enzymes in yeast also differ with respect to their substrate specificities. Dpp1p and Lpp1p utilize a variety of lipid phosphate substrates, including PA, DGPP, lysoPA, sphingoid base phosphates, and isoprenoid phosphates (Wu et al., 1996). But, Pah1p activity is specific for PA (Morlock et al., 1991; Pascual and Carman, 2013). Moreover, both the substrates and products of the reactions catalyzed by the PAP2 enzymes are important signaling molecules, suggesting that these enzymes are involved in lipid signaling, and not responsible for the de novo synthesis of phospholipids and TAG that occurs in the ER. Dpp1,

Lpp1 and App1 are thought to be involved in lipid signaling or membrane structural/curvature changes associated with vesicular trafficking.

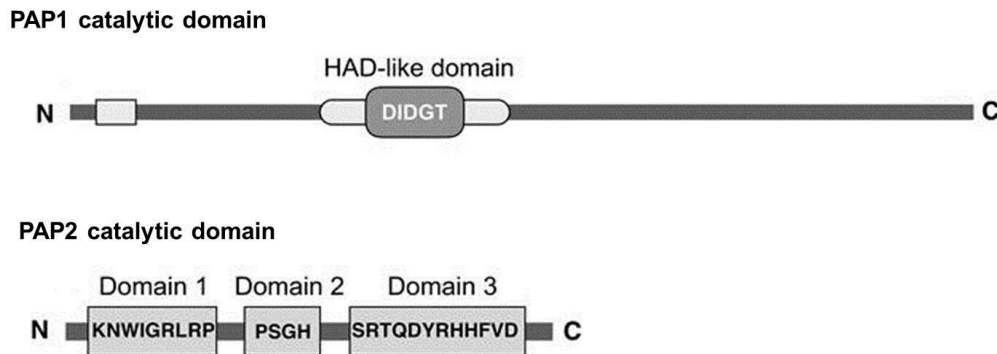


Figure 1.2: The domain organization of PAP1 and PAP2 enzymes

The essential catalytic motifs are indicated. The conserved amino acid residues in the catalytic motifs are indicated by the single letter code. HAD denotes Haloacid dehalogenase domain

The PAP reaction was first described in animal tissues by Smith et al. in 1957, providing a link between the neutral and phospholipid synthesis pathways in mammalian cells. Subsequent studies demonstrated that majority of this enzymatic activity resides in the soluble fraction of cell lysates, in contrast to other enzymes in the TAG and phospholipid synthesis pathways, which are integral membrane proteins. Also this enzymatic reaction requires Mg^{2+} ions, and that the. Due to the instability of the mammalian enzyme, the isolation of PAP remained elusive for more than three decades. In 1984, Hosaka and Yamashita identified PAP activity in the cytosolic and membrane fractions of the yeast *S. cerevisiae*. This simple eukaryote synthesizes lipids by pathways common to those of more complex organisms and is an attractive model system due to its molecular and genetic tractability(Botstein et al., 1997; Botstein and Fink, 2011; Duina et al., 2014). This helped in purification of a 104-kDa PAP enzyme from the total membrane fraction. Unfortunately the gene(s) encoding them could not be identified because of insufficient amount of protein available for sequencing by Edman degradation analysis. Later in a fortunate twist of scientific fate, a preparation of the 91-kDa enzyme was recovered from frozen storage,

analyzed for enzymatic activity, and sequenced by mass spectrometry and the gene was identified. This matched the protein sequence product of the SMP2 gene, which had been implicated in plasmid maintenance and respiration (Irie et al., 1993). The molecular function of Smp2p, however, had yet to be established. Overexpression of SMP2 was reported to complement the aberrant nuclear membrane expansion phenotype of *nem1Δ* and *spo7Δ*, mutants lacking the endoplasmic reticulum (ER)-associated Nem1p–Spo7p phosphatase complex. Upon identification of the molecular function as a PAP enzyme, the SMP2 gene was renamed *PAH1* (for phosphatidic acid phosphohydrolase). In *Sacharomyces cerevisiae* Pah1p is 862 amino acids in length and has a predicted molecular mass of 95-kDa; however, when expressed in *S. cerevisiae* it migrates as a 124-kDa protein on SDS-PAGE. Pah1p expressed in *E. coli* migrates as a 114-kDa protein product on SDS-PAGE. Therefore, observed size of Pah1p cannot be attributed solely to modification by phosphorylation. The identification and characterization of yeast Pah1p revealed its homology to the mammalian homolog known as lipins, encoded by the murine Lpin1, 2, and 3 genes. Lpin1 was identified as the gene whose mutation at the Glycine 80 residue is responsible for the transient fatty liver dystrophy (*fld*) phenotype of mice. A loss of lipin-1 was shown to prevent normal adipose tissue development, resulting in lipodystrophy and insulin resistance, while an excess of lipin-1 promoted obesity and insulin sensitivity.

Lipins/PAHs are relatively large proteins close to 100 kDa and contain a conserved amino-terminal domain (N-LIP) and carboxy-terminal catalytic domain (C-LIP) harbouring a DXDXT motif found in a superfamily of Mg²⁺-dependent phosphatases. This catalytic motif is important for Pahp function and mutation of Aspartate (Asp-398, and Asp-400) in the catalytic motif leads to loss of phosphatase activity (Han et al., 2007; Pascual and Carman, 2013). All lipins lack transmembrane domains and therefore must first translocate onto membranes in order to dephosphorylate PA (Karanasios et al., 2010). Recruitment requires

the transmembrane protein phosphatase complex Nem1p-Spo7p in yeast (Figure 1.3) which dephosphorylates Pah1p (Karanasios et al., 2010; Karanasios et al., 2013). Nem1p is the catalytic subunit while Spo7p is the regulatory subunit that binds to the catalytic domain of Nem1p and is required for the phosphatase activity of the holoenzyme (Santos-Rosa et al., 2005; Siniossoglou, 2009; Pascual and Carman, 2013). Once, dephosphorylated, Pah1p can associate with the nuclear/ER membrane independent of Nem1p-Spo7p. The mammalian counterparts of Nem1-spo7 are CTDNEP1 (formerly known as “dullard”) and NEP1-R1, the catalytic and regulatory subunits, respectively (Figure 1.3), of the phosphatase complex (Han et al., 2012). Pah1p contains an amphipathic helix in its extreme amino-terminal end from residues 1 to 18 (Karanasios et al., 2010). Dephosphorylation of Pah1p promotes membrane binding only in the presence of this amphipathic helix (Karanasios et al., 2010). PAH1 from yeast species carry an acidic stretch at their C-terminal ends (amino acid residues 837 to 862) (Siniossoglou, 2009; Karanasios et al., 2013). This C-terminal acidic stretch of Pah1p is required for its binding to the Nem1p-Spo7p phosphatase complex (Karanasios et al., 2013). The acidic tail is necessary and sufficient for Nem1p-Spo7p-dependent recruitment of Pah1p close to lipid droplets and is important for droplet biogenesis (Karanasios et al., 2013). A very recent study has found that C-terminal region of yeast Pah1 contains the sequence WRDPLVDID, which is important for the in vivo function of Pah1 (Park et al., 2017). This sequence contains residues conserved (or partially conserved) in Pah1/lipin proteins from yeast, mice, and humans. The analysis of the site-specific mutations of the conserved residues within the sequence WRDPLVDID revealed that Trp-637 is required for Pah1 function in vivo (Park et al., 2017). Unlike other conserved residues (e.g. Gly-80, Asp-398, and Asp-400 in yeast Pah1) that are essential for PAP activity and the in vivo function of Pah1, the mutations of Trp-637 did not compromise the enzyme activity (Park et al., 2017). This may

be explained by the fact that Gly-80, Asp-398, and Asp-400 are catalytic residues, whereas Trp-637 is presumably a regulatory residue.

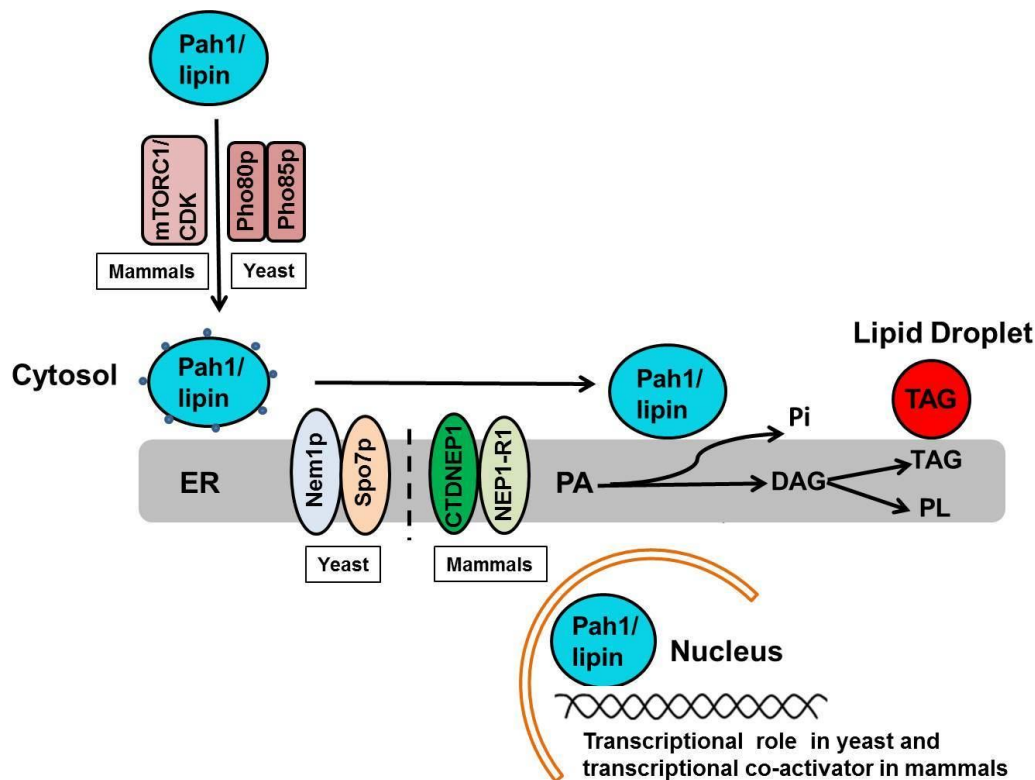


Figure 1.3: Schematic showing mechanisms of regulation of PA phosphatase PAH1 and its function

PAH1 is dephosphorylated by the Nem1-Spo7 phosphatase complex in yeast. The dephosphorylation activates Pah1 and recruits it to the membrane to catalyze the dephosphorylation of PA to generate DAG. DAG is converted to TAG and phospholipids. TAG form the major constituent of lipid droplet. In yeast Nem1p-Spo7p dephosphorylates Pah1. The mammalian counterparts of Nem1-spo7 are CTDNEP1 and NEP1-R1. In yeast Pah1 is phosphorylated by multiple protein kinases including like Pho85p-Pho80p. In mammals lipin is phosphorylated by mTOR. LD-lipid droplet; DAG-diacylglycerol; TAG-triacylglycerol; PL-phospholipids; ER-endoplasmic reticulum; NEM1- nuclear envelope morphology 1; SPO7- sporulation 7; CTDNEP1- C-terminal domain nuclear envelope phosphatase 1; NEP1-R1- nuclear envelope phosphatase 1-regulatory subunit 1.

1.4 Phosphatidic acid phosphohydrolase (*PAH1*) regulate lipid biosynthesis and lipid droplet biogenesis

The essential role of PAP1 in de novo lipid metabolism has been established using the yeast *pah1Δ* mutant (Figure 1.4) (Santos-Rosa et al., 2005; Pascual and Carman, 2013). Lack of enzyme activity in this mutant shows elevated levels of PA and decreased levels of

DAG/TAG(Siniooglou, 2009; Pascual and Carman, 2013). Moreover, the levels of phospholipids, fatty acids, and sterol esters are elevated in response to the *pah1Δ* mutation, indicating that PAP1 regulates overall lipid synthesis. In addition to the alteration in lipid metabolism, the *pah1Δ* mutant also exhibits slow growth, aberrant expansion of the nuclear/ER membrane, respiratory deficiency, defects in lipid droplet formation and morphology, vacuole homeostasis and fusion, fatty-acid induced lipotoxicity, and a growth sensitivity to elevated temperature (Santos-Rosa et al., 2005; Fakas et al., 2011; Adeyo et al., 2011; Sasser et al., 2012; Fernández-Murray and McMaster, 2016). Catalytically inactive mutant forms of PAP1, either mutation of a conserved glycine (e.g., G80R) at the N-terminus or of DIDGT catalytic motif (D398E or D400E) exhibit the same phenotypes associated with the *pah1Δ* mutation, indicating these effects are specifically linked to the loss of PAP activity (Han et al., 2007).

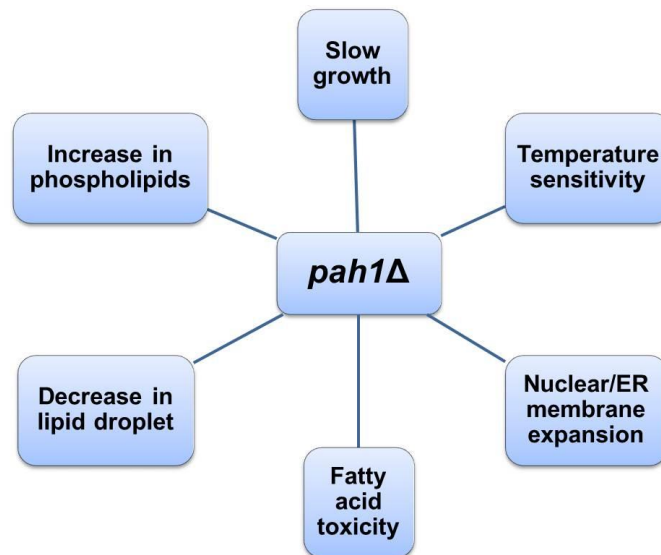


Figure 1.4: Major phenotypes shown by yeast *pah1Δ* strains

Yeast *pah1Δ* strains shows elevated levels of PA, phospholipids, fatty acids, and sterol esters and decreased levels of DAG and TAG. The *pah1Δ* mutant also exhibits slow growth, aberrant expansion of the nuclear membrane, respiratory deficiency, and decreased lipid droplet number, fatty-acid induced lipotoxicity, and growth sensitivity to elevated temperature.

A contributing factor for the increased amounts of phospholipids and fatty acids in the *pah1Δ* mutant is the derepression of lipid synthesis genes containing UASINO in response to elevated PA levels (Siniossoglou, 2009; Carman and Han, 2009). The UASINO element contains the binding site for the Ino2p-Ino4p complex and this binding of Ino2-Ino4 stimulates expression of lipid synthesis genes (Biosynthesis et al., 1995; Robinson and Lopes, 2000; Shetty and Lopes, 2010). The PA-mediated regulation of these genes is controlled by the transcriptional repressor Opi1p, whose function is determined by its localization (Loewen et al., 2004). In its inactive state, Opi1p is tethered to the nuclear/ ER membrane through interactions with Scs2p and PA (Gaspar et al., 2017). A reduction in PA levels destabilizes this interaction, allowing translocation of Opi1p into the nucleus, where it suppresses transcription of UASINO-containing genes by binding to the Ino2p subunit of the Ino2p-Ino4p activator complex (Siniossoglou, 2009; Pascual and Carman, 2013; Fernández-Murray and McMaster, 2016). Moreover, the decreased capacity of *pah1Δ* mutant cells to incorporate fatty acids into TAG may contribute to the alterations in phospholipids, fatty acids, and sterol esters. The yeast DAG kinase (Dgk1p) counterbalances the function of Pah1p PAP (Han et al., 2008; Adeyo et al., 2011). Dgk1 is an integral membrane protein localized at the ER/nuclear membrane. Similar to the *pah1Δ* mutation, overexpression of Dgk1p causes accumulation of PA at the nuclear/ ER membrane and the derepression of UASINO-containing genes, providing evidence that Dgk1p activity antagonizes the function of Pah1p enzyme by regulating cellular levels of PA(Han et al., 2008b).

The aberrant membrane expansion phenotype of the *pah1Δ* mutant has been attributed to the abnormal increase in phospholipid synthesis associated with this mutation. However, recent reports have shown that increased expression of phospholipid biosynthetic genes alone is not sufficient for nuclear/ER membrane expansion(Laura O’Hara, Gil-Soo Han, Sew Peak-Chew, Neil Grimsey, George M. Carman, 2006). Moreover, DGK1 overexpression results in

anomalous nuclear/ER membrane morphology, while the introduction of the *dgk1Δ* mutation in the *pah1Δ* background restores PA levels, the suppression of UASINO-containing genes, and a normal nuclear/ER membrane structure (Han et al., 2008a; Han et al., 2008b). Thus, increased phospholipid synthesis coupled to increased PA levels result in the aberrant nuclear/ER morphology displayed by the *pah1Δ* mutant. Among the phenotypes associated with the *pah1Δ* mutant, the defect in lipid droplet formation can also be complemented by the *dgk1Δ* mutation (Adeyo et al., 2011). In contrast with the *pah1Δ* mutant phenotypes described above, the defect in TAG synthesis, increase in fatty acid content, fatty acid-induced toxicity, and temperature sensitivity could not be suppressed by loss of Dgk1p function (Carman and Han, 2009). These observations seem to indicate that these phenotypes are related to depletion of DAG rather than increase in PA content. Another phenotype exhibited by the *pah1Δ* mutant is the defect in vacuole homeostasis and fusion. While this phenotype is due to the loss of PAP activity of Pah1p, it is not known whether it is based on alterations in PA and/or DAG. Additional phenotypes of *pah1Δ* cells are slow growth, and an impairment of *pah1Δ* cells to grow in non-fermentable carbon sources. The inability to grow on non-fermentable carbon sources is not believed to be due to a respiratory defect, instead a reduction of ATP level observed in *pah1Δ* cells as a consequence of deregulated PL synthesis (which consumes ATP) was proposed as the limiting factor for growth. In addition, *pah1Δ* cells exhibited an increased level of mitochondrial superoxides and a decreased tolerance to oxidative stress resulting in reduced chronological life span (Park et al., 2015; Fernández-Murray and McMaster, 2016). The susceptibility of *pah1Δ* cells to oxidative stress and their inability to grow in non-fermentable carbon sources were partially suppressed by loss of Dgk1.

Phosphatidic acid (PA) is the common precursor for the synthesis of both membrane phospholipids (PL), and TAG (the major component of lipid droplets) (Beller et al., 2010).

The de novo biosynthesis of PA, as well as its consumption for PL and TAG synthesis, takes place in the ER (Wolins et al., 2006; Zhang and Reue, 2017)(). LDs are the organelles responsible for the cellular storage of the neutral lipids (NLs) TAG and sterol esters (SE) (Czabany et al., 2007; Beller et al., 2010). Stored NLs are a source of precursors for membrane synthesis as well as substrates for energy production. LD is organized as a core of NLs wrapped in a PL monolayer (Farese and Walther, 2009; Beller et al., 2010). This PL monolayer allows specific association with many proteins, some of which are specifically present in LDs whereas others are shared with ER (the compartment from which LDs originate). Reflecting the most relevant function of LDs, the vast majority of proteins associated with LDs participate in NL synthesis and degradation. Consistent with a role for the ER in lipid homeostasis, and in particular as a site where the flux of lipid precursors is directed towards membrane synthesis or storage, LDs are not only formed from the ER but most of them remain physically connected with the ER. Interestingly, LDs are tightly associated with the ER at membrane contact sites (MCS). The activation and membrane recruitment of Pah1 takes place in the vicinity of LDs suggesting a channeling mechanism of DAG delivery for TAG synthesis and sorting into LDs. PA is synthesized in the ER where it is activated to CDP-diacylglycerol (CDP-DAG) for subsequent synthesis of membrane lipids(Carman and Han, 2009; Fernández-Murray and McMaster, 2016). The phospholipid PA functions at a critical branching point in lipid metabolism where lipid biosynthetic flux can be directed into membrane PL synthesis concomitant with membrane proliferation, or into TAG synthesis and LD formation. To generate TAG, PA at the ER is dephosphorylated to form DAG by the PA phosphatase Pah1(Carman and Han, 2009). DAG is acylated by the acyltransferases Dga1 and Lro1 to produce TAG for accumulation in LD. DAG can also be phosphorylated back to PA by the ER localized lipid kinase Dgk1.

Yeast lipin, Pah1p, controls the formation of cytosolic lipid droplets (Adeyo et al., 2011). Disruption of *PAH1* resulted in decrease in droplet number, although total neutral lipid levels did not change. This was accompanied by an accumulation of neutral lipids in the endoplasmic reticulum. The requirement of *PAH1* for normal droplet formation can be bypassed by a knockout of *DGK1* (Adeyo et al., 2011). Nem1p, the activator of Pah1p, localizes to a single punctum per cell on the ER that is usually next to a droplet, suggesting that it is a site of droplet assembly. DAG generated by Pah1p is important for droplet biogenesis. Pah1 has its greatest effect on lipid synthesis in the stationary phase of growth, when the synthesis of TAG occurs at the expense of membrane phospholipids (Pascual and Carman, 2013). Cell growth transition from exponential growth phase into stationary phase encompasses major metabolic changes. At the lipid level this transition involves a switch from membrane synthesis to lipid storage as revealed by the increase in cellular TAG and the accumulation of LDs. The localization of Pah1 with LDs and the increase in neutral lipid synthesis take place simultaneously.

1.5 Regulation of yeast PAH1 by phosphorylation and dephosphorylation

In *S. cerevisiae* Pah1p is a relatively abundant enzyme. While Pah1p is found mostly in the cytosol, its substrate PA resides in the nuclear/ER membrane, and therefore translocation of the PAH1 to membrane is vital for in vivo function (Han et al., 2006; Karanasios et al., 2010). This membrane association is regulated by phosphorylation-dephosphorylation and hence governs the sub-cellular localization of PAH1. Phosphorylated Pah1p resides in the cytosol, whereas dephosphorylated form of PAH1 is associated with the membrane (Hyeon-Son Choi 2011). Phosphoproteomic studies have shown that yeast PAH1 is a target for multiple protein kinases including CDC28 (CDK1)- cyclin B, PHO85-Pho80, protein kinases A and C, casein kinases I and II, DBF2, and MAPK. PAH1 is phosphorylated at more than 30 Serine/Threonine sites(Choi et al., 2011; Choi et al., 2012, Hsieh et al., 2016). This indicates

that the regulation of PAH1 by phosphorylation is complex. The physiological relevance of phosphorylation at different sites by multiple protein kinases vary. Some of the phosphorylation sites regulate the subcellular localization, its phosphatidic acid phosphatase activity, or half- life of the protein. Also phosphorylation of PAH1 on some sites influences phosphorylation on other sites by the same or different protein kinases. The first study to identify the phosphorylated residues of PAH1 showed that Pah1p is phosphorylated on seven multiple Serine/Threonine sites *in vivo*. The phosphorylation sites matching the minimal Serine/Threonine-Pro motif are Serine-110, Serine -114, Serine-168, Serine-602, Threonine-723, Serine-744, and Serine-748. All these seven sites are targets for cell cycle-regulated protein kinases like cdk1-cyclin B, Pho85p–Pho80p (Su et al., 2014). Alanine substitution of this Serine/Threonine-Pro motif completely inhibits the Nem1p-Spo7p-dependent mobility shift in SDSPAGE. The phosphorylation- deficient PAH1-7A (Serine-168, Serine-602, Serine-744, Serine-748, and Threonine-723, Serine-110 and Serine -114 mutated to alanine) exhibits a 2-fold increase in the specific activity and increased interaction with phospholipid vesicles when compared with the wild-type PAH1. Cells lacking the Nem1p–Spo7p complex exhibit reduced TAG due to loss of PAP function. The phosphorylation deficient PAH1-7A facilitates the translocation of Pah1p from the cytosol to the membrane and causes an increase in the synthesis of TAG in *nem1Δ* yeast. This indicates that the lack of phosphorylation of the seven sites renders Pah1p bypass the Nem1p–Spo7p dephosphorylation for *in vivo* function. Gene expression studies using Pah1p-7P- mutant showed that dephosphorylation of Pah1p promotes repression of INO1 and OPI3. Thus Phosphorylation of PAH1 on the Ser/Thr-Pro sites by Cdk1 has role in the expression of phospholipid biosynthetic enzymes.

Additional phosphorylation sites that do not fit the Cdk consensus include Serine-773, Serine-774, Serine-800, Serine-805, Serine-810, Serine-814, and Serine-818. Inhibition of

phosphorylation by mutating these serine residues did not significantly change the migration of PAH1, suggesting that the residues contributing to the mobility shift during the cell cycle are among mainly the seven Ser/Thr-Pro sites which fit the Cdk phosphorylation consensus. Though the role of the additional phosphorylation is not known, it does not overlap with the function of the Ser/Thr-Pro-dependent phosphorylation in transcription and PA production.

Protein kinase A phosphorylates Pah1p on Ser10, Ser677, Ser773, Ser774, and Ser788 with specificity similar to that shown by Pho85p–Pho80p and Cdc28p-cyclin B(Su et al., 2012)(Huffman et al., 2002). The protein kinase A mediated phosphorylation of Pah1p inhibits its PAP activity by decreasing catalytic efficiency. The inhibitory effect of protein kinase A on PAP activity is primarily conferred by phosphorylation at Ser10 (Su et al., 2012). Phosphorylation by protein kinase A at Ser10 also inhibits its association with membranes, and TAG synthesis.

Pah1p is also phosphorylated by protein kinase C and casein kinase II. Phosphorylation of Pah1p by protein kinase C and casein kinase II decreases its interaction with model membranes, suggesting an inhibitory effect of phosphorylation on PAP activity *in vivo*. Protein kinase C has the effect of decreasing Pah1 abundance when it is not phosphorylated by Pho85-Pho80. Phosphorylation of Pah1 by protein kinase C had a small stimulatory effect on its 20S proteasomal degradation, reducing the half-life of the protein from 6 min (unphosphorylated) to 5 min (phosphorylated). Casein Kinase II phosphorylates Pah1 on Thr-170, Ser-250, Ser-313, Ser- 705, Ser-814, and Ser-818 residues(Hsieh et al., 2016). The CKII phosphorylation of Pah1 did not have a significant effect on the K_m but had a small (13%) inhibitory effect on the V_{max} of the reaction. Phosphorylation of Pah1 by CKII had no significant effect on its proteasomal degradation by the 20S proteasome. Also, pre-phosphorylation by CKII reduces subsequent phosphorylation by protein kinase A (Hsieh et al., 2016). The S705A mutant, expressed in either *pah1*Δ or *pah1*Δ *nem1*Δ cells, showed a 2-

fold increase in membrane association when compared with the wild type control. Except for S705A, mutations of other residues phosphorylated by the CKII showed little effect on the subcellular localization of Pah1. Pah1p has been reported as a putative target of the Dbf2p-Mob1p kinase complex, a component of the mitotic exit network (MEN) cascade in phospho-site array screening(Mah et al., 2005; Laura O’Hara, Gil-Soo Han, Sew Peak-Chew, Neil Grimsey, George M. Carman, 2006).

A balance between PA and DAG levels mediated by Pah1p PAP activity is important to maintain lipid homeostasis and normal cell physiology. In view of the variety of cellular processes in which PA and DAG play a role, the regulatory mechanisms governing PAP activity are complex affecting transcription, posttranslational modification, subcellular localization, and biochemical properties of Pah1p. Several transcription factors have been shown to interact with the *Lpin1* promoter, including the glucocorticoid receptor (GR), sterol response element binding protein-1 (SREBP-1), and cAMP response element binding protein (CREBP).Recent work by Soto-Cardalda and colleagues has shown that the expression of *PAHI*-encoded PAP activity is affected by intracellular levels of zinc (Soto-Cardalda et al., 2012). Pah1p PAP activity is stimulated by the phospholipids CDP-DAG, PI and CL, which act as mixed competitive activators of PAP activity (Pascual and Carman, 2013).

1.6 Lipins - the metazoan *PAHI* homolog

The founding member of the lipin protein family, lipin-1 was identified in 2001 by positional cloning of the mutant gene underlying lipodystrophy in the fatty liver dystrophy (*fld*) mouse (Péterfy et al., 2001; Reue and Zhang, 2008). The *fld* mouse is named for two key features of the mutant phenotype – the presence of a fatty liver for the first 2 weeks of the postnatal period, and the subsequent development of a peripheral neuropathy characterized by poorly compacted myelin sheaths, abnormal Schwann cells, and myelin breakdown (Péterfy et al., 2001; Harris and Finck, 2011; Csaki et al., 2013). The *fld* mouse also lacks normal adipose

tissue depots throughout the body (Reue and Zhang, 2008). This phenotype is reminiscent of some forms of generalized lipodystrophy in humans.

In mammals, there are three members of the lipin gene family, which encode five lipin protein isoforms (Péterfy et al., 2005; Donkor et al., 2007; Gil-Soo Han and George M. Carman, 2010). Lpin1 mRNA undergoes alternative splicing to generate three isoforms: lipin 1 α , lipin 1 β and lipin-1 γ (Péterfy et al., 2005). Lipin-2 and lipin-3 were identified through sequence similarity to lipin-1. The three mammalian lipin genes differ in their tissue expression patterns, suggesting that they have unique physiological roles (Donkor et al., 2007; Gil-Soo Han and George M. Carman, 2010; Csaki et al., 2013).

Lipin 1 α is localized predominantly in the nucleus, whereas lipin 1 β is primarily present in the cytoplasm (Péterfy et al., 2005). Lipin 1 α and 1 β isoforms are present in most of the tissues that express Lpin1, but the relative levels of the two isoforms varies with tissue type. Lipin-1 γ is present primarily in brain (Harris and Finck, 2011). Lipin 1 α and 1 β isoforms have distinct cellular functions in processes such as preadipocyte differentiation. Lipin 1 α is associated with expression of adipogenic differentiation factors such as PPAR γ and C/EBP α , and lipin 1 β is associated with induction of lipogenic genes such as fatty acid synthase, stearoyl CoA desaturase, and DGAT (Kim et al., 2013).

Lipin proteins in all species share two highly conserved regions, termed the N-terminal lipin (N-LIP) and C-terminal lipin (C-LIP) domains, based on their locations (Siniosoglou, 2009). Lipin proteins in most species also contain at least one nuclear localization sequence unlike the yeast homolog. The C-LIP domain contains the DIDGT motif, which is present in all species and constitutes the catalytic site for phosphatidate phosphatase (PAP) enzyme activity (24), and mammalian lipin proteins contain an additional LXXIL motif, required for transcriptional coactivator activity (Reue and Zhang, 2008). Also a conserved serine residue at 734th position is required for the phosphatidate phosphatase activity of Lipin-1 and Lipin-2

(Donkor et al., 2009). But this residue is not important for the transcriptional coactivator functions. Although all three mammalian lipin proteins have the DIDGT motif and demonstrable PAP activity, lipin-1 exhibits higher PAP specific activity than lipin-2 and lipin-3 as assessed by an in vitro assay. The DIDGT motif is absolutely required for PAP enzyme activity, but mutation of this motif does not affect transcriptional coactivator function. Lipin 1 can form homo-dimers, as well as heterodimers with lipin 2 or lipin 3 (Liu et al., 2010; Pascual and Carman, 2013). Despite the formation of oligomers, it appears that the individual lipin molecules present within oligomers act independently as phosphatases, rather than forming an active site through oligomerization (Liu et al., 2010). Little is known about the physiological role of lipin2 and lipin3 compared to lipin1.

C. elegans has only one putative lipin homolog and is needed for lipid storage and development. Down regulation of *LPIN-1* in *C.elegans* resulted in disorganization of the peripheral ER with more membrane sheets compared to control. Down regulation of *LPIN-1* promoted bi-nucleation resulting in abnormal nuclear morphology (Gorjánác and Mattaj, 2009; Golden et al., 2009). In *C.elegans* *Lpin-1* had no effect on timely entry into mitosis or on the early steps of NEBD, but was required for disassembly of the nuclear lamina during late NEBD (Bahmanyar, 2015). This *Lpin-1* requirement appears to be separable from the effect of *Lpin-1* on the peripheral ER. In *Drosophila melanogaster* the single lipin orthologue (*dLipin*) is essential for normal adipose tissue (fat body) development and TAG storage (Ugrankar et al., 2011). *dLipin* mutants are characterized by reductions in larval fat body mass, whole-animal TAG content, and lipid droplet size. In *Lipin* mutants cells of *Drosophila*, the underdeveloped fat body are characterized by increased size and ultrastructural defects affecting cell nuclei, mitochondria, and autophagosomes (Ugrankar et al., 2011).

Arabidopsis have two lipin homologs, *AtPAH1* and *AtPAH2* that encode the phosphatidate phosphatase activity (Nakamura et al., 2009; Mietkiewska et al., 2011). Double mutant

pah1pah2 in *Arabidopsis thaliana* had decreased phosphatidic acid hydrolysis. Decreased phosphatidic acid hydrolysis, affects the eukaryotic pathway of galactolipid synthesis and the membrane lipid remodeling mediated by these two enzymes is an essential adaptation mechanism to cope with phosphate starvation in *Arabidopsis* (Nakamura et al., 2009). In *Arabidopsis thaliana* disruption of PAH activity elevates phosphatidic acid (PA) levels and stimulates PC biosynthesis and biogenesis of the endoplasmic reticulum (ER). PAH activity controls the abundance of PA, which in turn can modulate CCT (Phosphocholinecytidyltransferase) activity to govern the rate of PC biosynthesis in *Arabidopsis* (Craddock et al., 2015). It has been recently shown that in mammals Lipin-1 regulation of phospholipid synthesis maintains endoplasmic reticulum homeostasis and is critical for triple-negative breast cancer cell survival (He et al., 2017).

1.6.1 Lipin transcriptional co-regulator activity

In addition to its role as a PAP enzyme in the glycerol 3-phosphate pathway, lipin proteins are implicated in the regulation of gene expression through interactions with nuclear receptors and other DNA-bound transcription factors. The first demonstration of this was the requirement for lipin 1 in mouse hepatocytes for activation of genes regulated by peroxisome proliferator activated receptor α (PPAR α) and its coactivator protein, PPAR γ coactivator-1 α (PCG-1 α) (Zhang et al., 2012; Kim et al., 2013). It is clear that lipin 1 also associates with additional transcription factors, including PPAR γ , myocyte enhancer factor 2 (MEF2), and the nuclear factor of activated T-cells c4 (NFATc4) to either co-activate or co-repress gene expression (Koh et al., 2008; Kim et al., 2010). Lipin 1 mediated co-repression of MEF2 possibly modulate inflammatory cytokine signaling in adipocytes (Chen et al., 2015). Lipin 2 also has the ability to co-activate PPAR α /PGC-1 α . The ability of lipin proteins to regulate both triacylglycerol synthesis through PAP activity, and fatty acid oxidation through

transcriptional co-activation, suggests a unique mechanism for coordination of fat synthesis and turnover.

1.6.2 Lipin regulation by phosphorylation

As mentioned earlier the mammalian counterparts of Nem1p-spo7p proteins; the CTDNEP1 and NEP1-R1 complex dephosphorylates lipin 1 and promotes its association with the ER/nuclear envelope membrane, and stimulates its PAP activity in metazoan species ranging from *C. elegans* to mammals. A combination of three-dimensional structure analysis and *in vitro* steady-state kinetic analysis of CTDNEP1 showed that the phosphatase prefers to act at Ser106, one of the target sites for mTOR complex 1 phosphorylation. mTOR mediates insulin-induced lipin 1 phosphorylation at multiple sites leading to its cytosolic localization and reduced enzyme activity (Huffman et al., 2002; Laplante and Sabatini, 2009; Kim and Chen, 2004). Inhibition of mTOR favors lipin 1 membrane association and increases its PAP activity. The phosphorylation sites in yeast and mammalian lipin proteins are not directly comparable, such that the sites, the kinases, and the physiological consequences require specific investigation in mammalian systems. Lipin 2 is also a highly phosphorylated protein, but unlike lipin 1, phosphorylation is not responsive to insulin or mTOR. Little is known about the phosphorylation of lipin 3 and the effect of its subcellular translocation. There is a complex relationship between mTOR, lipin 1 and PA, and the interplay between mTOR and lipin 1 enzyme function is more complex than simply kinase and phosphorylation substrate (Laplante and Sabatini, 2009; Peterson et al., 2011; Soliman et al., 2010).

The movement of mammalian lipin within the cell is closely associated with its phosphorylation status as in case of yeast PAH1. The lipins are highly phosphorylated with over 25 sites identified in the founding member, lipin 1. Both phosphorylated and dephosphorylated lipin 1 showed similar activity when measured as a function of PA concentration. But subsequent studies showed that reduced PAP activity during mitosis has

been linked to lipin-1 and -2 phosphorylation, confirming phosphorylation as a modulator of PAP activity. Phosphorylation of lipin 1 inhibits physiological activity by decreasing membrane association. Mutation of 21 of Ser/Thr residues to Ala promoted localization to the ER/nucleus suggesting an increase in membrane association. Inhibition of mTOR causes a dramatic change in the intracellular localization of lipin 1, suggesting that mTOR activity is sufficient to regulate lipin 1 association with membranes. Not all of the phosphorylated sites identified play a significant role in controlling lipin 1 association with membranes. The majority of the effects of phosphorylation on lipin 1 PAP activity require mTOR kinase activity, suggesting that other kinase(s) have a less significant contribution on PAP activity. Lipin 1 has a highly basic stretch (PBD) of amino acid residues with 9 lysine and arginine residues in a row at amino acid residues 153–161. This motif is required for interaction with PA but had no effect on lipin 1 enzymatic activity. Mutation of the PBD sites completely eliminates the effect of phosphorylation on lipin 1 PAP activity, suggesting that the function of phosphorylation is to prevent the PBD from interacting with PA (He et al., 2017). Phosphorylation regulates the ability of the polybasic domain of lipin 1 to recognize dianionic PA. When measured by biochemical fractionation of cells, hyper-phosphorylated lipin 1 is found in the cytosol of 3T3-L1 adipocytes, whereas hypo-phosphorylated lipin 1 is localized to microsomal membranes. Overexpression of wild type lipin 1 shows cytosolic localization by immune fluorescent microscopy, whereas the 21xA mutant (mutation in all 21 phosphorylation sites) localizes to the ER/nucleus. Microscopic analysis of endogenous lipin 1 in 3T3-L1 adipocytes shows lipin 1 spread across the cytosol and localized to discrete punctuate spots, whereas treatment with torin1(mTOR inhibitor) causes a dramatic relocation to the ER/nucleus. These changes in localization were found to play a crucial role in the regulation of the transcriptional activity of SREB1. In addition, lipin 1 phosphorylation is thought to play a critical role in its enzymatic function, although evidence

for this has been lacking until now. mTOR activity is required for phosphorylation of lipin 1 to negatively regulate lipin 1 PAP activity. This clearly depicts the importance of phosphorylation on the regulation of lipin function by affecting localization, catalytic activity and stability.

1.6.3 Lipin gene mutations and disease

As discussed earlier a spontaneous mutation in the mouse LIPIN1 gene manifested a severe disease phenotype, indicating the physiological significance and non-redundancy of lipin 1 protein function. Individuals that carry bi-allelic pathogenic mutations in LIPIN1 shows severe, potentially life-threatening rhabdomyolysis in childhood (Müller-felber et al., 2010). In contrast, individuals with bi-allelic pathogenic LPIN2 mutations develop an auto inflammatory syndrome called Majeed syndrome characterized by recurrent fever, bone lesions, anemia and inflammatory skin lesions (Al-Mosawi et al., 2007; Ferguson, 2005). Majeed syndrome is caused by S734L mutation in the *LPIN2* (Donkor et al., 2009). It is not known whether LPIN3 mutations cause any disease. The disparate symptoms associated with lipin- 1 or lipin-2 dysfunction/deficiency indicate that these lipin proteins each have unique roles *in vivo*.

1.7 Phosphatidic acid phosphohydrolase (PAH) in the phylogeny

The eukaryotic lineages can be divided into five supergroups which includes Opisthokonta, Archaeplastida (Plantae), Amoebozoa, Excavata and SAR (stramenopiles, alveolates, and Rhizaria) (Parfrey et al., 2006; Koonin, 2010; Adl and Needs Authors, 2013). Opisthokonta supergroup contains animals (Metazoa) and fungi, as well as several lines of heterotrophic protists. Amoebozoa includes mostly amoeboid, heterotrophic protists (e.g., *Amoeba*) or the mycetozoon slime molds capable of aggregative multicellularity (e.g., *Dictyostelium*). Excavata supergroup is composed of diverse and mainly heterotrophic protists, many of which are anaerobes and/or parasites and possess hydrogenosomes or mitosomes instead of

mitochondria (e.g., *Giardia*, *Trypanosoma*). Plantae supergroup is composed of the three main lineages of primary photosynthetic taxa: organisms that harbor plastids directly derived from the cyanobacterial endosymbiosis. SAR supergroup an acronym of its constituents: stramenopiles, alveolates, and Rhizaria is the most recently recognized supergroup. Stramenopiles (also known as heterokonts) are a very large diversity of protists, including, ecologically important algal groups such as diatoms or large multicellular seaweeds, as well as heterotrophic, often parasitic species. Alveolates include the dinoflagellate algae, apicomplexan (parasites such as the malaria agent *Plasmodium*) or ciliate protozoans (e.g., *Tetrahymena*). Rhizaria is based only on molecular characters and includes naked and testate amoeboid, heterotrophic protists such as foraminiferans and radiolarians.

The mostly used model for studying PAH function has been animal or fungus which belongs to the Opisthokont clade (Péterfy et al., 2001; Donkor et al., 2007; Soto-Cardalda et al., 2012). PAH proteins are conserved among members of Opisthokonts with counterpart enzymes in humans, mice, flies, worms, and plants. Few studies on PAH functions are known in plants that belongs to Archeplastidia (Nakamura et al., 2009; Mietkiewska et al., 2011). A comparison of cell biological features between different eukaryotic lineages would be a better strategy for understanding the evolutionary conservation than between organisms within the same lineage. The remaining three clades Excavata, Amoebozoa, and SAR consist largely of unicellular organisms (both parasitic and free-living) are distantly related to Opisthokonta and are very poorly represented in PAH studies.

By comparing PAH functions between organisms belonging to different lineages would provide a more accurate understanding of conserved features, and the variation that exists within them, and also of features that are limited to specific lineages. A broader, taxonomy-informed sampling would therefore provide a more accurate picture of the relative contributions made by inheritance versus innovation in the emergence of modern cells.

As discussed above studies of phosphatidic acid phosphatase have focused on Opisthokonta (fungi, nematode, fly and animals) and Plantae clades (Santos-Rosa et al., 2005; Han et al., 2006; Donkor et al., 2007; Nakamura et al., 2009, Golden et al., 2009; Gorjánác and Mattaj, 2009; Ugrankar et al., 2011; Schmitt et al., 2015). In contrast, these enzymes and the regulatory cascades in which they participate have not been reported in organisms including Amoebozoa, Alveolata, and Excavata. *Tetrahymena thermophila* belongs to the Alveolata, a major evolutionary branch of eukaryotic protists in which cells display functional complexity comparable to the cells of humans and other metazoans. *T. thermophila* is a free-swimming unicellular eukaryote belonging to protist, with size of $\sim 30 \times 50 \mu\text{m}$ and larger than many mammalian cells (Mobberley et al., 1999). *Tetrahymena* (and ciliates in general) are unique for their nuclear dimorphism. *Tetrahymena* have two nuclei each, the micronucleus (MIC) and the macronucleus (MAC) (Mobberley et al., 1999; Edurado Orias, 2011). The transcriptionally active macronucleus, is the primary source of gene transcripts in the cell; its proteins and non-protein coding RNAs which maintain the functions required for the life of the organism and thus the MAC genome directly determines the phenotype of cell. The silent micronucleus is transcriptionally silent in vegetative cells, is the store of genetic information for the sexual progeny. The micronucleus is diploid and has five different chromosomes, while the macronucleus is roughly 45-ploid with around 180-200 different chromosomes. The two genomes are genetically and developmentally related but exhibit dramatic differences in structure and function (Mobberley et al., 1999; Edurado Orias, 2011).

The life cycle of *T. thermophila* has two major components: asexual reproduction by binary fission and conjugation, the non-reproductive sexual stage (Figure 1.5) (Turkewitz et al., 2002; Edurado Orias, 2011). During asexual reproduction, the MIC genome divides mitotically, while the MAC divides amitotically. Under starved conditions two different strains of *Tetrahymena* undergo conjugation, during which the parental MIC in each

conjugant undergoes meiosis, haploid gamete nuclei are formed and reciprocal fertilization gives rise to a diploid zygotic nucleus. Progeny MICs and MACs differentiate from mitotic copies of the zygote nucleus. The parental MAC genome contributes no DNA to the sexual progeny and is destroyed through autophagy-mediated programmed nuclear death (Eduardo Orias, 2011).

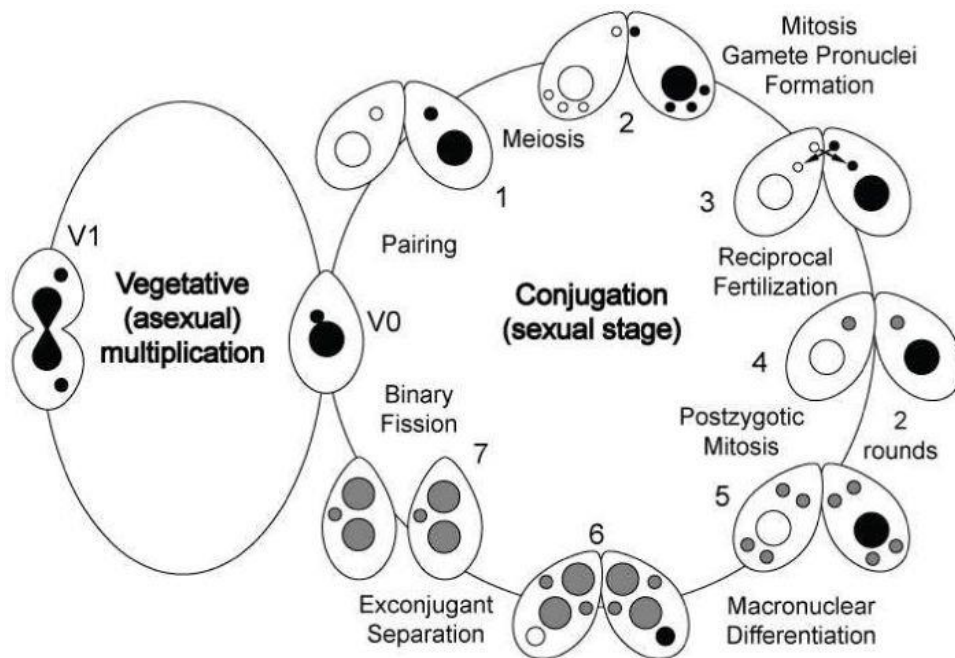


Figure 1.5: The *Tetrahymena* life cycle

Left: vegetative (asexual) reproduction phase. V0: vegetative cell. V1: cell undergoing binary fission. MIC and MAC divide mitotically and amitotically, respectively. Right: conjugation, the sexual (non-reproductive) stage of the life cycle. The following events occur in synchrony in each conjugant. 1. Starved cells of different mating type meet and form pairs. 2. Meiosis generates four haploid products, three of which are resorbed by programmed nuclear death (PND). 3. The functional meiotic product undergoes mitosis, generating the haploid migratory (anterior) and stationary (posterior) gamete pronuclei. Migratory pronuclei are reciprocally exchanged. 4. Incoming migratory and resident stationary pronuclei fuse, generating the diploid fertilization nucleus. 5. The fertilization nucleus undergoes two rounds of mitosis, generating four diploid anlagen, which will differentiate into new polyploid MACs (anterior two) and new diploid MICs (posterior two). 6. New MACs and MICs take up central position and characteristic arrangement. Parental MAC migrates posteriorly and is resorbed by PND. 7. Exconjugant cells separate. One new MIC is resorbed by PND. Not shown: at the first post-conjugation cell division (directly following stage 7), a new MAC and a mitotic daughter of the surviving new MIC are distributed to each daughter cell, thus restoring the vegetative -- one MIC, one MAC -- nuclear organization (stage V0). (Taken from Eduardo Orias *et.al. Res Microbiol. 2011.*

Three distinct modes of genome distribution at nuclear division have been documented in *Tetrahymena*: MIC mitosis, MIC meiosis and MAC amitosis. Nuclear divisions are classically defined as being closed or open based on the retention or breakdown of the nuclear envelope during nuclear division(Boettcher and Barral, 2012)(Ebrahimi and Cooper, 2012). By this criterion, all nuclear divisions in *Tetrahymena* are closed. Also in *Tetrahymena*, during conjugation the new macronucleus develops from micronucleus which involves 10 to 15 fold of nuclear membrane expansion.

Tetrahymena Genome contains two homologs of phosphatidic acid phosphatase (*PAH1/LIPIN*) and we have designated them as *TtPAH1* (TTHERM_00189270) and *TtPAH2* (TTHERM_00215970) in this study. With this background, the work is presented in four different chapters as mentioned below:

- 1) Elucidation of the role of *Tetrahymena PAH1* in membrane biogenesis and lipid homeostasis.
- 2) Investigation of the role of *Tetrahymena PAH1* in mediating cell cycle regulation of nuclear expansion.
- 3) Analysis of conservation of *PAH* functions across eukaryotic clades.
- 4) Functional characterisation of *Tetrahymena PAH2*.

In this study the role of phosphatidic acid phosphatase (*PAH1*) in regulating lipid homeostasis, membrane biogenesis coupled with organelle morphology(ER/nuclear) in *Tetrahymena thermophila* is investigated. Also the cellular functions of lipin homologs in Excavata, Amoebozoa and Plantae are investigated to understand the evolutionary conservation of this cascade. Overall, evidence for the evolutionary conservation of this Mg²⁺ dependent phosphatidic acid phosphatase across phylogeny is provided.

CHAPTER 2

Role of Tetrahymena PAH1 in membrane biogenesis and lipid homeostasis.

2.1 INTRODUCTION

Regulation of lipid homeostasis and membrane biogenesis is important for normal growth and development of all eukaryotes. The magnesium dependent form of the enzyme phosphatidic acid phosphatase (PAP; EC 3.1.3.4) is a key player in eukaryotic lipid homeostasis with both structural and regulatory roles (Finck et al., 2006; Donkor et al., 2007; Carman and Henry, 2013; Pascual and Carman, 2013). Yeast contains a single PAP protein called Pah1 (Han et al., 2006), while mammals possess 3 homologs lipin1, 2, and 3 (Péterfy et al., 2001) which are reviewed in detail in chapter 1. This phosphatidate phosphatase (PAH1 in yeast and lipin in mammals) converts phosphatidic acid (PA) to diacylglycerol (DAG), which then serves as a substrate for both phospholipid and triacylglycerol (TAG) biosynthesis (Carman and Henry, 2013).

In *Saccharomyces pombe*, and in *Saccharomyces cerevisiae*, loss of Ned1/Pah1p causes dramatic abnormalities in the structure of the ER and the nuclear envelope, as a result of increased membrane proliferation (Tange, 2002). Deletion of *PAH1* showed disruption in ER structure and defects in lipid droplet number and morphology, with neutral lipid accumulating around the ER in stationary phase. Loss of the single lipin homolog in *C. elegans* causes defect in the breakdown ability of the nuclear envelope, decreased formation of LD, and disorganization of the ER. In Arabidopsis the loss of both lipin homologs PAH1 and PAH2 increased the level of PA and most other phospholipids. Loss-of-function mutations in lipin 1 produce the dramatic metabolic abnormalities displaying growth retardation, hypertriglyceridemia and the development of severe hepatic steatosis. Human mutations in the gene encoding lipin 2 (LPIN2) lead to an autoinflammatory bone disease known as Majeed syndrome (Ferguson, 2005; Al-Mosawi et al., 2007). Expression of peroxisome proliferator-activated receptor γ (PPAR γ), a key player in adipogenesis is

influenced by lipin by regulating levels of PA (Finck et al., 2006; Harris and Finck, 2011; Kim et al., 2013).

The existence of a single lipin ortholog in genetically tractable organisms above described such as *S. cerevisiae*, *C.elegans*, *Drosophila melanogaster* has simplified the functional analysis of the role of lipin in these species. But plants (*Arabidopsis thaliana* and *Brassica napus*) contain two lipin paralogs which are result of post-speciation duplication events.

Tetrahymena thermophile, a single cell ciliate represents lower eukaryote that contains all subcellular organelles typically found in eukaryotic cells, such as mitochondria, lysosomes, endoplasmic reticulum and peroxisomes. *Tetrahymena* cells grow well in lipid-free media and can be therefore considered a closed system with respect to the budget of its membrane components. *Tetrahymena* has already been chosen as an appropriate model for the use in structure function of biological membranes, membrane fluidity and membrane homeostasis studies particularly membrane biogenesis. *Tetrahymena* shows no requirements for fatty acids or sterols or phospholipids under normal conditions as they can synthesize all complex lipid from small molecules needed for growth. *Tetrahymena* has membrane complexities comparable to cells of higher organisms (Frances and Bryn, 1975). Hence *Tetrahymena* serve as a good model system to study lipid homeostasis and membrane biogenesis in lower eukaryotes which are evolutionarily distant from organisms where *PAH* functions has been characterized (Eduardo Orias, 2011; Briguglio and Turkewitz, 2014). *Tetrahymena thermophila* possesses two *PAH* homologs, *TtPAH1* and *TtPAH2*, which are disparate in their size (Pillai et al., 2017a). *TtPah1* has a length of 872 amino acids and is comparable to the size of previously characterized lipins, whereas *TtPah2* is a low molecular protein. This chapter focusses on the role of *Tetrahymena PAH1* in regulating functions which are known to be performed by this family of proteins in other model organisms. For this purpose, a knockout strain of *TtPAH1* was generated by deleting all copies of *TtPAH1* from the

macronucleus. Role of *TtPAH1* in regulating cell viability, lipid droplet number, endoplasmic reticulum and nuclear morphology are discussed in this chapter.

2.2 MATERIALS

2.2 .1 Plasmids

Tetrahymena specific expression vector pIGF was a gift from Doug Chalker, Washington University. *Tetrahymena* expression vector pVGF was from Meng-Chao Yao, University of Washington. The *NUP3-GFP* in NCVB vector was obtained from Aaron Turkewitz, University of Chicago. pCRII vector was from Invitrogen.

2.2 .2 *Tetrahymena thermophila* strains and culture media

Wild type *Tetrahymena thermophila* strains CU428.1 and B2086 were procured from *Tetrahymena* Stock Centre, Cornell University, USA. Proteose peptone and Yeast extracts were purchased from BD Biosciences, USA, and Dextrose and Paramomycin Streptomycin pencillin (PSA/fungizone) from MP Biomedicals

2.2 .3 Other reagents:

ER Tracker Red, DiOC6(3) and DAPI were from Invitrogen. Oil Red O dye was from Hi-Media. Phosphatidic acid was obtained from MP Biomedicals. Other chemicals and media components were from Sigma-Aldrich unless mentioned otherwise.

2.3 METHODS

2.3.1 Competent cells preparation

For plasmid transformation *E. coli* strain DH5 α was used and the competent cells of these strains were prepared by following Methodology. DH5 α was streaked from freezer stock on to LB-agar plate and was grown overnight at 37 $^{\circ}$ C. Single colony was picked and inoculated into 25 ml of LB media in a 250 ml flask. This was grown for 6-8 hours at 37 $^{\circ}$ C with 220 rpm. This culture was used to inoculate 100 ml of LB media in a 500 ml flask to get an OD₆₀₀ of 0.025. Incubate the flask at 18 $^{\circ}$ C. OD of the culture was constantly monitored after 24

hours so as to collect cells at $OD_{600} = 0.55$. The culture flask was transferred onto ice for 10 minutes with occasional mixing. The cells were collected by centrifuging at 3500 rpm for 10 minutes at 4°C . The cell pellet was resuspended in 16 ml ice cold transformation buffer (55 mM MnCl_2 , 15 mM CaCl_2 , 250 mM KCl , 10 mM PIPES (pH 6.7)). Cells were again collected by spinning at 3500 rpm for 10 minutes and removing all residual buffer. 4 ml of ice cold transformation buffer and 300 μl of DMSO was added and cells were resuspended slowly. The bacterial suspension was mixed by swirling and allowed to incubate on ice for 15 minutes. Dispense aliquots into pre-chilled centrifuge tubes and snap freeze in liquid nitrogen to store in -80°C .

2.3.2 *Tetrahymena* culture conditions

Wild-type CU428.1 and B2086 strains of *T. thermophila* were grown at 30°C in SPP medium (2% proteose peptone, 0.2% dextrose, 0.1% yeast extract, 0.003% ferric EDTA) with 250 $\mu\text{g/ml}$ penicillin and streptomycin and 1.25 $\mu\text{g/ml}$ Fungizone (amphotericin B). Cultures were generally not allowed to exceed a concentration of 5×10^5 cells/ml. Cells were transferred to fresh medium at maximum of 1: 100 dilution. For short term storage, stocks were maintained at room temperature in test tubes in low aeration in 2% SPP for 3 to 6 months. For long term storage, wild-type or knockout cells were starved and frozen in liquid nitrogen in 4% DMSO (Bruns et al., 2000).

For conjugation, cells of different mating types (CU428.1 and B2086 strains) were grown to log phase ($3-4 \times 10^5/\text{ml}$), washed and starved in DMC (0.17 mM sodium citrate, 0.1 mM NaH_2PO_4 , 0.1 mM Na_2HPO_4 , 0.65 mM CaCl_2 , and 0.1 mM MgCl_2) for 16-24 hours at 30°C (Orias et al., 2000). Equal numbers of starved cells of two different mating types were mixed to initiate conjugation. Conjugation efficiency was checked at the fourth hour post mixing after fixation with formalin by counting number of paired *tetrahymena* cells versus number of

unpaired cells after fixing with PFA. Conjugation cultures showing more than 80% of paired cells (conjugation efficiency) are used for transformation.

2.3.3 *Tetrahymena* Genomic DNA Extraction

25 ml stationary cultures (1×10^6 cells/ml) were used for genomic DNA isolation. Cells were resuspended in 3.5 ml Urea buffer (42% urea, 0.35 M NaCl, 0.01M Tris pH 7.4, 0.01M EDTA, 1% SDS) and shaken gently for 5 minutes until the cells are homogenized/lysed. The lysate was extracted twice with equal volume of phenol: chloroform: isoamylalcohol (25:24:1). Then it was extracted once with chloroform isoamyl alcohol. 1ml of 5M NaCl was added to approximately 3ml of lysate to reduce carbohydrate content. DNA was precipitated with an equal volume of isopropyl alcohol. The precipitated DNA was spooled onto a glass capillary tube, washed with 70% ethanol and dried. DNA was resuspended in 600 μ l TE containing 6 μ l RNase A (10mg/ml). This was kept in a heating block at 55 $^{\circ}$ C overnight and used as for PCR reactions.

2.3.4 Cloning

To generate the *TtPAH1-GFP* construct, full-length *TtPAH1* was amplified from genomic DNA using specific primers (Table 2.1). Table 2.2 mentions the PCR reactions and conditions used for amplification of the gene. The amplified product was cloned into an entry vector using pENTR/D-TOPO kit (Invitrogen). This was further cloned into the destination vector pIGF (an rDNA-based expression vector from Meng-Chao Yao, University of Washington, USA) using LR clonase (Invitrogen). The construct was screened by mobility shift in agarose gel, confirmed by PCR amplification and further confirmed by sequencing.

For expressing *TtPAH1* as TAP-tagged protein, full-length *TtPAH1* was PCR amplified using specific primers with Xho1 restriction site in forward primer and Apa1 restriction site in the reverse primer (Table 2.1). Table 2.2 mentions the PCR reactions and conditions used for amplification of the gene. The amplified product was cloned into *Tetrahymena* specific

vector pVGF (an rDNA-based expression vector) using XhoI and ApaI restriction sites. Positive clones were identified by screening by digestion with Xho I and Apa I and constructs with right-sized releases were selected. Positive constructs were further confirmed by sequencing and used for transformation and expression of the protein.

5'UTR and 3'UTR of *TtPAH1* were PCR amplified and cloned into the pCRII vector (Invitrogen – Life technologies, Carlsbad, U.S.A.). To amplify 5'UTR, SacI and EcoRI restriction sites were incorporated in forward and reverse primers respectively (Table 2.1). For amplification of 3'UTR, EcoRI and XhoI restriction sites were included in the forward and reverse primer respectively (Table 2.1). Finally, the *NEO3* cassette was introduced between 5'UTR and 3'UTR using EcoRI restriction sites.

Table 2.1: Oligonucleotides used chapter 2

No.	Oligo Name	Sequence (5' to 3')
1	TtPAH1-GFP FP	CACCATGCATCACCATCACCATCACACTACTAGCAGT ATGAGTGTTTTAA
2	TtPAH1-GFP RP	TCATTCGCTTAATAGTTAGTTAATATCTT
3	TtPAH1-TAP FP	<u>GCCTCGAGACT</u> AGCAGTATGAGTGTTTTAA
4	TtPAH1-TAP RP	<u>GCGGGCCCTCATT</u> CGCTTAATAGTTAGTTAATATCTT
5	5'UTR FP	<u>GAGCTCGTGA</u> ATAGTAGTAATCTTAA
6	5'UTR RP	<u>GAATTCCTTAAT</u> CAGAAATTATGATAATATATCT
7	3'UTR FP	<u>GAATTCCTTCCT</u> CCCATCAAGCAG
8	3'UTR RP	<u>CTCGAGTTCTAT</u> TTATATTTTTTGTTAA
9	TtPAH1 RT FP	GCTATTGGGCAATCGGAGTA
10	TtPAH1 RT RP	TCCAAATCCTGCATAATAGACG
11	Alpha tubulin RT FP	CCTCCCCCTAAGTCTCAACC
12	Alpha tubulin RT RP	CGAAGGCAGAGTTGGTGATT

Table 2.2: PCR reaction components and conditions for amplification of *TtPAH1* using Phusion Polymerase

Reaction components	Volume (µl)	Temperature	Time	No. of cycles
Template (100 ng/µl)	1	98°C	1 minute	1
5X Phusion buffer	10	98°C	5 seconds	35
10mM dNTP	1	58 °C	30 seconds	
Forward primer	1	72°C	1 minute 30 seconds	
Reverse primer	1	72°C	10 minutes	1
Magnesium chloride	1			
Phusion polymerase	0.5			
Water	34.5			
Total	50			

2.3.5 Transformation of *Tetrahymena* cells by electroporation method

TtPAH1-TAP and *TtPAH1-GFP* were transformed into wild-type *Tetrahymena* cells through electroporation using 20 to 25 µg of the plasmid DNA (Gaertig et al., 1994). Conjugating cultures of *Tetrahymena* cells (3×10^5 cells/ml) were washed with 10 mM HEPES buffer and concentrated to a final volume of around 500 µl in the same buffer. In an electroporation cuvette with 0.2-mm gap (Thermo scientific), 125 µl of concentrated cells are mixed with 125 µl of plasmid DNA. Electro-pulsing was done exactly at the tenth hour post-mixing of the two different wild type strains. Electro-transformation was carried out using Gene Pulser (Biorad) electroporation unit at 250 V for 5 milli seconds under time constant protocol. Post

one minute of pulsing electro-pulsed cells were diluted in SPP medium and 125 µl of these cells were later aliquoted in 96 well plates and incubated at 30⁰ C. The selection antibiotic paromomycin sulphate was added at a concentration of 100µg/ml after 14 hours of transformation. Transformants were selected within 3 to 5 days post drugging, which grow efficiently in the presence of Paramomycin sulfate.

Screen for wells containing drug-resistant cells 3–4 days after plating which grow vigorously and swim rapidly while drug sensitive cells are swollen and grow and divide slowly.

2.3.6 Biolistic method for knockout generation

The knockout cassette was released from the knockout construct by SacI and XhoI digestion and was further ethanol precipitated. 20 µg of the knockout construct was used. The purified construct was used to coat 0.6 micron gold microcarrier beads, which were introduced to the macronuclei of starved, vegetative CU428 and B2086 *Tetrahymena* by biolistic bombardment as described previously (Gaertig et al., 1994) (Cassidy-Hanley, 2003). Biolistic transformation was carried out using PDS1000/He Biolistic particle delivery system (BioRad) according to manufacturer's instructions. Following bombardment, cells were recovered in beakers of SPP media for approximately 12 hours. Next, paromomycin sulfate was added to a concentration of 100µg/ml and cadmium chloride was added to a concentration of 2.0 µg/ml. These cells were transferred to 96-well microtiter plates, using a multichannel pipette to deliver 150 µl per well and incubated at 30°C.

2.3.7 Phenotypic Assortment

After 2-3 days, the resistant lines were observed. This initial low-level resistance indicates that the Neomycin cassette allele has replaced at least one of the endogenous *TtPAH1* genes in the polyploid macronuclei. In *Tetrahymena* macronucleus is polyploidy and contains 45 or more copies of each gene. In order to drive this initial Neomycin allele to replace all of the estimated 45 endogenous copies of *TtPAH1* in the macronuclei, the Cadmium concentration

was lowered to 0.5 µg/ml and the paromomycin concentration was increased gradually as cells were transferred to fresh media every 1-2 days. The amitotic nature of macronuclear division in *Tetrahymena* leads to an imperfect segregation of the macronuclear genome during vegetative growth. As a consequence, alleles are unequally partitioned to daughter cells following division. Gradual increase of the paromomycin sulphate concentration results in survival of only those cells which receive more copies of NEO3 cassette. This will bias the culture towards replacing all the endogenous copies of *TtPAH1* with *NEO3* cassette. The result is a phenomenon termed phenotypic assortment (Sonneborn, 1974). The knock out cells showed resistance to paromomycin as high as 20 mg/ml. Single-cell isolates were prepared from these resistant lines and expanded to 8 ml standing tube cultures.

2.3.8 RNA Isolation, cDNA synthesis and semiquantitative PCR

Total RNA was isolated from 20 ml cultures (8×10^5) of both $\Delta Ttpah1$ cell lines and respective wild type cells using Rneasy Mini Kit (Qiagen) according to manufacturer's instruction. cDNA synthesis was done with QuantiTect Rev. Transcription Kit (Qiagen) using random hexamers according to manufacturer's instruction. PCR reactions were performed with 100 ng cDNA using *TtPAH1* specific primers and with control alpha tubulin (ATU1) primers for 34 cycles. Table 2.3 mentions the PCR reactions and conditions used for amplification of the product. Identical PCR reactions were performed without adding reverse transcriptase during cDNA synthesis.

Table 2.3: PCR reaction components and conditions for amplification of alpha tubulin and *TtPAH1* using Taq polymerase for semiquantitative PCR

Reaction components	Volume (μl)	Temperature	Time	No. of cycles
Template (100 ng/μl)	1	94°C	4 minute	1
10X Taq buffer	10	94°C	30 seconds	34
10mM dNTP	1	56°C	30 seconds	
Forward primer (ATU RT)	1	72°C	50 seconds	
Reverse primer (ATU RT)	1	72°C	5 minutes	1
Forward primer (TtPAH1 RT)	1			
Reverse primer (TtPAH1 RT)	1			
Magnesium chloride	1			
Phusion polymerase	0.5			
Water	34.5			
Total	30			

2.3.9 Growth assay

Mid-log-phase cultures of wild-type and $\Delta Ttpah1$ *Tetrahymena* cells were used to inoculate 20 ml of fresh SPP medium at an initial cell density of 0.4×10^5 . When cell number reached 1×10^5 /ml, cells were counted at every 2 hour interval using a hemocytometer after fixation with formalin. The averaged cell density was plotted against time.

2.3.10 Isolation of nuclei

The *NUP3-GFP* in NCVB vector was linearized and introduced biolistically into vegetative *Tetrahymena* by particle bombardment, and the transformants were selected using 60μg/ml

blasticidin in the presence of 1 µg/ml cadmium chloride (Rahaman et al., 2008). The wild type and $\Delta Ttpah1$ cells expressing *NUP3-GFP* was used for nuclear isolation. 50 ml of *Tetrahymena* cells (5×10^5 cells/ml) were centrifuged (5 min at 1100g) at 4°C and cell pellets were washed with pre-chilled Solution A (sucrose 0.1M, gum arabic 4% v/v, MgCl₂ 0.0015M, Spermidine Hydrochloride 0.01% v/v) and resuspended in pre-chilled Solution B (sucrose 0.1M, gum arabic 4% v/v, MgCl₂ 0.0015M, Spermidine Hydrochloride 0.01% v/v, octanol 24mM). The suspension was shaken vigorously for 5 min followed by centrifugation (Allen, 2000). The nuclear pellet was resuspended in Buffer A and was imaged by fluorescence microscope after staining with DAPI.

2.3.11 Staining and microscopy:

2.3.11.1 Fixation with Paraformaldehyde

Tetrahymena cells were fixed with 4% paraformaldehyde (PFA) in 50mM HEPES pH 7.5. The cells were spun down at 1100 RCF and the supernatant was discarded. The cell pellet was dislodged by tapping and PFA was added to the cells by dispensing quickly and incubated at room temperature for 30 min. Cells were recovered by centrifugation and washed with 10mM HEPES pH 7.5. The fixed cells were further used for staining purpose.

2.3.11.2 Lipid droplet staining

For staining lipid droplets, *Tetrahymena* cells ($4-5 \times 10^5$ cells/ml) were pelleted down by centrifugation (1100g for 2 min) at room temperature, washed with DMC and fixed with 4% paraformaldehyde. Fixed cells were washed with 10mM HEPES pH 7.5 and resuspended in the freshly prepared oil red O solution. To prepare fresh Oil red O stain, stock of 1 g oil red O in 100 ml isopropanol was diluted with water (3:2 vol/vol) and filtered through 0.45- and 0.22-µm syringe filters (Binns et al., 2006). *Tetrahymena* cells were pelleted down by centrifugation (1100g for 2 min at room temperature, washed with DMC and fixed with 4% paraformaldehyde. Cells were tapped briefly and incubated in the dark in nutating mixer at

room temperature for 10 min. Stained cells were washed thrice with 1 ml of 10mM HEPES each time. Finally cells were re suspended in 50 μ l of 10mM HEPES pH 7.5 and mounted on glass slides for confocal microscopy and viewed under 63X oil objective.

2.3.11.3 Endoplasmic Reticulum staining

For Endoplasmic Reticulum staining, *Tetrahymena* cells were grown to a density of $3-4 \times 10^5$ cells/ml. To the *Tetrahymena* culture 0.5 μ M ER-Tracker™ Red dye was added and incubated for 60 minutes. The stained cells were fixed with 4% paraformaldehyde in 50 mM HEPES pH 7.5. Fixed cells were washed once with 10mM HEPES to remove traces of paraformaldehyde. To rule out any effect of differential pressure (during placing coverslips) on ER morphology in different samples, we imaged both wild-type cells and knockout cells simultaneously. 3-5 μ l of cells were mounted on glass slides, covered with cover glasses, and sealed with nail polish and imaged under a 63X oil immersion objective in a Zeiss LSM780 confocal microscope.

2.3.11.4 DiOC6 (3) Staining

For staining isolated *Tetrahymena* nucleus, it was incubated with 5 μ g/ml of 3,3'-dihexyloxacarbocyanine iodide (DiOC6(3)) and 0.5 μ g/ml of 4',6-diamidino-2-phenylindole, dihydrochloride (DAPI) for 10 minutes in dark, washed thrice with Solution A and was resuspended in the same solution before imaging in a Nikon Eclipse Ti fluorescence microscope. Slides were viewed under a under a 60X oil immersion lens.

2.3.11.5 Imaging and Analysis

All the confocal imaging was performed using a Zeiss LSM780 confocal microscope. Lipid droplets were counted manually from the confocal images. To quantitate ER content, the stacked images of ER tracker red stained cells were analyzed by image J after sum intensity projection. The mean intensity values were plotted for both wild-type (n= 34) and $\Delta Ttpah1$ (n=32) cells using box plot.

2.3.12 Preparation of cell extracts and Western blotting

Wild type cells expressing *TtPAH1GFP* ($4\text{-}5 \times 10^5$) was used to prepare cell lysate. Cell lysis was performed in ice-cold buffer containing 10 mM Tris-HCl (pH 7.5), 1 mM MgCl₂, 10% glycerol, 0.02% NP-40 and 10 mM β-mercaptoethanol supplemented with protease inhibitors (1 μg/ml leupeptin, 2 μg/ml pepstatin, 1 μg/ml E-64, 1 μg/ml aprotinin and protease inhibitor cocktail). The cells were lysed by cell homogenizer (Isobiotec), and cell lysate was clarified by centrifugation at 16,000 rpm for 1 hour at 4°C. After centrifugation the lysate was separated into membrane fraction (pellet) and cytosolic fraction (supernatant). Protein estimation of lysate, membrane and cytosolic fractions was done by Bradford. Equivalent amount of supernatant and pellet fractions along with clarified total cell lysate were resolved by 10% SDS-PAGE at 120 V for 3 h. Protein was transferred to a nitrocellulose membrane using a semidry electroblotter at 0.01 mA and blocked overnight in 3% milk in Tris -buffered saline with Tween 20 (TBST). TtPah1-GFP was detected using anti-GFP polyclonal antibody. For this purpose membrane was incubated with horseradish peroxidase (HRP)-conjugated *anti-GFP* polyclonal antibody with (from Stefan Kircher, University of Freiburg), washed and detected. Images were collected with a Gel doc gel documentation system (BioRad).

2.3.13 Expression and Purification of TtPah1-TAP

3 ml of *Tetrahymena* transformant cultures were induced with 1 μg of Cadmium Chloride and kept for 5 hours. After 5 hours of induction cells were spun at 3000 rpm for 2 minutes. Media was discarded and the pellet was resuspended in the residual media. 50 μl of these cells were added to 50 μl of boiling 2x SDS gel loading dye kept in the dry bath at 103°C. This was kept for 12 minutes and once incubation is over tubes containing the cells were immediately transferred to ice and kept for 2 minutes. The cells were now spun at 13000 rpm for 5 minutes and the supernatant was loaded into 10% SDS gel. The gel was run at 150 V, 50Mv.

Protein was transferred to a PVDF membrane by western semidry and the transfer of protein was confirmed by staining the membrane with ponceau S stain (Sigma). The membrane was blocked for 1 hour in 3% skimmed milk TBST Solution. The membrane was incubated for another 1 hour in 1^o antibody (Rabbit IgG – 2mg/ml 1:3500). The membrane was washed 3 times for 10 minutes each time with TBST containing 3% skimmed milk. Then membrane was again incubated with 2^o antibody (α Rabbit HRP 1:7000) and then washed thrice with TBST containing 3% skimmed milk for 10 minutes each. The membrane was then washed with TBS and blot was developed with Supersignal West Femto Maximum Sensitivity substrate (Thermo Scientific) and detected with BioRad Quantity One (Chemi Hi sensitivity)

Tetrahymena cells harboring *TtPAHI-pVGF* and expressing TtPah1-TAP were grown to a density of 3x10⁵ cells per ml. The culture was induced with 1 μ g/ml cadmium chloride for 5 hours at 30°C to express *TtPAHI-TAP*, and cells from 300 ml cultures were collected by centrifugation. The cell pellet was resuspended in 10 ml lysis buffer (20 mM Tris-HCl (pH 8.00), 100 mM NaCl, 0.5% NP-40, 10% glycerol) supplemented with a mixture of protease inhibitor (pepstatin, E-64, aprotinin, and protease inhibitor cocktail). The lysate was clarified by ultracentrifugation (Beckman Coulter Optima L100K, 70Ti rotor) for 1 hour at 250,000g. To minimize proteolysis, all subsequent steps were carried out at 4°C unless mentioned otherwise. Rabbit-IgG agarose slurry (Sigma) pre-equilibrated with wash buffer was added to the clarified lysate and was kept for binding for 2 hours. Resin was collected by centrifugation (1 min at 3,000 g) and washed with 50 bed volumes of wash buffer (20 mM Tris-HCL (pH 8.00), 2 mM MgCl₂, 0.2 mM EGTA, 0.1 % Tween 20, 10 % glycerol, 1 mM DTT, 0.1mM PMSF). Resin was incubated with 2 μ l of TeV protease in 200 μ L cleavage buffer (10 mM Tris-HCl (pH 8.00), 0.1 M NaCl, 0.1% Tween 20, 0.5 mM EDTA, 1 mM DTT) for 1.5 hours at room temperature followed by further incubation at 4°C overnight. The eluate after proteolytic cleavage was adjusted to 3 mM CaCl₂ and mixed with 3 volumes of

calmodulin binding buffer (10 mM Tris-HCl (pH 8.00), 100 mM NaCl, 1 mM Mg acetate, 1 mM imidazole, 2 mM CaCl₂, 0.1 % Tween 20, 10 mM βME). This was incubated with 100 μL of calmodulin resin (GE Biosciences) at 4°C for 1 hour. The resin was recovered by centrifugation and washed with calmodulin binding buffer. Protein was eluted with calmodulin elution buffer (10 mM Tris-HCl (pH 8.00), 100 mM NaCl, and 1 mM Mg acetate, 1 mM imidazole, 10 mM EGTA, 0.1 % Tween 20, 10 mM 2-mercaptoethanol) (Witkin and Collins, 2004). Eluted fractions were loaded on 10 % SDS polyacrylamide gel, and the protein was detected by silver staining.

2.3.14 Preparation of Triton X-100/Lipid-mixed Micelles

PA in chloroform was transferred to a round bottom flask, and the solvent was eliminated in vacuum for 1 hour. Triton X-100 was added to PA to prepare Triton X-100/PA-mixed micelles. The mol % of a lipid in a Triton X-100/lipid-mixed micelle was calculated using the following formula, $\text{mol \%}_{\text{lipid}} = 100 \times \text{lipid (molar)} / ([\text{lipid (molar)}] + [\text{Triton X-100 (molar)}])$. The total lipid concentration in the Triton X-100/lipid-mixed micelles was kept below 15 mol % to ensure that the structure of the lipid-mixed micelles was similar to that of pure Triton X-100 micelles (Gil-Soo Han and George M. Carman, 2010).

2.3.15 Phosphatase Assay

Phosphatidic acid phosphatase activity was measured by following the release of water-soluble Pi from chloroform-soluble PA (Gil-Soo Han and George M. Carman, 2010). The standard reaction contained 50 mM Tris-HCl buffer (pH 7.5), 1 mM MgCl₂, 10 mM Triton X 100, 10 mM 2-mercaptoethanol and 1 mM phosphatidic acid in a total volume of 100 μL. Reactions were initiated by the addition of recombinant proteins and carried out in triplicates at 30°C for 20 min. The reaction was terminated by adding 0.5 ml of 0.1 M HCl in methanol, 1 ml of chloroform, and 1 ml of water. This was allowed to stand for phase separation and upper volume was collected. One volume of upper phase was mixed with two volumes of

Biomol Green (malachite green-molybdate reagent), and the color was allowed to develop. The absorbance of this was measured at 620 nm, and the amount of phosphate produced was quantified using a standard curve. Enzyme assays were conducted in triplicate.

2.4 RESULTS

2.4.1 Sequence analysis of Ttpah1

Ttpah1 is a large protein comparable to size of PAH1 proteins in other organisms. Sequence contains 872 amino acids. We analysed the sequence of TtPah1 using Interpro: protein sequence analysis & classification (<https://www.ebi.ac.uk/interpro/>) to predict the presence of domains and important residues within Ttpah1. Interpro predicted an N-terminal domain (10 to 83 amino acid sequences), and a C-terminal HAD like domains (614 to 837 amino acid sequences) which are characteristic for lipin proteins (Figure 2.1A). Moreover, all Magnesium dependent phosphatidic acid phosphatases contain an essential catalytic DXDXT/V motif in the HAD-like domain of the C-LIP region (Figure 2.1B). We found similar domain DIDGT (666 to 670) within the C-terminal HAD like domain of TtPah1 suggesting it to be a Mg²⁺-dependent phosphatidate phosphatase (Figure 2.1A). A conserved Glycine residue in N-terminal domain is critical for PAH function since its mutation in mammalian lipin1 causes lipodystrophy. Similar conserved glycine residue is present at the 75th position of TtPah1 at the N-LIP region (Figure 2.1A and B).

Amino acid sequences of PAH1 are generally conserved in the N-LIP and C-Lip domain. Similar to other Phosphatidic acid phosphatases, the amino acids are mostly conserved in the N-LIP and C-LIP region in TtPah1. TtPah1 shares 50% sequence identity with yeast Pah1 N-LIP and 49% identity with N-LIP of human lipin. C-LIP domain of TtPah1 has sequence identity of 49% with corresponding domain of yeast Pah1 and 44% with human lipin. Overall sequence identity of TtPah1 with yeast equivalent is 24% and 31% with human lipin.

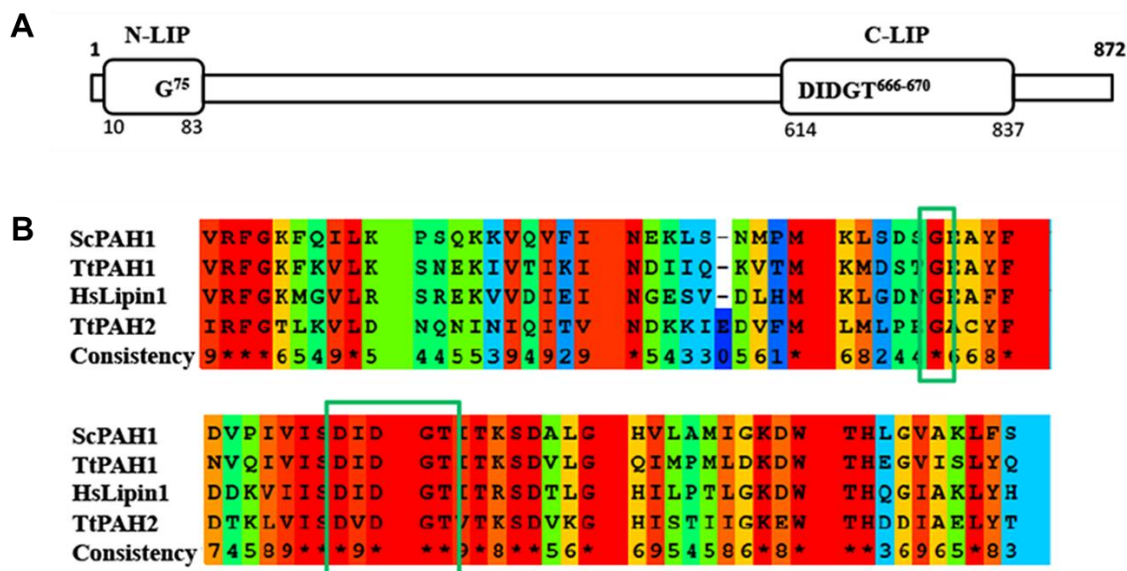


Figure 2.1: Domain Organization of TtPAH1.

(A) Predicted N-LIP and C-LIP domains are indicated in the boxes. Also shown are the positions of a conserved glycine residue in N-LIP and the haloacid dehalogenase (HAD) with its conserved DXDXT/V motif in C-LIP. (B) Multiple sequence alignment showing partial sequences of N-LIP and C-LIP of PAH1 proteins. Sequences of PAH1 proteins from *Tetrahymena thermophile* (TtPAH1), *Saccharomyces cerevisiae* (ScPAH1), and *Homo sapiens* (Hslipin1) were analyzed using PRALINE. Assigned colors of the specific residues are based on alignment consensus. Conserved Glycine in N-LIP and catalytic motif (DXDGT/V) in C-LIP are indicated inside the box. The numbers indicate the level of conservation where 9 is the maximum (identical) and 1 is the minimum.

2.4.2 Phosphatidate phosphatase activity of TtPah1

Sequence analysis showed that TtPah1 is a magnesium dependent phosphatidic phosphatase. To examine if *TtPAH1* encodes a functional phosphatidate phosphatase, it was expressed as a TAP-tag fusion protein in *Tetrahymena* cells and was purified from the cell lysates. The purified protein migrated at its expected size near 100 kDa in SDS-PAGE. However, there were also more abundant smaller species, probably corresponding to proteolytic products (Figure 2.2A).

Phosphatase activity was measured following the release of inorganic phosphate (Pi) from PA using malachite based colorimetric assay. The recombinant TtPah1 dephosphorylated PA in a time dependent manner (Figure 2.2B). The purified protein did not show any phosphatase

activity in the absence of magnesium (Figure 2.2C). These results confirm that TtPah1 is a functional magnesium dependent phosphatidate phosphatase in *Tetrahymena*.

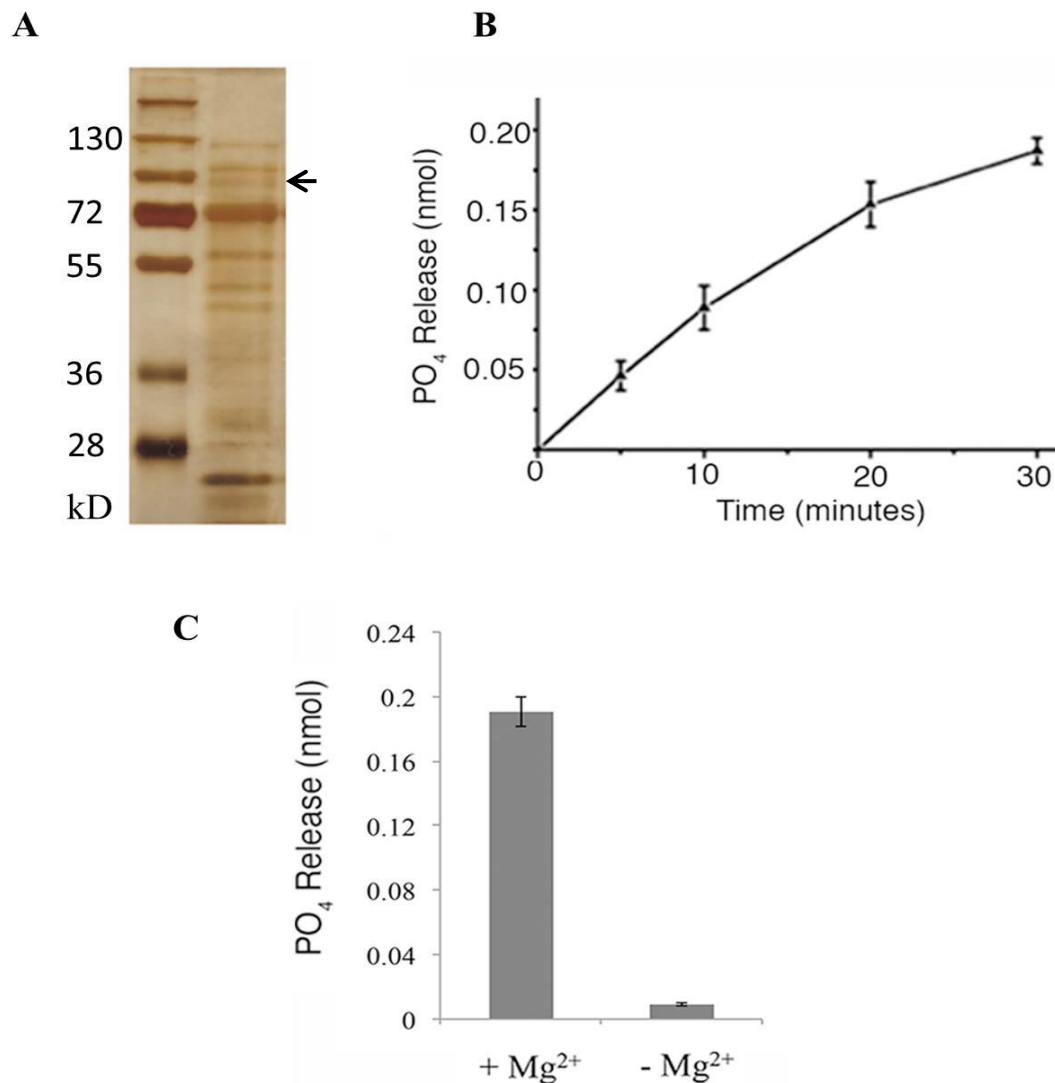


Figure 2.2: TtPah1 displays magnesium dependent phosphatidate phosphatase activity. A) Silver stained gel of purified TtPah1 along with standard molecular weight marker. The molecular weight is indicated on left (Arrow indicates the putative band ~ 100 kD). In addition to the expected band of ~100 kD, many smaller species are likely to reflect partial proteolysis of the full-length protein. B) TtPah1 protein (10 μ g in 100 μ l) partially purified from *Tetrahymena* was used to measure phosphatidic acid phosphatase activity. The average phosphate released (nmol) (n=3) was plotted against time. C) The phosphatidate phosphatase assay performed either in the presence (+Mg²⁺) or absence (-Mg²⁺) of magnesium. TtPah1 showed activity only in the presence of Mg²⁺ confirming it to be a PAP1 enzyme.

2.4.3 Subcellular localization of Tt-PAH1

To assess localization of TtPah1, *TtPAH1* bearing an N-terminal GFP tag was overexpressed in wild type *Tetrahymena* cells. Analysis of confocal images of *TtPAH1-GFP* overexpressed cells showed TtPah1-GFP was distributed throughout the cell, both in cytoplasm and membrane (Figure 2.3A). Total lysate of cells expressing *TtPAH1-GFP* was fractionated into the membrane and cytosolic fractions. TtPah1 was detected in both the fractions with anti-GFP antibody in western blot analysis, showing its localization both in cytosol and in membrane (Figure 2.3B).

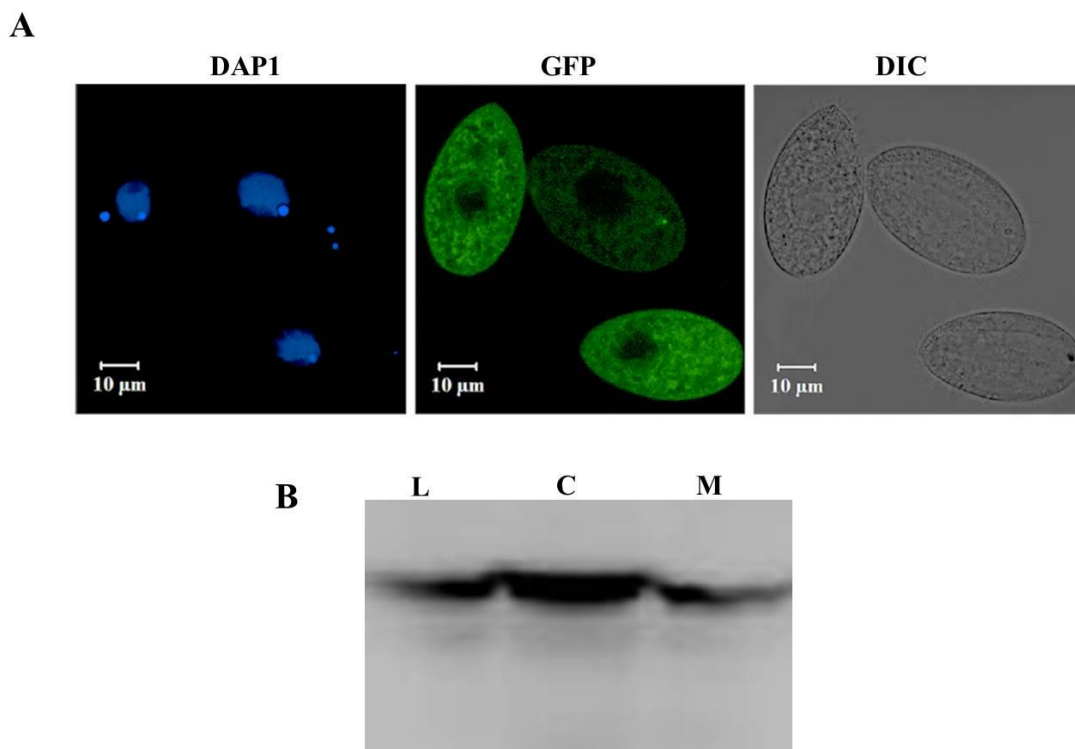


Figure 2.3: TtPah1 is distributed both in cytosol and in membranes.

(A) Localization of *TtPAH1-GFP* in *Tetrahymena* cells. Fixed *Tetrahymena* cells expressing *TtPAH1-GFP* was imaged after DAPI staining. DAPI stained nuclei (left panel), TtPah1-GFP (middle panel) and DIC image (right panel) of the fixed growing cell. (B) Western blot analysis of the total lysate (L), cytosolic fraction (C) and membrane fraction (M) isolated from *Tetrahymena* cells expressing *TtPAH2-GFP*. Polyclonal anti-GFP antibody was used for Western blot analysis.

2.4.4 TtPah1 localizes to endoplasmic reticulum

Phosphatidic acid, the substrate of PAH1 protein is enriched on ER membrane and dephosphorylation of PA generates DAG (Carman and Han, 2009). To evaluate if TtPah1 associates with ER membrane, *Tetrahymena* cells expressing *TtPAH1-GFP* were stained with ER-Tracker dye and visualized by confocal microscopy. Analysis of images showed that TtPah1-GFP co-localized with ER tracker dye (Figure 2.4) suggesting that TtPah1 localizes on ER membrane.

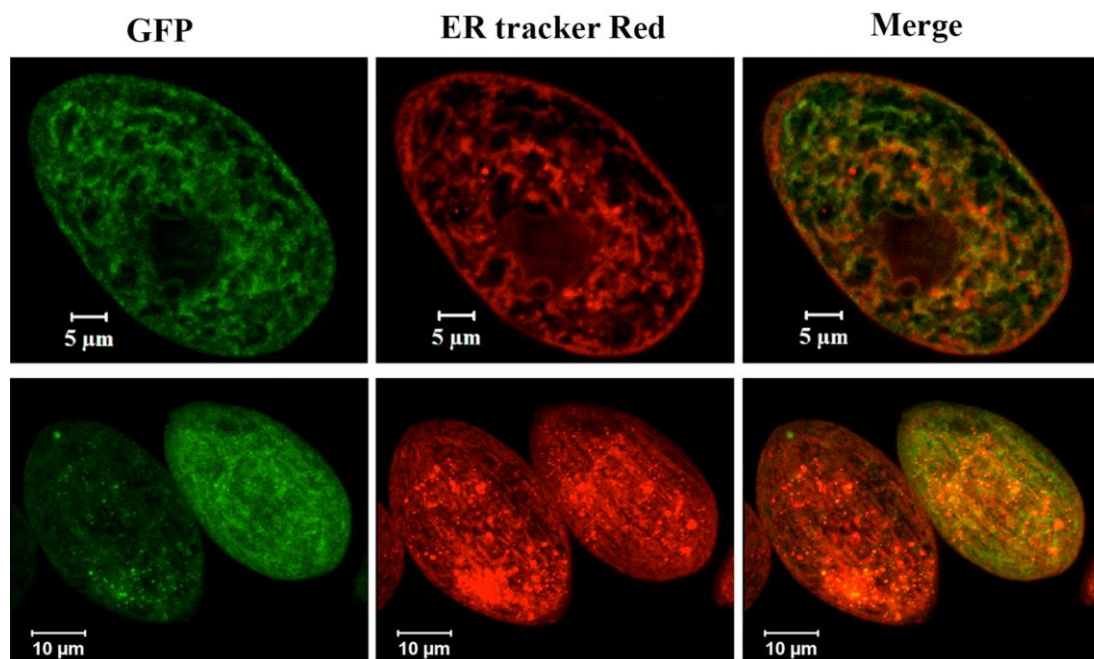


Figure 2.4: TtPah1 localizes to ER.

Upper panel shows confocal images of fixed *Tetrahymena* cells expressing *TtPAH1-GFP* after staining with ER tracker Red. TtPAH1-GFP (left panel), ER tracker Red (middle panel) and merge (right panel). Lower panel shows the confocal stack of a different *Tetrahymena* cell expressing *TtPAH1-GFP* and stained with ER tracker Red.

2.4.5 Generation of $\Delta TtPAH1$ (TtPAH1KO)

$\Delta Ttpah1$ strain was generated from wild-type *tetrahymena* strains by removing all 45 copies of *TtPAH1* from the macronucleus of wild-type *Tetrahymena* by homologous recombination (Figure 2.5A). The knockout strains thus generated ($\Delta Ttpah1$) were analyzed by semi-quantitative RT-PCR (Figure 2.5B). Reverse transcription PCR analysis of wild-type and

$\Delta Ttpah1$ cells was carried out using cDNA from wild-type cells and from $\Delta Ttpah1$ cells. The band corresponding to alpha tubulin (387 bp) is present in both $\Delta Ttpah1$ cells and wild-type cells (Figure 2.5B). The presence of *TtPAH1* band (300 bp) in wild-type cells and absence of band corresponding to *TtPAH1* (300bp) in $\Delta Ttpah1$ cells confirms that knockout is complete (Figure 2.5B). *TtPAH1* specific product was not amplified even after 34 cycles of PCR when cDNA from $\Delta Ttpah1$ cells were used as template, confirming it to be a complete *TtPAH1* knockout.

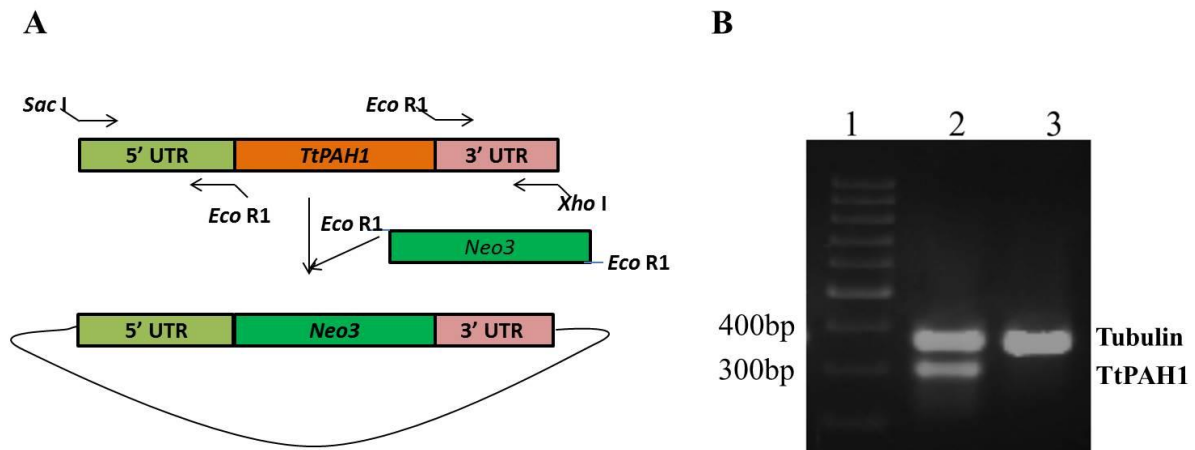


Figure 2.5: Generation of *TtPAH1* knockouts ($\Delta TtPah1$)

A) Schematic showing organization of the knockout construct used to disrupt *TtPAH1* in the macronucleus. Gene disruption was done by replacing the *TtPAH1* ORF with *NEO3* gene cassette, by homologous recombination. The *NEO3* cassette confers resistance to paromomycin. B) Reverse transcription PCR analysis of wild-type and $\Delta Ttpah1$ cells. Lane 1 is standard molecular weight marker, lane 2 is amplified products of cDNA from wild-type cells and lane 3 is amplified products of cDNA from $\Delta Ttpah1$ cells. The top band just below 400 bp marker corresponds to alpha-tubulin (387 bp), and the band near 300 bp represents *TtPAH1*. The absence of 300 bp band corresponding to *TtPAH1* confirms that knockout is complete.

2.4.6 Growth analysis of $\Delta TtPAH1$ (*TtPAH1*KO)

In many organisms such as *Saccharomyces cerevisiae*, *C. elegans*, and *Drosophila melanogaster*, *PAH* is required for normal growth. To assess whether *TtPAH1* is essential for normal growth of *Tetrahymena* we assessed growth rate of $\Delta Ttpah1$ cells and compared with

growth rate of wild-type *Tetrahymena*. The growth of $\Delta Ttpah1$ cells was not significantly different from that of wild-type cells (Figure 2.6).

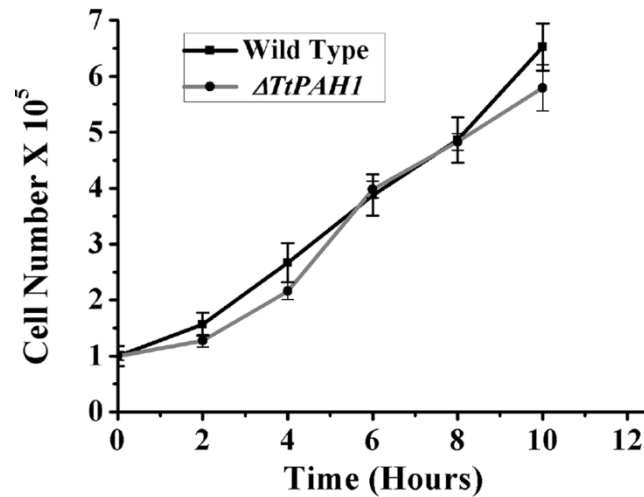


Figure 2.6: Growth curve of *Tetrahymena* wild-type versus $\Delta Ttpah1$ cells.

The cell numbers were counted every two hours, and the number of cells was plotted against time. Loss of *TtPAH1* does not affect *Tetrahymena* growth significantly.

Moreover, $\Delta Ttpah1$ cells did not show any visible defect in their morphology. To rule out the possibility that the lack of growth defect in $\Delta Ttpah1$ is due to compensatory overexpression of another homolog *TtPAH2* in these cells, the expression of *TtPAH2* in $\Delta Ttpah1$ was compared with wild-type cells. To check the expression of *TtPAH2* in $\Delta Ttpah1$ and wild-type cells, *TtPAH2* was amplified with specific primers using cDNA from $\Delta Ttpah1$ and from wild-type cells as templates for 30 cycles (Figure 2.7A). Alpha tubulin primers were used as control. The band corresponding to *TtPAH2* from $\Delta Ttpah1$ and wild-type cells were quantitated and normalised with respect to alpha tubulin bands. The expression of *TtPAH2* was not enhanced in $\Delta Ttpah1$ cells as compared to wild-type cells (Figure 2.7A and 2.7B). Taken together, these results suggest that *TtPAH1* is dispensable for normal growth of *Tetrahymena*.

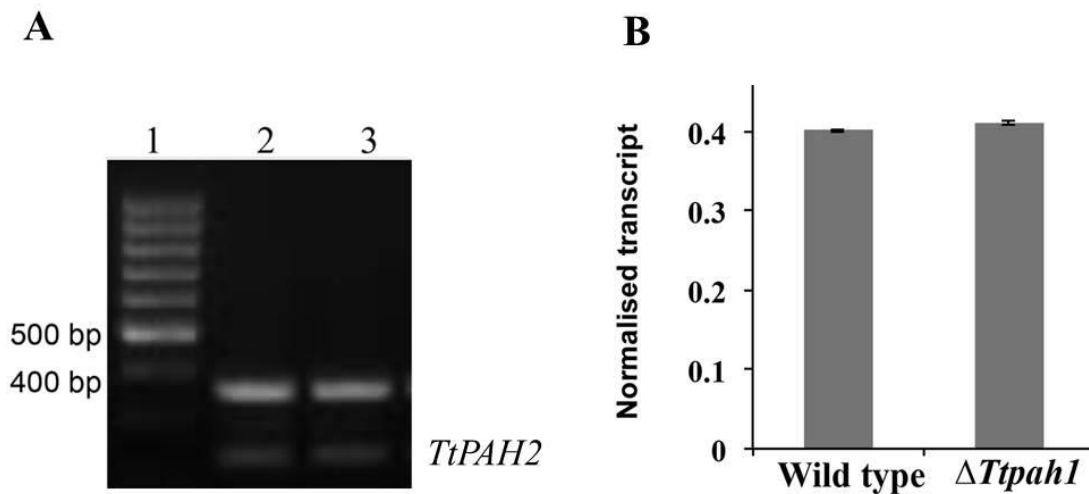


Figure 2.7: Lack of growth defect in $\Delta Ttpah1$ is not due to compensatory overexpression of the other homolog *TtPAH2*

A) Semi-quantitative RT-PCR showing expression of *TtPAH2* in wild-type and $\Delta Ttpah1$ cells. Lane1 is standard molecular weight marker; lane2, amplified products of cDNA from wild-type cells; lane3, amplified products of cDNA from $\Delta Ttpah1$ cells. The top band in lane 2 and 3 corresponds to alpha-tubulin (387 bp), and the band near 238 bp represents *TtPAH2*. (B) The graph shows quantitation of *TtPAH2* after normalization with alpha tubulin band. The expression of *TtPAH2* is not enhanced by the loss of *TtPAH1*

2.4.7 *TtPAH1* regulates lipid droplet biogenesis in *Tetrahymena*

Lipid droplets are ubiquitous eukaryotic organelles mainly used for storing lipids (Murphy, 2001). They consist of a hydrophobic core of neutral lipids such as triacylglycerol, sterols and sterol esters surrounded by a phospholipid monolayer originating from the ER (Farese and Walther, 2009; Radulovic et al., 2013; Tauchi-Sato et al., 2002). Lipid droplets growth occurs either by localized synthesis of lipids or by fusion with other lipid droplets (Thiele and Spandl, 2008). PAH proteins generate DAG by dephosphorylating PA and the DAG thus produced gets converted into TAG, the storage lipid. TAG thus produced from DAG forms the major constituent of lipid droplet along with steryl esters and any change in the conversion of PA to DAG could affect lipid droplet. Since PAH proteins are required for the synthesis of triacylglycerol, lipid droplet numbers were compared between $\Delta Ttpah1$ and wild-type cells. $\Delta Ttpah1$ and wild-type cells were grown to stationary phase (10×10^5), fixed

with 4% PFA and lipid droplets were visualized by staining with Oil Red O and imaged in confocal microscope (Figure 2.8A).

The number of lipid droplet in both $\Delta Ttpah1$ and wild-type cells were counted manually after analyzing images by LSM Image analyzer. The average lipid droplet number in $\Delta Ttpah1$ cells were 134 where as it was 340 in wild-type cells (Figure 2.8B). Approximately 65% reduction of lipid droplet in $\Delta Ttpah1$ cells numbers compared to wild-type strongly supports that *TtPAH1* is required for lipid droplet biogenesis. There was no visible difference in the size of lipid droplets between $\Delta Ttpah1$ and wild-type cells (Figure 2.8A).

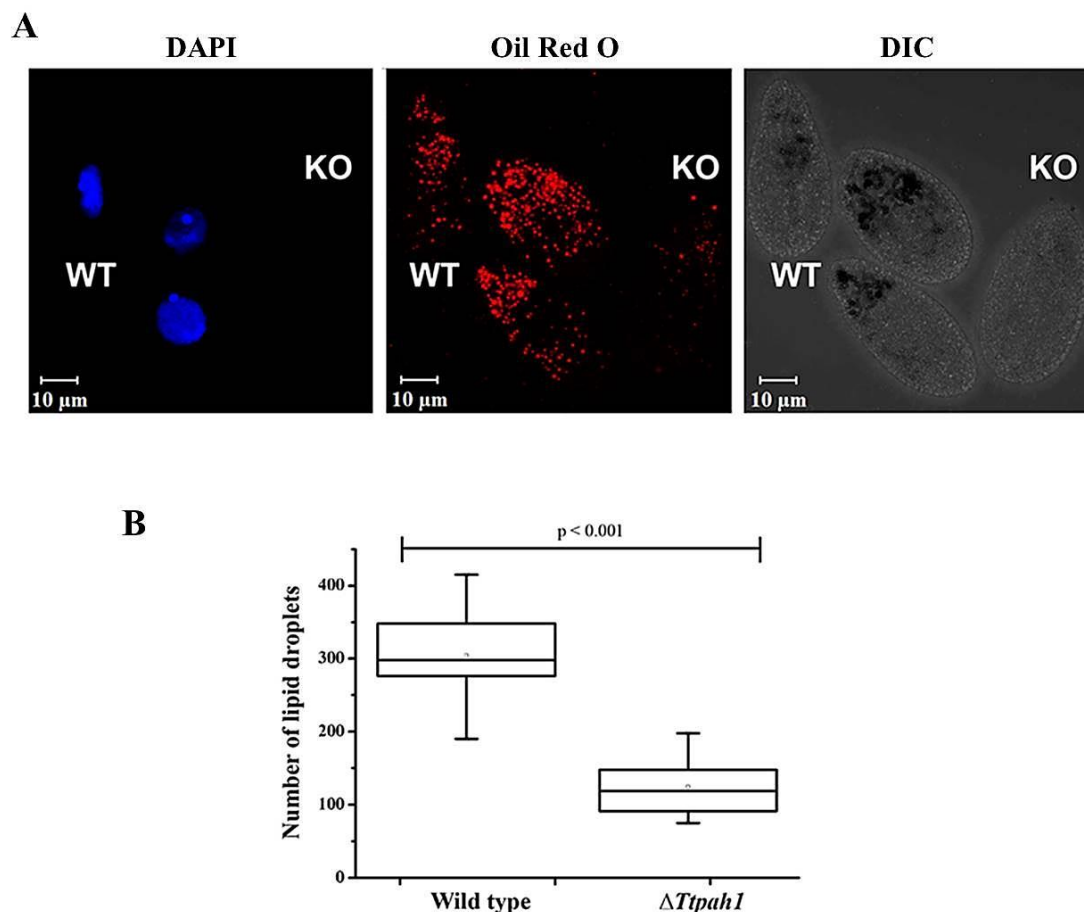


Figure 2.8: Deletion of *TtPAH1* reduces lipid droplet number in *Tetrahymena*.

A) Confocal images of *Tetrahymena* cells showing lipid droplets as stained with Oil Red O dye. Wild-type cells and knockout cells were imaged together simultaneously. The wild-type cells were stained with DAPI to distinguish them from knockout cells. B) Box plot showing the distribution of lipid droplet numbers in wild-type (n=35) vs. $\Delta Ttpah1$ (n=38) cells.

Lipid droplets were also compared between $\Delta Ttpah1$ and wild-type under starvation. As in case of growing *Tetrahymena*, lipid droplet number was also strikingly reduced in $\Delta Ttpah1$ cells compared to wild type cells in starved condition as well (Figure 2.9A and 2.9B). This suggests that reduction in lipid droplet number in growing condition was not due to decreased nutrient uptake. The average lipid droplet number of $\Delta Ttpah1$ under starved condition was 108 while the average lipid droplet number in wild-type cells is 276. Under starvation conditions (starved for 10 to 12 hours), there was ~ 60% reduction in lipid droplet number in $\Delta Ttpah1$ cells (Figure 2.9B). Unlike in growing *Tetrahymena* cells, the size of lipid droplet in $\Delta Ttpah1$ was smaller than wild-type cells under starvation (Figure 2.9A). These results suggest that *TtPAH1* regulates lipid droplet number and size in *Tetrahymena*.

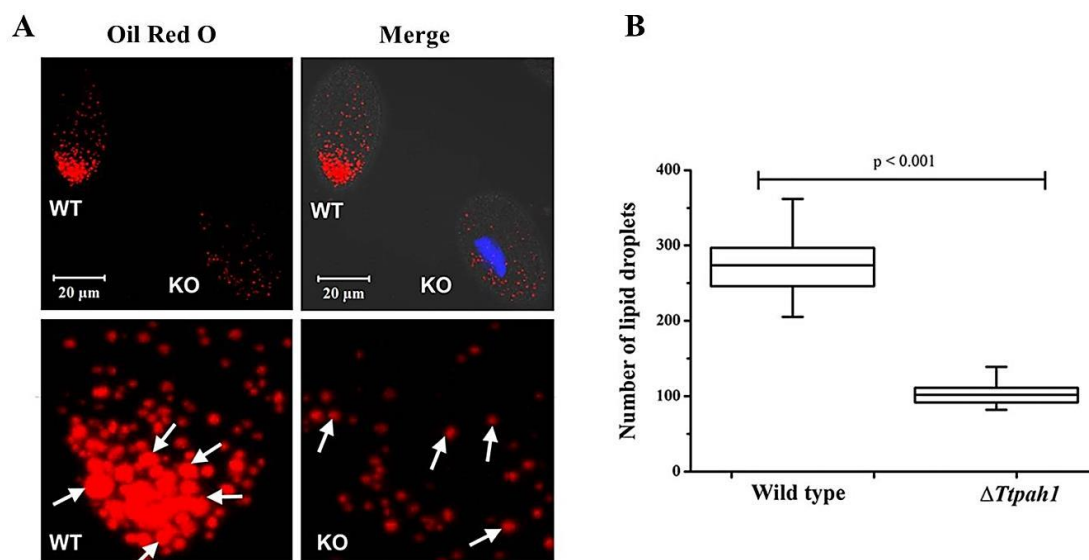


Figure 2.9: Deletion of *TtPAH1* showed reduced lipid droplet number in starved conditions.

A) Confocal images of *Tetrahymena* cells showing lipid droplets as stained with Oil Red O dye. Wild-type and knockout cells after starvation were imaged together simultaneously. Knockout cells were stained with DAPI to distinguish them from wild-type cells. Lipid droplet size in wild-type cells appears to be larger than in the knockout cells as indicated by arrows (lower panel). B) Box plot showing lipid droplet numbers in wild-type (n=22) and $\Delta Ttpah1$ (n=22) cells under starved condition.

To provide further evidence that *TtPAH1* is involved in lipid droplet biogenesis, we overexpressed *TtPAH1-GFP* in wild-type *Tetrahymena* cells. The mean lipid droplet number in cells overexpressing *TtPAH1-GFP* is 425, a significant increase (~ 25 %) in lipid droplet number as compared to wild-type cells (Figure 2.10A and 2.10B). To demonstrate that this increase in lipid droplet number is not due to overexpression of any transgene, *DRP6-GFP* (a dynamin-related protein in *Tetrahymena*) was similarly overexpressed and checked for lipid droplet number. The average lipid droplet number in *DRP6-GFP* overexpressed *tetrahymena* cells is 357 which are not significantly different from the average lipid droplet number of wild type (Figure 2.10A and 2.10B). Taken together these results suggest that *TtPAH1* influences the number and size of the lipid droplet in *Tetrahymena*.

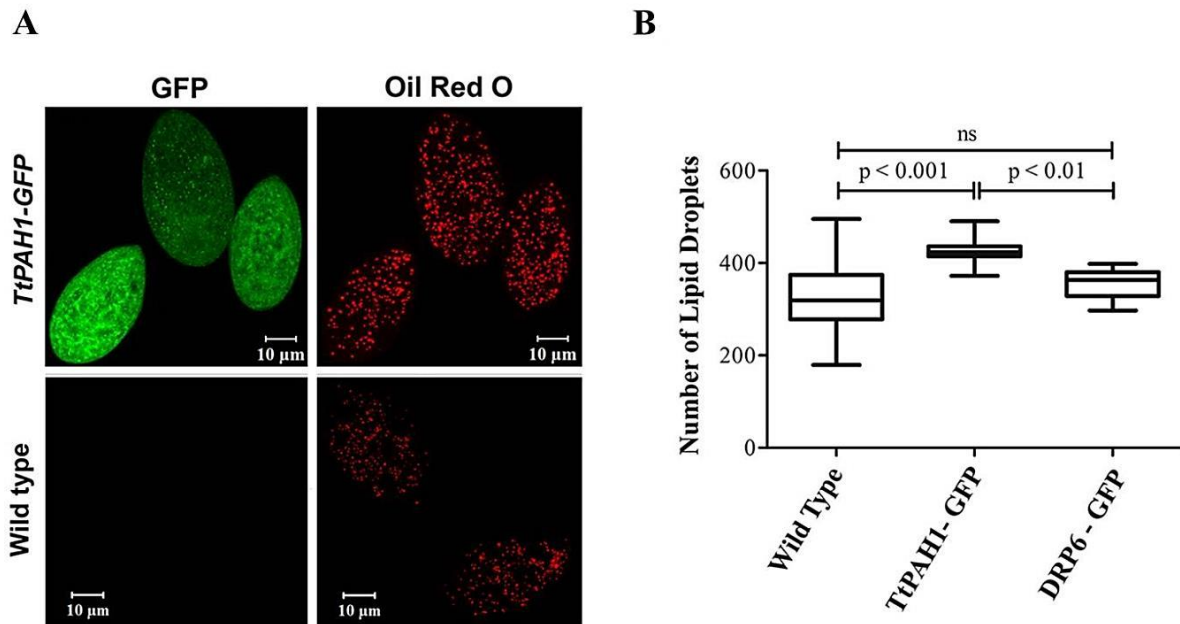


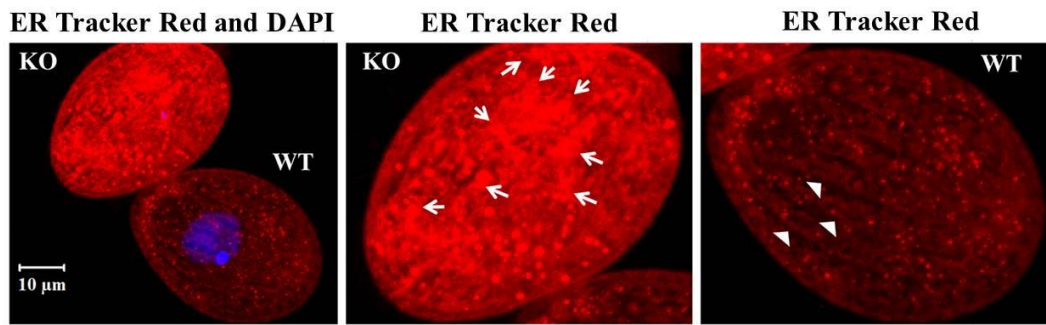
Figure 2.10: Overexpression of *TtPAH1* causes increase in lipid droplet number
A) Confocal images of wild-type and *TtPAH1-GFP* expressing cells showing lipid droplets after staining with Oil Red O dye. (B) Box plot showing lipid droplet numbers in wild-type cells (n=35), cells overexpressing *TtPAH1-GFP* (n=20), and cells overexpressing *GFP-DRP6* (n=20). The increase in lipid droplet number is observed in cells expressing *TtPAH1-GFP*.

2.4.8 *TtPAH1* is needed for maintaining tubular ER in *Tetrahymena*

The ER is a complex network consisting of flat sheets and highly curved tubules, and their abundance varies with cell cycle stages. The ER serves as the primary site for *de novo* lipid biosynthesis. We hypothesized that *PAH* regulates ER morphology since phosphatidic acid (PA) is present on ER membrane and is converted to DAG by PAH. To determine whether *TtPAH1* is important in maintaining ER morphology, we stained both $\Delta Ttpah1$ and wild-type cells with ER-tracker dye and analyzed morphology by confocal microscopy (Figure 2.11A). In wild-type cells, the ER appeared mainly as a network of fine tubules with occasional small patches, likely to represent ER sheets (Figure 2.11A). $\Delta Ttpah1$ cells had abundance of membrane sheets and patches compared to wild-type cells (Figure 2.11A). As compared to wild-type cells, tubules are less and sheet like structures are more in $\Delta Ttpah1$ cells.

The ER content in both $\Delta Ttpah1$ and wild-type cells were quantitated using Image J software (<https://imagej.nih.gov/ij/>). The mean density was significant more in $\Delta Ttpah1$ cells as compared to wild-type cells (Figure 2.11B). This shows that ER content increased considerably in cells lacking *TtPAH1*, as measured by the mean density of ER-tracker red staining. Taken together, these results suggest that *TtPAH1* is required for maintaining ER content and structure in *Tetrahymena*.

A



B

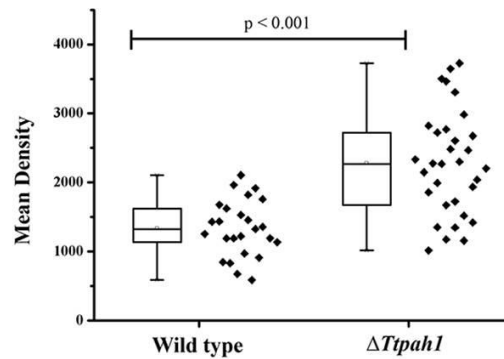


Figure 2.11: *TtPAH1* is needed for maintaining tubular ER and deletion of *TtPAH1* results in increased ER content.

A) Wild-type (WT) and $\Delta Ttpah1$ (KO) cells were imaged simultaneously in the same field. Wild-type cells were stained with DAPI to distinguish them from $\Delta Ttpah1$ cells. The enlarged images of $\Delta Ttpah1$ (middle panel) and wild-type (right panel) cells are shown indicating ER sheet (arrow) and ER tubule (arrowhead) structures. B) Box plot showing the mean density of ER tracker stain in $\Delta Ttpah1$ and wild-type cells. The mean intensity of $\Delta Ttpah1$ (n=32) is significantly higher than that of wild-type (n=25).

2.4.9 Loss of *TtPAH1* does not manifest visible nuclear envelope defect in *Tetrahymena*

Tetrahymena harbors one polyploid, phenotypically active macronucleus (MAC) and a diploid transcriptionally silent germline micronucleus (MIC). Deletion of yeast PAH1 causes aberrant nuclear membrane morphology. Lipin inactivation in higher organisms like *Caenorhabditis elegans* and *Drosophila melanogaster* also leads to nuclear defects. The outer nuclear membrane is continuous with the endoplasmic reticulum and any defect in ER morphology is expected to affect nuclear membrane. Since nuclear-ER membranes form one continuous compartment, changes in the structural organization of the ER could impact on the morphology of the nucleus. To see whether change in ER morphology due to PAH1

deletion affected nuclear morphology, the NE was analyzed by expressing and visualizing *NUP3-GFP* (a nuclear pore component marker specifically localizing to macronucleus) in $\Delta Ttpah1$ cells and wild-type cells (Figure 2.12). This comparison did not reveal any visible defect in size or shape of the nucleus in $\Delta Ttpah1$ cells (Figure 2.12). Like in wild-type, the DAPI-stained DNA appeared round, compact, and non-fragmented. Consistent with this, isolated DAPI-stained nuclei from wild-type and mutant cells expressing *NUP3-GFP* seemed identical (Figure 2.12A).

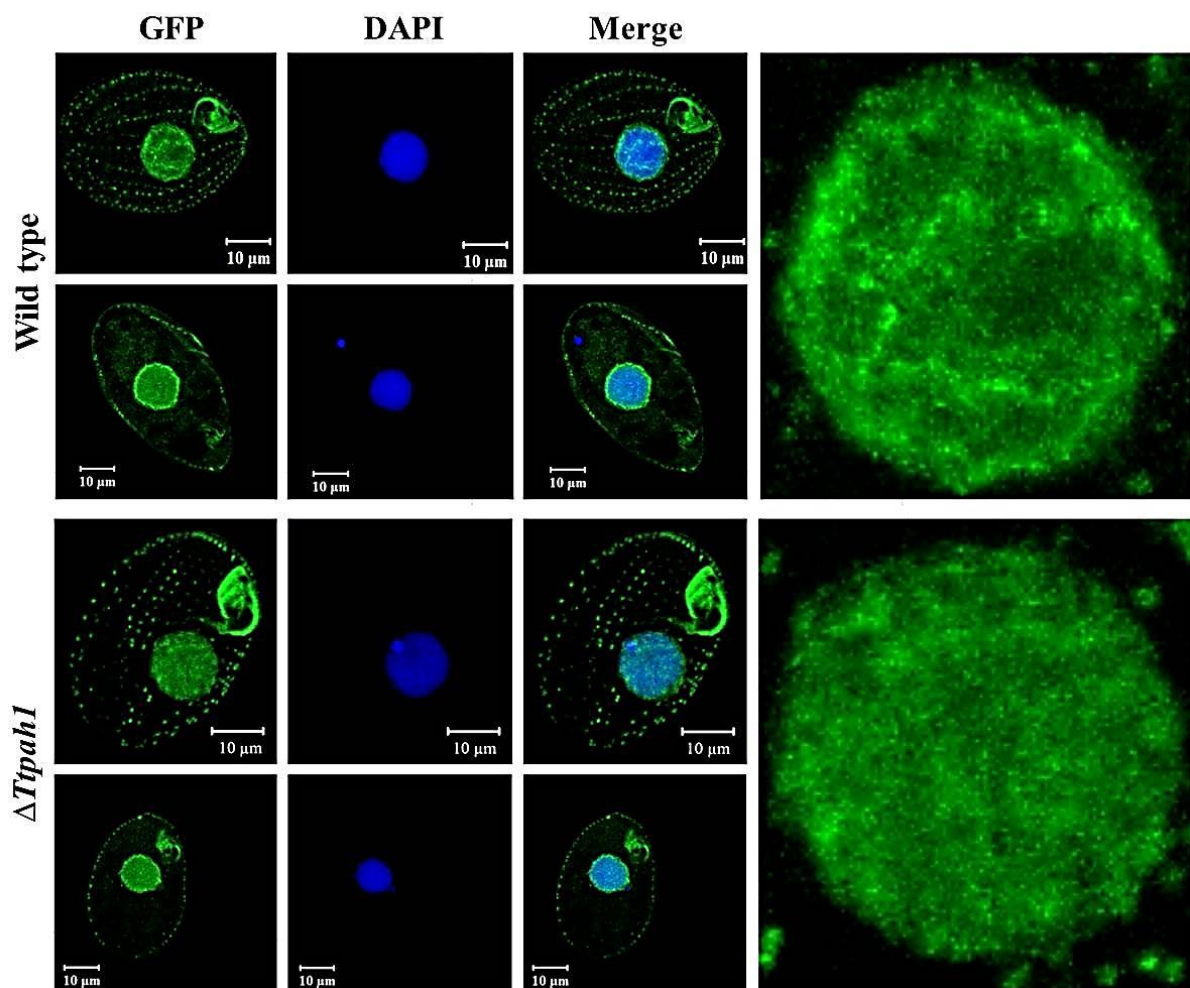


Figure 2.12: Loss of *TtPAH1* does not show visible nuclear envelope defect in *Tetrahymena*.

Confocal images of wild-type and $\Delta Ttpah1$ cells expressing *NUP3-GFP* after DAPI staining. In both wild-type and $\Delta Ttpah1$, upper panel is Z-stack and lower panel is a single slice. The enlarged nucleus from Z-stack is shown on the right side.

To further confirm that deletion of *TiPAH1* did not affect nuclear morphology, isolated nuclei (both MAC and MIC) of $\Delta Ttpah1$ cells and wild-type cells were stained with a lipophilic dye (DHCC) and the nuclear membrane was visualized. Similar to Nup3-GFP labelled nuclei, there was no visible defect in nuclear membranes of MAC (Figure 2.13B). Nuclear envelope of micronucleus also did not show any visible change in morphology (Figure 2.13B).

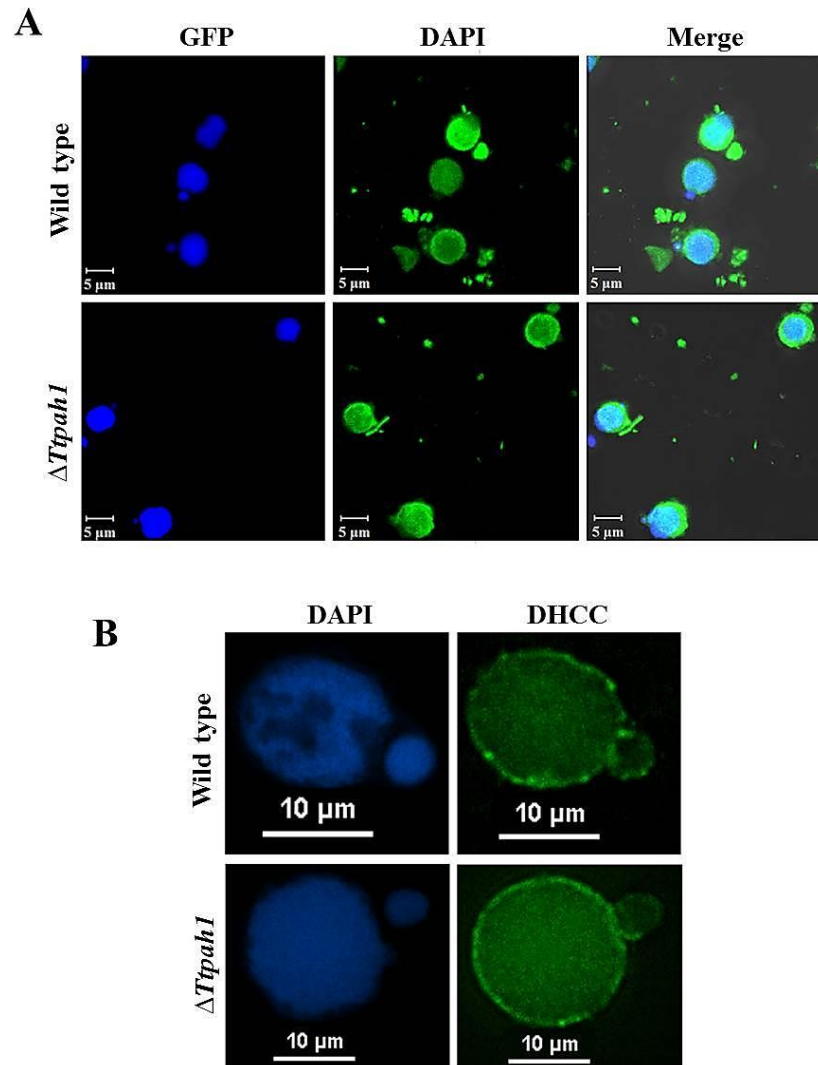


Figure 2.13: Loss of *TiPAH1* does not show nuclear membrane expansion in *Tetrahymena*

A) Confocal images of DAPI stained nuclei isolated from wild-type (upper panel) and $\Delta Ttpah1$ (lower panel) cells expressing *NUP3-GFP*. B) Fluorescence images of *Tetrahymena* nuclei of wild type (Top panel) and $\Delta Ttpah1$ (Bottom panel) after staining with DHCC and DAPI. The images are deconvoluted using NIS Advanced Research software.

These results suggest that *TtPAH1* is not essential for maintaining normal nuclear morphology in *Tetrahymena*. These results also suggest that defects in ER morphology in *Tetrahymena* do not necessarily affect nuclear morphology, unlike the coupling of ER morphology change with nuclear envelope as in other organisms. Our results are in contrast to findings in *S. cerevisiae*, where cells lacking *PAH1* showed abnormal expansion of nuclear envelope that appeared as a nuclear membrane projections lacking DNA along with difference in ER.

2.5 DISCUSSION

Regulation of lipid homeostasis and membrane biogenesis is fundamental to all eukaryotes, and the presence of a regulation cascade comprising Pah1 and its phosphatase complex Nem1-Spo7 has been shown in yeast (Siniossoglou et al., 1998; Péterfy et al., 2001; Han et al., 2006). Similar cascades are also reported in plants (Nakamura et al., 2009; Mietkiewska et al., 2011), mammals (Kim et al., 2007), worms, (Golden et al., 2009) and flies (Ugrankar et al., 2011). Two homologs of *LIPIN/PAH* in *Tetrahymena thermophila* are identified in *Tetrahymena* Genome database. The presence of two lipin homologs in a single celled eukaryote is quite interesting as multiple homologs are not found in any lower organism. *In vitro* phosphatase activity showed that large homolog TtPah1 is a PAPH1 enzyme requiring magnesium for its phosphatase activity.

Earlier studies have shown that deletion or depletion of PAH1 in organisms caused defect in the viability and growth. PAH1 deletion in yeast leads to slow growth, while in *Caenorhabditis elegans* lipin depleted adult worms were smaller in size. In *Drosophila melanogaster* lipin depletion caused delayed development of larvae and overall less viability. Contrary to this, deletion of *TtPAH1* caused no growth defect in *Tetrahymena thermophila* suggesting that the gene is not essential for its survival. The normal growth and development of *TtPAH1* knockout cells may be attributed to the presence of another homolog, *TtPAH2*. But the expression of TtPAH2 is not increased in $\Delta Ttpah1$ cells as compared to wild-type

cells. TtPah1 displays cytoplasmic as well as membrane localization consistent with previously characterized mammalian lipin and yeast Pah1 (Péterfy et al., 2001; Han et al., 2006). Dephosphorylation of Pah1 regulates its subcellular localization and promotes its translocation from the cytoplasm into ER, where it converts PA to DAG (Karanasios et al., 2010). PA phosphatase converts its substrate PA into DAG. DAG is used for the synthesis of the membrane phospholipids and triacylglycerol; the storage lipid majorly constituting lipid droplet. In *Sacharomyces cerevisiae* DAG generated by Pah1p is important for lipid droplet biogenesis and deletion of PAH1 leads to decrease in lipid droplet number (Adeyo et al., 2011). Also in *C.elegans*, reduced lipin activity leads to decrease in lipid droplet number causing defects in lipid storage (Golden et al., 2009), a phenotype similar to LPIN1-null mice. Ugrankar *et.al* found that in *Drosophila melanogaster*, the functions of the fat body (the central metabolic organ and energy store of insects) were severely impaired in $\Delta lipin$ mutants. These mutant larvae looked transparent with under developed fat body. While mutations in mammalian *lipin* genes prevent normal development of adipose tissue resulting in lipodystrophy, lipin overexpression promotes obesity (Péterfy et al., 2001; Phan and Reue, 2004). Thus lipin/PAH1 is known to regulate lipid storage.

Deletion of *TtPAH1* in *Tetrahymena* caused severe reduction in lipid droplet number thus demonstrating its role in lipid droplet biogenesis. This reduction in lipid droplet number in $\Delta Ttpah1$ is due to defect in TAG production. TAG in *Tetrahymena* forms the bulk of neutral lipid which is used as a precursor for phospholipids other than energy storage. Overexpression of *TtPAH1* in wild-type cells leads to an increase in lipid droplet number, further corroborating its role in lipid droplet biogenesis. The observations from lipid droplet number suggest that similar to all other PAH homologs studied till date *TtPAH1* also has a direct role in the production of TAG by dephosphorylating PA to DAG. This observation is significant because it suggests that the function of lipin protein is conserved.

The role of PAH proteins in maintaining ER structure is well established in yeast and *C.elegans* (Siniossoglou et al., 1998; Joseph L. Campbell, Alexander Lorenz, Keren L. Witkin, Thomas Hays Josef Loidl, 2006; Golden et al., 2009; Gorjánác and Mattaj, 2009) . In yeast, loss of *PAH1* leads to over developed ER membrane. Depletion of single copy of PAH1 homolog in drosophila caused morphology change in cell nuclei, autophagosomes, and mitochondria but any perturbation in ER morphology is not reported (Ugrankar et al., 2011). Interestingly, deletion of macronuclear copies of *TtPAH1* in *Tetrahymena* alters ER morphology resulting in an increased proportion of sheet to tubule structure. *TtPAH1* is required for maintaining ER structure by controlling the ER sheet to tubule volume. A possibility for the altered ER morphology could be the change in phospholipid flux arising from the loss of *PAH1* leading to change in the phospholipid composition of ER.

As discussed above, loss of *PAH1* in *Tetrahymena* demonstrates a change in ER content and structure. Although the loss of *TtPAH1* increases the ER sheet structure, it does not manifest visible defect in the nuclear envelope. It appears that in *Tetrahymena*, unlike other organisms, ER content and structure are functionally isolated from mechanisms underlying nuclear expansion. However, further studies are required to clearly understand the regulation of nuclear expansion and its relation to ER in *Tetrahymena*.

Irregular nuclear morphology has been observed in lipin-deficient yeast, *C. elegans* and Drosophila cells. Golden et.al proposed that in *C.elegans* the nuclear morphology changes may be because of an indirect effect of ER morphology. Loss of *PAH* in mammals and *C.elegans* results in a defect in nuclear envelope break down (NEBD) without any defect in nuclear expansion (Golden et al., 2009; Gorjánác and Mattaj, 2009). This has been proposed to result from a reduction in DAG levels, which in turn could decrease the activity of DAG-dependent protein kinase Cs that phosphorylate lamins to promote their disassembly (Mall et al., 2012). The regulation of nuclear membrane expansion by *PAH* is restricted to yeast,

which could be explained by the presence of CDP-DAG pathway in yeast and its absence in mammals and *C.elegans* (Bahmanyar et al., 2014; Bahmanyar, 2015). Loss of *PAH1* results in accumulation of PA which leads to the excess synthesis of phospholipids PE and PC via the CDP-DAG pathway. This excessive synthesis of membrane phospholipids results in a massive nuclear expansion in yeast (Santos-Rosa et al., 2005; Han et al., 2006; Bahmanyar et al., 2014). *Tetrahymena*, though possessing the CDP-DAG pathway for phospholipid synthesis it is interesting to note that, nuclear expansion was not visible in $\Delta Tpah1$. Although *NUP3-GFP* is a reliable marker since nuclear membrane flares seen in yeast contain assembled nuclear pore structures (Siniosoglou et al., 1998) it might be useful to test with other nuclear markers as well. Further, staining the nuclear membrane with a lipophilic dye also failed to detect any visible flares in both micronucleus and macronucleus of $\Delta Tpah1$. These results suggest that unlike yeast, where the expansion of nuclear membrane is very prominent, there is no extensive expansion of the nuclear membrane in *Tetrahymena* upon deletion of *TtPAH1*.

Macronucleus and micronucleus in *Tetrahymena* have distinct cell cycles, with distinct cycles of DNA replication and nuclear division at different times within the same cell. A new MAC is generated from the MIC through sexual reproduction (conjugation). It is remarkable that at the time of exconjugant separation (a stage during conjugation) there are five nuclei experiencing four extremely diverse fates, all within a common cytoplasm. CLEFFMAN (1968) and DOERDER *et al.* (1975) have provided cytological evidence for frequent inequalities in the amounts of macronuclear DNA distributed to daughter cells (CLEFFMANN, 1968; FLACKS, 1974; Doerder FP, Frankel J, Jenkins LM, 1975). The G-I macronucleus contains approximately 45 subunits. The number 45, in as much as it is not part of a geometric progression starting with a diploid nucleus indicates at least some disparity between replication and division during the formation of the macronucleus from a diploid

synkaryon. Gorovsky also had proposed that there could be difference in the ploidy of macronuclear DNA but not in the number of macronuclear subnuclei as proposed by Nanney et.al. This shows that nuclear volume in *Tetrahymena* is variable presumably due to differential ploidy level in the MAC (Raikov IB, 1976; Gorovsky MA, 1980; Bodenbender J, Prohaska A, Jauker F, Hipke H, 1992). In view of these complicated process of nuclear division, differential amount of DNA being distributed to different daughter cells and the concern in ploidy number points to a fact that *Tetrahymena thermophila* nuclear membrane has to maintain a high degree of plasticity in order to being flexible for these process. Therefore, different mechanism that allows plasticity in nuclear expansion to accommodate different nuclear volumes may be present in *Tetrahymena*. Thus unlike other known *PAH* homologs, *TtPAH1* does not regulate nuclear morphology.

Membrane biogenesis itself has to be regulated, especially for nucleus since size control of the nucleus is particularly important because changes in nuclear size and shape are associated with disease like cancer and processes including aging and senescence. Therefore there is spatial and temporal regulation in maintaining nuclear size and nuclear envelope membrane biogenesis. The mechanism of nuclear membrane size and shape regulation in organisms having nuclear dimorphism will definitely add to our understandings to the basic mechanism of nuclear expansion conserved within all eukaryotes.

CHAPTER 3

Role of Tetrahymena PAH1 in mediating cell cycle regulation of nuclear expansion in yeast.

3.1 INTRODUCTION

In yeast, PAH1 was initially identified as a gene whose mutation results in increased plasmid maintenance, slow growth, temperature sensitivity, and respiratory deficiency. The physiological relevance of Pah1 has been revealed by studying *pah1Δ* yeast strains. The absence of *PAH1* leads to elevated levels of PA and other phospholipids causing the hyper proliferation of the nuclear ER (Siniossoglou, 2009; Pascual and Carman, 2013; Fernández-Murray and McMaster, 2016). This deletion of PAH1 also caused reduced amounts of DAG and TAG, reduced number of lipid droplet, and lipotoxicity. *Pah1Δ* cells also show phenotypes like slow growth, thermosensitivity, and impaired growth in non-fermentable carbon sources known as respiratory deficiency (Pascual and Carman, 2013)(Fernández-Murray and McMaster, 2016). The inability to grow on non-fermentable substrate is correlated with a reduction of ATP level observed in *pah1Δ* cells (Park et al., 2015; Fernández-Murray and McMaster, 2016). In addition, *pah1Δ* cells exhibit an increased level of mitochondrial superoxides and a decreased tolerance to oxidative stress resulting in reduced chronological life span (Park et al., 2015). Cells defective in PAH1 activity also display vacuolar fragmentation (Sasser et al., 2012). Pah1p in yeast regulates transcription of phospholipid biosynthetic genes and nuclear/ER membrane growth (Santos-Rosa et al., 2005). Deletion of *PAH1* or its phosphatase complex *NEM1/SPO7* has a unique effect on nuclear structure. In *Saccharomyces cerevisiae* the mutant display irregularly shaped nuclei with long stacks of membranes that contain nuclear pores and appear to be in contact with the nuclear envelope(Santos-Rosa et al., 2005; Siniossoglou, 2009). Similar defects were described in mutants of *Saccharomyces pombe NED1*(Tange, 2002).

TtPAH1 has the same domain organisation with DXDX (T/V) catalytic motif within a haloacid dehalogenase-like domain like yeast PAH1. Deletion of TtPAH1 in *Tetrahymena*

causes severe reduction in lipid droplet number and affected endoplasmic reticulum morphology (Pillai et al., 2017a).

Cell expansion and proliferation (division) are the two most important mechanisms underlying cell growth and both rely on membrane biogenesis. For example cell expansion requires production of plasma membrane while, during the mitotic phase of the cell cycle, division of the nucleus also demands rapid production of nuclear-endoplasmic reticulum (ER) membrane. The outer nuclear membrane is continuous with the endoplasmic reticulum and any difference in ER morphology in general affects nuclear membrane. However in *Tetrahymena*, changes in the structural organization of the ER does not impact nuclear membrane morphology, since $\Delta TtPAHI$ cells does not manifest visible defect in size or shape of the nucleus (Pillai et al., 2017a). To find out whether *TtPAHI* retain the function of regulating nuclear membrane expansion, *pah1Δ* yeast cells were complemented with *TtPAHI* and rescue of the aberrant nuclear shape of *pah1Δ* cells were assessed. *TtPAHI* rescued the nuclear defects of *pah1Δ* yeast cells. Other phenotypes such as slow growth, temperature sensitivity, respiratory deficiency, derepression of lipid biosynthetic genes shown by *pah1Δ* cells were also assessed for rescue in complemented cells. This chapter discusses on the functional conservation of PAH proteins between yeast and *Tetrahymena* assessed by complementation of *pah1Δ* yeast cells with *TtPAHI*.

3.2 MATERIALS

3.2.1 Plasmids

pRS316-URA3-PUS1- GFP plasmid was obtained from Symeon Siniosoglou (University of Cambridge). Yeast centromeric plasmid YCplac 111with a LEU2 (Gietz and Akio, 1988)marker was obtained from Pankaj Alone (NISER, Bhubaneswar). *TtPAHI* coding sequence was commercially synthesised and obtained in the pUC57 vector from Eurofins.

3.2.2 Yeast strains and culture media

Δ *pah1* yeast strain (RS453 *smp2* Δ : *ade2 his3 leu2 trp1 ura3 smp2::TRP1*) was obtained from Symeon Siniosoglou (University of Cambridge). This was cultured at 30 °C in minimal medium containing 2.0 % glucose, 0.67 % Yeast Nitrogen Base along with adenine, leucine, uracil and histidine supplements or in YPD.

3.2.3 Other reagents

RNA Isolation kit was obtained from Promega. Superscript II reverse transcriptase for cDNA synthesis was from Invitrogen. SYBR Green qPCR mix for qPCR was obtained from Roche. Dextrose, yeast nitrogenous base, yeast extract, peptone and agar were from MP Biomedicals. Other chemicals and media components were from Sigma-Aldrich unless mentioned otherwise.

3.3 METHODS

3.3.1 Yeast culture conditions

Yeast cells were grown either in YPD media [nutrient base = 1% Yeast Extract + 2% Peptone and carbon source = 2% Dextrose] or Synthetic Defined (SD) medium (nutrient base = Yeast Nitrogenous Base with ammonium sulphate (0.67 %) and a carbon source = 2% Dextrose) with appropriate amino acids (Table 3.1) (Sherman, 2002). For growing Δ *pah1* cells adenine, leucine, uracil and histidine were added as supplements to complete the synthetic defined media. For selection of transformants and their culturing synthetic defined media containing adenine and histidine but lacking leucine and uracil were used. To check respiratory deficiency, dextrose was replaced by 2% glycerol as the carbon source. 2% agar was added to SD media or YPD media to make solid media plates.

Table 3.1: Amino acid composition for yeast in SD media

Sl. No	Amino acid	Stock concentration/100 ml of MQ Water	Amount needed to add for 250 ml media
1	Adenine	0.135 gm	3.75 ml
2	Leucine	1.31 gm	5 ml
3	Uracil	0.224 gm	2.5 ml
4	Tryptophan	0.8 gm	2.5 ml
5	Histidine	2.09 gm	750 µl

3.3.2 Gene Synthesis

The coding region of *TtPAH1* was commercially synthesized (Eurofins) after codon optimization and obtained in the pUC57 vector. This commercially synthesized gene was used for complementation assays in yeast. Before commercial synthesis TAA and TAG codons in the coding region of *TtPAH1* was replaced with CAA and CAG respectively. This codon change was done because TAA and TAG which codes glutamate in *Tetrahymena* (Horowitz and Gorovsky, 1985) represent stop codon in *Saccharomyces cerevisiae*. This sequence was further codon optimized using Integrated DNA Technology codon optimisation software for efficient expression in yeast and bacterial systems.

3.3.3 Cloning

The full-length coding sequence of *TtPAH1* was amplified using specific primers (Table 3.2) containing Sal I and BamH I restriction sites from the commercially synthesized *TtPAH1* in pUC57 vector. Table 3.3 mentions the PCR reactions and conditions used for amplification. The amplified product of right size was and cloned into YCplac111 (LEU) using SalI and

BamH1 restriction sites. The construct was confirmed by release of right sized product by restriction digestion and was further verified by sequencing. This construct (YCplac 111 *TtPAH1*) was used to complement Δ *pah1* yeast strain.

Table 3.2: Oligonucleotides used in chapter 3

No	Oligo Name	Sequence
1	TtPAH1 FP	GCGTCGACATGAGTGTTTTAAAAAACTACAG
2	TtPAH1 RP	GCGGATCCTCATTGCTTAATAGCTGGTTAAT
3	INO1 FP	CATGGTTAGCCCAAACGACT
4	INO1 RP	CGTGGTTACGTTGCCTTTTT
5	INO2 FP	TTCCAGCCAATATCGAGGAC
6	INO2 RP	AGTGCTTCATTTGCGCTTCT
7	OPI3 FP	ACATGGTGTACGAGTCTGCA
8	OPI3 RP	CATGGGGTTGTTGGAAACGT
9	SEC-63 FP	TCCTTGTCACAGGTGAGAAC
10	SEC-63 RP	ATGGGACGAGTGGCTGTTTA
11	TtPAH1mut FP	ATGTCCAGATTGTAATTCAGAGATAGAGGGAA CAATCACCAAATCTGATG
12	TtPAH1mut RP	CATCAGATTTGGTGATTGTTCCCTCTATCTCTGAA ATTACAATCTGGACAT

Table 3.3: PCR reaction mixture and conditions for amplification of *TtPAH1* using phusion polymerase to clone in YCplac 111

Reaction components	Volume (µl)	Temperature	Time	No. of cycles
Template (100 ng/µl)	1	98°C	1 minute	1
5X Phusion buffer	10	98°C	5 seconds	35
10mM dNTP	1	54	30 seconds	
Forward primer	1	72°C	1 minute 30 seconds	
Reverse primer	1	72°C	10 minutes	1
Magnesium chloride	1			
Phusion polymerase	0.5			
Water	34.5			
Total	50			

3.3.4 Site-directed mutagenesis

Point mutations (D666 to E666 and D668 to 668E) at the corresponding sites of *TtPAH1* coding region in *YCplac111-PAH1* fusion construct were introduced using Quik Change Site-directed mutagenesis protocol (Stratagene), and the mutations were confirmed by DNA sequencing. The primers used for mutagenesis are listed in Table 3.1.

3.3.5 Yeast Transformation

Pah1Δ cells were initially grown in 4ml YPD media at 30°C at 220 rpm for overnight. Next day this was culture was used to inoculate 10 ml SD media with appropriate amino acid supplements to get a starting OD₆₀₀ of 0.05. Cells were harvested at the mid-log phase (OD₆₀₀

around 0.7-0.8), in a sterile 50 ml centrifuge tube at 3000 x g (5000 rpm) for 5 min. The medium was poured off and the cells were washed once with TE (10 mM Tris-HCl. Cell pellet was further collected by centrifuging (5000 rpm for 5 min) and resuspended in 5ml of 100mM lithium acetate. Cells were again pelleted and further resuspended in 500µl of 100mM lithium acetate and was incubated for 30 minutes at 30⁰C in a water bath. After 30 minutes this was removed and kept in ice or stored at 4⁰C. This forms the *pah1Δ* competent cell which is ready to be transformed (Gietz and Woods, 2001).

3µg each of pRS316-URA3-PUS1-GFP (PUS –GFP) and YCplac 111 *TiPAHI* were added to a 1.5 ml centrifuge tube followed by 50µl of *pah1Δ* competent cells and 300µl of polyethelene glycol (PEG). This mixture was vortexed for 5 seconds and incubated at 30⁰C for 30 minutes followed by incubation at 42⁰C for 20 minutes. The pellet was collected by centrifuging for 4 min at 4,500 rpm at 4⁰C, dissolved in 150µl of water and spread plated on to SD plates with adenine and histidine but lacking leucine and uracil. The plates were incubated at 30⁰C in an incubator. The growth of transformants colonies was observed after 48 hours of spreading. The colonies were later picked and grown on SD media with corresponding amino acids.

3.3.6 Spotting

For growth analysis, yeast cells were grown in the SD media lacking leucine and uracil to early logarithmic phase ($OD_{600} \approx 0.8$ to 1.0). O.D. of each culture to be tested was normalised to 0.8 and was further serially diluted to 5 tenfold dilutions (10^{-1} , 10^{-2} , 10^{-3} , 10^{-4} , and 10^{-5}). 5µl of each dilution was spotted onto the solid SD media lacking leucine and uracil and incubated at either 30⁰C or 37⁰C for 2–3 days. Plates were examined and photographed at ≥ 72 h.

3.3.7 Confocal Microscopy

To visualise nucleus *pah1*Δ cells expressing PUS GFP and either YCplac111 (empty vector) or YCplac111-*TtPAH1* were grown in liquid SD media lacking uracil and leucine. When the cells reached OD₆₀₀ of 0.8 to 1.0, cells were harvested by centrifuging at 4000 rpm for 2 minutes. Cells were resuspended in minimum amount of media, 5 μl of these were dispensed on a glass slide, covered with cover slip and imaged at 63X oil objective in Zeiss 780 confocal microscope. Images were processed using LSM analyzer. The percentage of cells containing round nucleus was calculated. Three different transformants per strain were analyzed and the number of cells counted for each one was 200-250 (n= 600 to 750).

3.3.8 RNA isolation from yeast cells

All glasswares were washed with diethylpyrocarbonate (DEPC) treated water. Nitrile gloves were used to prevent RNase contamination. For RNA isolation cells at the exponential phase (OD₆₀₀ = 0.8) were pelleted down at 3,500 rpm for 5 minutes. The pellet was resuspended in 375 μl of Trizol. Glass beads were added to 1/10th volume of cell suspension and was lysed in a Fast prep bead beater (alternate 30 sec lysis and 1minute ice incubation with 15 repeats). 375 μl of Trizol was added again, mixed thoroughly and incubated at room temperature for 5 minutes. To this 150μl of chloroform: isoamyl alcohol was added, mixed by shaking for 15 seconds and further incubated for 2-3 minutes at room temperature. The tubes were spun at 12,000 g for 5 minutes at 4^oC and the topmost layer which contains the RNA was transferred to a new 1.5 ml centrifuge tube. 375μl of isopropanol was added to this and was incubated for 10 min. Pellet was collected (12,000 g for 5 minutes at 4^oC) and washed with 1 ml of 75% ethanol. This was centrifuged again at 7,500g for 5 min at 4^oC to collect the pellet. The pellet was air dried and was resuspended in 27μl of nuclease free water. The resuspended RNA pellet was further treated with DNAase 1(Table 3.4).

Table 3.4: DNase treatment mixture for RNA isolated from yeast cells

Components	Volume
RNA	25µl
DNAase 1	3µl
10x DNAase1 Buffer	1 µl

This mixture was incubated at 37⁰C for 2 hours. 1 µl of 0.5 M EDTA was added and the tube containing the mixture was heated at 75⁰C for 10 minutes in water bath to stop the reaction.

To this 70 µl of nuclease free water, 250 µl of RLT Buffer (RNA Isolation Kit Quiagen) and 350 µl of 70% ethanol was added. This mix was loaded on to a column (RNA Isolation Kit Quiagen) and further washed and eluted as per manufacturer's (RNA Isolation Kit Quiagen) instruction. RNA was eluted in 30 µl nuclease free water. RNA was quantitated by reading at A260. Quality of RNA was confirmed by A260/A280 (1.9-2.0), A260/A230 (2.0-2.2). RNA was stored at -80°C.

3.3.9 cDNA synthesis

10 µg of total RNA was used for cDNA synthesis (Invitrogen) using Superscript II reverse transcriptase with random hexamers as per the manufacturer's instructions.

3.3.10 Analysis of Gene Expression by quantitative real time PCR

Gene expression was analysed by reverse transcription PCR. For quantitative RT-PCR the product of these reactions was used using the Platinum SYBR Green qPCR (Roche) following manufacturer's instructions. Primer sequences used are summarized in Table 3.1. Normalization of each complemented strain was to the level of the empty vector control of the same cell type. The quantitative PCR was performed in 7500 Real-Time PCR System (Applied Biosystems) and the relative expression level of *INO1*, *INO2* and *OPI3* was calculated using the comparative Ct method after normalizing to SEC 63 as a control. Fold change was determined by relative quantitation method by determining 2- $\Delta\Delta$ Ct values. The

graph was plotted and significance was determined using the Student's t-test in GraphPad Prism V5 software.

3.3.11 Lipid Extraction from yeast

Yeast cells from a 50 ml culture at $OD_{600} = 1$ were harvested, washed in TE buffer were used for lipid extraction. Lipids were extracted using chloroform and methanol using Bligh and Dyer method. The cell pellet obtained was resuspended in 9 mL of autoclaved Milli Q water. Glass beads were added to $1/10^{\text{th}}$ volume of cell suspension and was lysed in a Fast prep bead beater (alternate 30 sec lysis and 1minute ice incubation with 15 repeats). Supernatant was collected and transferred to a separating funnel capped with the ground glass stopper and 10 ml of chloroform and 20 ml of methanol was added. The mixture was shaken thoroughly and then allowed to stand for 10 minutes. Then extra 10 ml of chloroform was added, mixed thoroughly and trapped gases were released. This was allowed to stand until two phases of separate out; a lower organic phase of lipid dissolved in chloroform and an upper polar phase. The lower phase was carefully drained and collected, avoiding any contamination from interface. The sample is then dried in a rotary evaporator at 40°C . This was further dried under a gentle stream of nitrogen in vacuum. The dried lipid was resuspended in 500 μl of chloroform: methanol (6:1 volume / volume ratio) by dissolving the entire lipid on the wall of the flask. This lipid dissolved in chloroform is transferred on to a glass vial and a gentle steam of nitrogen was passed before storing at -20°C . Extracted lipids were used within a month.

3.3.12 Thin layer chromatography

TLC tank was washed, dried completely and rinsed tank with chloroform and methanol. The solvent system was made consisting of Hexane: di-Ethyl Ether: Acetic Acid = 80:20:2 (80ml: 20ml: 2ml). The solvents were mixed in the order: acetic acid, di-ethyl ether and then hexane. Solvents were mixed to make sure it is uniform and quickly poured 100ml of solvent system

to the tank. Top of tank was covered with saran wrap and further covered with lid on top of saran wrap. The tank was allowed tank to equilibrate for 2 hr.

A line was drawn with a pencil across the plate with origin (~1 cm from bottom of plate). A vertical column, ½ inch from each end of the plate was cut using a razor blade with equal distance. Each column was marked with the name of the sample with the pencil. These plates were treated with 1.2% Potassium Oxalate 2mM EDTA in MeOH/H₂O (2:3). The plates were dried in an oven (110°C). Apply equal amount of isolated lipids on to the columns made on plate by pipetting the lipid + chloroform drop by drop so that it makes a small spot. The plates were dried using hair dryer between drops. 50ug of TAG (triacylglycerol) standard was also spotted. This plate was placed on the TLC tank with solvents and closed with lid to separate lipids. The samples were allowed to run till solvent front is around 1 inch from top. The plates were removed, dried and processed to develop spots for the lipids. Solution containing 3% Copper (II) acetate in 8% (v/v) phosphoric acid was applied to the TLC plate by a spray bottle in a fume hood. The plate is then heated in an oven set at 160⁰C for at least 10 min to develop darker spots. The plate was removed, scanned and the intensity of spots were analysed by Image J.

3.4 RESULTS

3.4.1 *TtPAH1* restores aberrant nuclear morphology of *pah1*Δ yeast strain

Though *TtPAH1* is not required for regulating nuclear expansion and nuclear shape in *Tetrahymena*, we asked whether the ciliate protein could rescue the nuclear defects in *S. cerevisiae pah1*Δ, which might be expected if the homologous proteins retain the same enzymatic activity. In Δ*pah1* yeast strain the nucleus in a non-dividing cell often consists of two lobes interconnected by a long nuclear membrane extension. *i.e.* the nuclear envelope is no longer spherical, but exhibits long protrusions extending into the cytoplasm. We also could observe single cells contain two nuclear compartments connected by a thin

membranous filament. The nuclear membrane organization is drastically altered in yeast mutants lacking *PAHI*. Long extensions of nuclear membrane which extend into the cytoplasm contained NPCs and an intranuclear content, but lacked any DNA.

To assess nuclear morphology in budding yeast, we expressed nucleoplasmic protein PUS as a GFP-fusion. As expected in *pah1* Δ cells, the nuclei in non-dividing cells appeared as two lobes interconnected by a long nuclear membrane extension (Figure 3.1, top panel). In contrast, *pah1* Δ cells expressing *TtPAHI* showed nearly normal nuclear morphology (Figure 3.1, bottom panel). This result suggests that *TtPAHI* retain the regulation of nuclear expansion function of the yeast homolog.

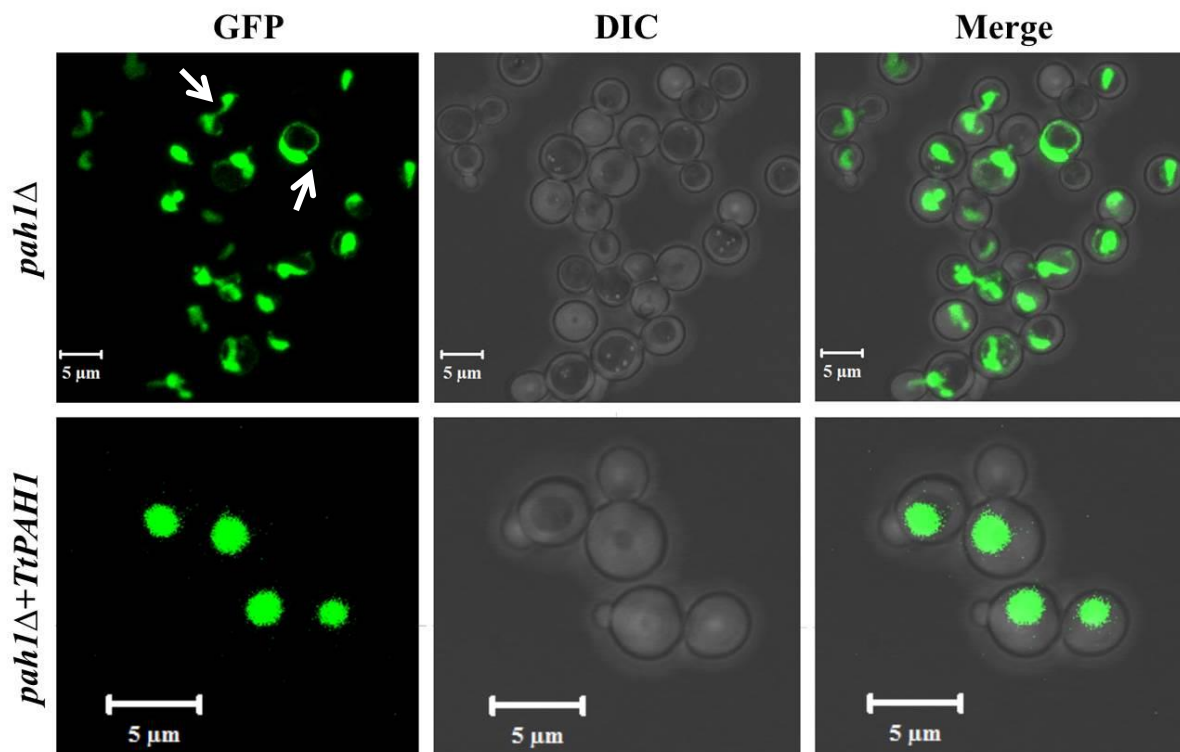


Figure 3.1: *TtPAHI* rescues the nuclear structure defect

Pah1 Δ yeast cells were transformed either with empty vector (top panel) or with *TtPAHI* (bottom panel) along with PUS1-GFP (an intranuclear reporter) and visualized by confocal microscope. *TtPAHI* restores defective aberrant nuclei of *pah1* Δ to wild-type spherical shape. Arrows indicate the aberrant nuclei of *pah1* Δ yeast cells

3.4.2 *TtPAH1* restores slow growth phenotype, temperature sensitivity and respiratory deficiency of *pah1*Δ yeast strain

*pah1*Δ yeast cell also exhibits slow growth at 30°C, temperature sensitive growth at 37°C and respiratory deficiency i.e. *growth* defect on non-fermentable carbon sources (Han et al., 2007; Han et al., 2006). Along with rescue of the nuclear morphology defect, expression of *TtPAH1* restored growth both at 30°C and 37°C (Figure 3.2A). To evaluate the role of *TtPAH1* in rescuing respiratory deficiency, we grew cells on plates containing either glycerol or acetate as non-fermentable carbon sources. The *pah1*Δ expressing *TtPAH1* grew faster than control *pah1*Δ cells (Figure 3.2B) suggesting that *TtPAH1* restores respiratory function of yeast homolog.

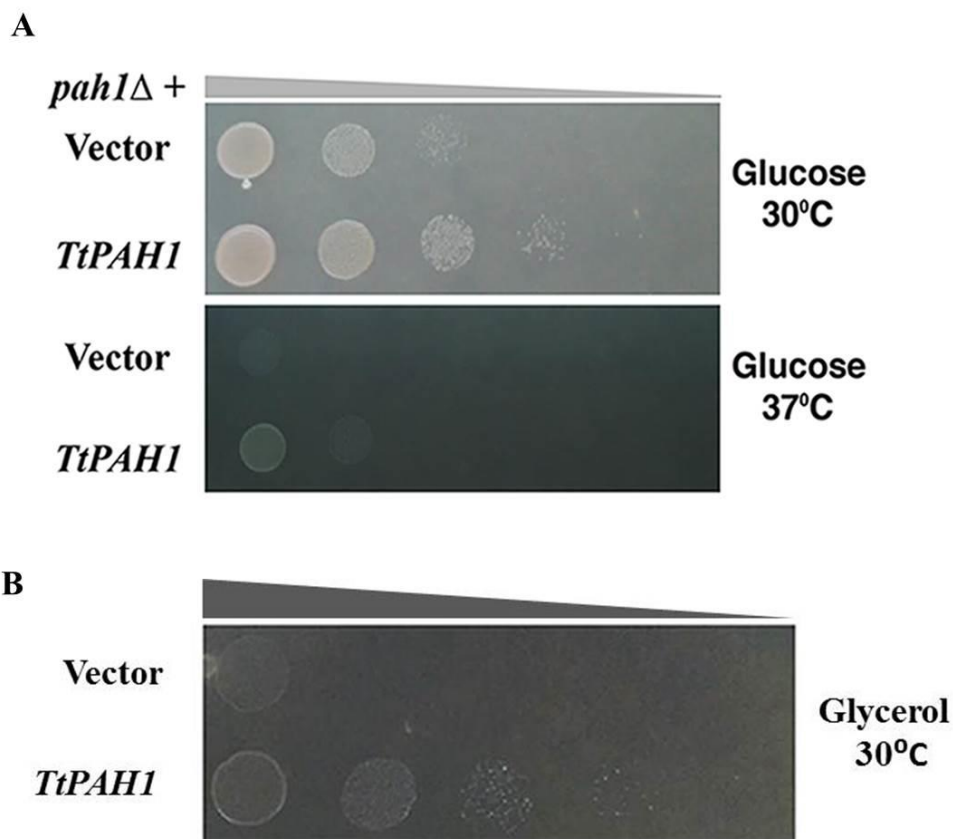


Figure 3.2: *TtPAH1* rescues the slow growth, temperature sensitivity and respiratory deficiency phenotypes of *pah1*Δ yeast cells.

A) *Pah1*Δ yeast cells transformed with either empty vector or *TtPAH1* were spotted on SD plates and grown at 30°C or 37°C for 2 to 4 days. B) For checking respiratory deficiency *pah1*Δ yeast cells transformed with either empty vector or *TtPAH1* were spotted on SD plates containing glycerol as carbon source and grown at 30°C for 2 to 4 days.

3.4.3 *TtPAH1* represses expression of genes involved in lipid biosynthesis and increases TAG level in *pah1*Δ yeast strain

Deletion of *PAH1* induces the expression of *INO1*, *INO2*, and *OPI3* involved in the induction of phospholipid biosynthetic genes leading to overly developed ER and aberrant expansion of nuclear membrane (Santos-Rosa et al., 2005). To test if *TtPAH1* inhibits abnormal nuclear expansion in *pah1*Δ yeast by inhibiting the phospholipid biosynthesis genes, we have analyzed the mRNA levels of *INO1*, *OPI3*, and *INO2* by quantitative real-time PCR using Sec 63 (a resident ER membrane protein unaffected by *PAH1* deletion) as a control. *TtPAH1* repressed expression of all the three genes tested (Figure 3.4A) suggesting that *TtPAH1* could replace yeast *PAH1* in regulating expression of phospholipid biosynthesis genes.

TAG content of the Δ*pah1* yeast strain was 62% lower than that of the wild type yeast. To check whether *TtPAH1* expression could increase level of TAG in Δ*pah1* cells, total lipids were extracted from both *pah1*Δ yeast and *pah1*Δ yeast complemented with *TtPAH1*. Extracted lipids were subjected to one dimensional thin layer chromatography to separate neutral lipids. Complementing *pah1*Δ yeast cells with *TtPAH1* could increase TAG levels of *pah1*Δ yeast cells (Figure 3.4B) suggesting *TtPAH2* could dephosphorylate PA in the yeast cells.

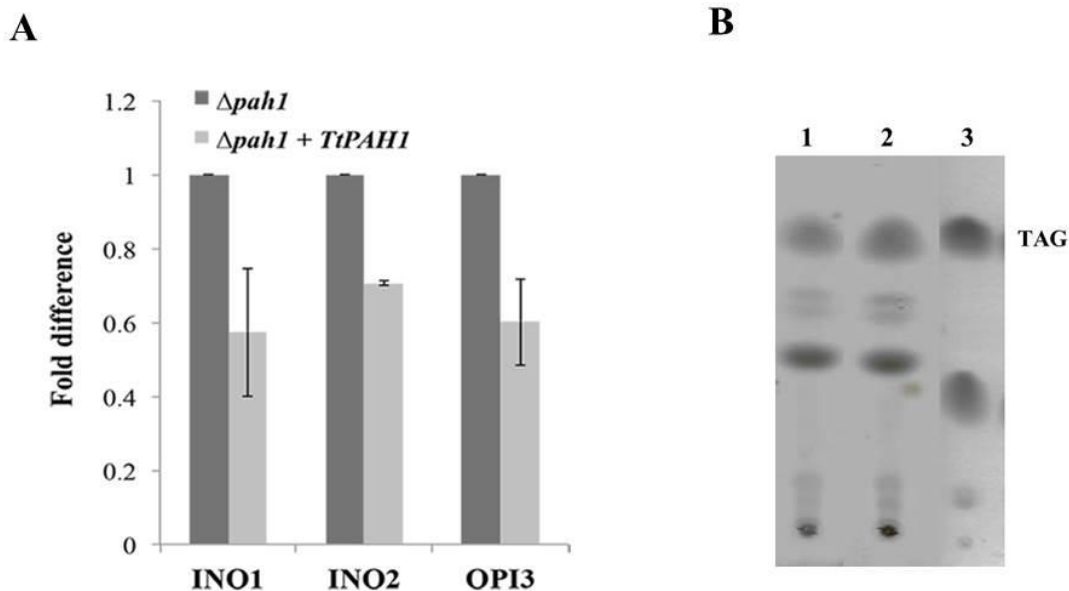


Figure 3.4: *TtPAH1* repress expression of genes involved in lipid biosynthesis

A) Levels of *INO1*, *INO2*, and *OPI3* mRNAs were analyzed by quantitative RT-PCR in *pah1* Δ yeast cells transformed with either empty vector or *TtPAH1*. Amplification of each sample was performed in triplicates and normalized to a control gene *SEC63*. B) *TtPAH1* increases TAG level in *pah1* Δ yeast strain. Total lipid isolated from yeast cells transformed with either empty vector or *TtPAH1* was spotted and run on one dimensional on TLC.

3.4.4 Catalytic motif of *TtPAH1* is essential for function

A conserved DXDXT/V motif at C-LIP is essential for the catalytic activity of PAH1/Lipin in yeast and mammals (Han et al., 2007; Finck et al., 2006). We have identified a similar motif (666 DIDGT 670) in the predicted C-LIP of *TtPAH1* and evaluated if the motif is important for the function of *TtPAH1* by mutating two aspartate residues (D666, 668E) (*TtPAH1_{mut}*). Since *TtPAH1* functionally replaces yeast *PAH1*, we complemented *pah1* Δ yeast cells with *TtPAH1_{mut}* and evaluated nuclear morphology, growth in different temperatures and media, and expression of phospholipid biosynthesis genes. Unlike wild-type *TtPAH1*, the mutant protein was unable to rescue aberrant nuclear morphology, slow growth at 30°C, and the respiratory defect (Figure 3.5A, 3.5B). As expected the catalytic motif mutant also did not reduce the expression of lipid biosynthetic genes such as *INO1*, *INO2*, and *OPI3* to the wild

type *TtPAH1* level (Figure 3.5C). These results suggest that catalytic activity of *TtPAH1* is important for its function.

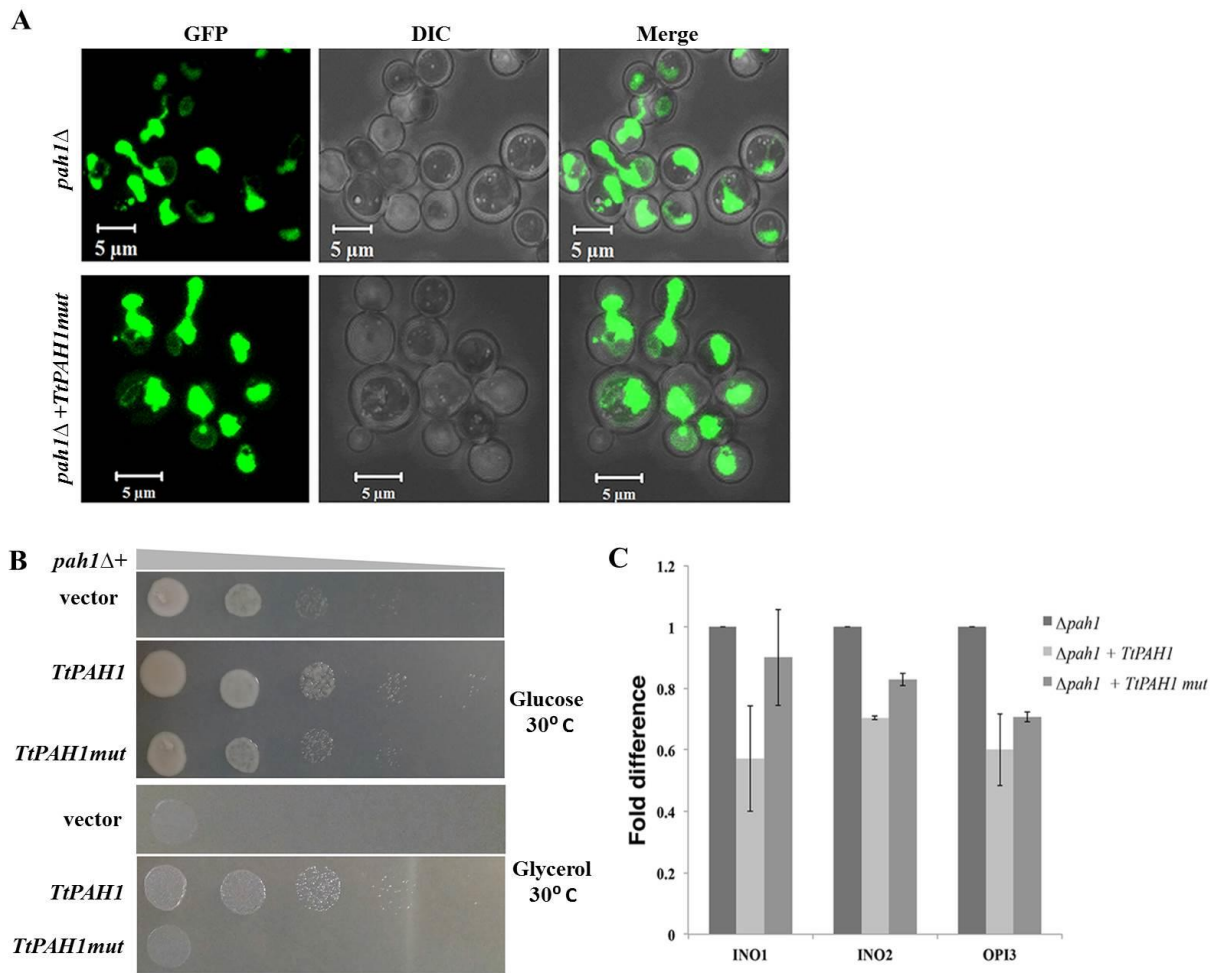


Figure 3.5: Catalytic mutant of *TtPAH1* could not rescue phenotypes of *pah1* Δ yeast cells.

A) *TtPAHmut* could not restore aberrant nuclei of *pah1* Δ yeast to wild-type spherical shape. Three different transformants per strain were analyzed and the number of cells counted for each transformant was 200-250. B) The growth of *pah1* Δ yeast cells transformed with either with empty vector, *TtPAH1* or *TtPAHmut* grown on SD media lacking leucine and uracil and containing either glucose or glycerol as indicated. C) Levels of *INO1*, *INO2*, and *OPI3* mRNAs were analyzed by quantitative RT-PCR in *pah1* Δ yeast cells transformed with either empty vector, *TtPAH1* or *TtPAHmut*.

3.5 DISCUSSION

Regulation of lipid homeostasis and membrane biogenesis is fundamental to all eukaryotes, and the presence of a regulation cascade comprising Pah1 and its phosphatase complex Nem1-Spo7 has been shown in yeast (Siniossoglou et al., 1998; Péterfy et al., 2001; Han et al., 2006; Golden et al., 2009, Nakamura et al., 2009). Previous work on mammalian lipins indicated that the *pah1*Δ yeast expression system could be used as a predictive model for confirming the functions of PAH1-homolog genes. *Tetrahymena* PAHs complemented the growth phenotype, temperature sensitive phenotype from the yeast *pah1*Δ strain.

Nuclear volume in *Tetrahymena* is variable likely due to differential ploidy level in the micronucleus (Raikov IB, 1976; Gorovsky MA, 1980; Bodenbender J, Prohaska A, Jauker F, Hipke H, 1992). In *Tetrahymena* there could be different mechanism that allows plasticity in nuclear expansion to accommodate different nuclear volumes. This could be the reason why nuclear membrane expansion or nuclear defect was not seen in Δ *TtPAH1* cells. Even though *TtPAH1* could not regulate nuclear morphology in *Tetrahymena* it could rescue the irregular shaped nucleus of *pah1*Δ yeast to round wild type nucleus. Similarly *LIPINs* in mammals do not regulate nuclear expansion, but have a role in nuclear envelope disassembly. This suggests that the regulation of nuclear expansion function is not intrinsic to the PAH family proteins and may have been adopted in yeast after divergence from other lineages. Similar to *PAH* from other organisms, mutation of the catalytic motif in *TtPAH1* leads to loss of function suggesting that the catalytic activity is necessary for its function. Taken together our results suggest that *TtPAH1* is orthologous to yeast *PAH1*.

CHAPTER 4

Analysis of conservation of PAH functions across eukaryotic clades

4.1 INTRODUCTION

The most used model for studying PAH function has been animal or fungal (Reue and Brindley, 2008)(Pascual and Carman, 2013). As a result the data of PAH function is biased towards a single eukaryotic lineage, Opisthokonta. PAH proteins are conserved among Opisthokonts with counterpart enzymes in humans, mice, flies, worms. In addition to Opisthokonta, PAH function is also known in plant that belongs to Archaeplastida clade. The PAH encodes a PAP enzyme is discovered in yeast and made studies on the orthologous PAP enzymes of other organisms possible. The PAH functions and the cascade they participate in are not known in organisms belonging to Amoebozoa, Alveolata, and Excavata A comparison of this enzyme between different eukaryotic lineages would help understanding the evolutionary conservation across eukaryotic lineages. By comparing PAH functions between organisms belonging to different lineages could produce a more accurate understanding of conserved features, and the variation that exists within them, and also of features that are limited to specific lineages. A broader, taxonomy-informed sampling would therefore provide a more accurate picture of the relative contributions made by inheritance versus innovation in the emergence of modern cells. In this chapter functional conservation of PAH across eukaryotic lineages is studied by complementation of *pah1*Δ yeast cells with *PAH* sequences from organisms belonging to different clades of eukaryotic lineages.

4.2 MATERIALS

4.2.1 Yeast strain, Plasmids and Other reagents

Yeast strains, plasmids and reagents used are the same as mentioned in chapter 3. *Trypanosoma brucei* genomic DNA was obtained from Dr. Laurie K. Read (SUNY at Buffalo). *Dictyostelium discoideum* cells were given by Dr. Roop Mallik, TIFR, Mumbai. *Arabidopsis thaliana* cDNA was obtained from Dr. KC Panigrahi, NISER, Bhubaneswar.

4.3 METHODS

4.3.1 Yeast culture conditions

Yeast culture media, conditions, and methods are exactly same as described in detail in chapter 3

4.3.2 Genomic DNA Isolation of *Dictyostelium discoideum*

For genomic DNA isolation $2-3 \times 10^7$ dictyostelium cells were used. The Cell pellet was loosened by scraping and were resuspended in 1 ml of nuclei buffer (20 mM Tris- HCl Ph-7.4, 5mM Magnesium Acetate, 0.5mM EDTA pH-8.0, 5% (w/v) sucrose) by gentle pipetting. 20% Triton X-100 was added and incubated on ice for 5min to lyse cells. The pellet containing the nuclei was collected by centrifuging at 12,000g for 5 min. The pellet was loosened by brief vortexing and resuspended in 300 μ l proteinase K buffer (100mM Tris HCl Ph-7.4, 5mM EDTA (Ph -8.0), 0.1 mg/ml proteinase K (add just before each use), 1% (v/v) SDS). This was incubated at 65^oC for 30 min. Nucleic acids were extracted by adding an equal volume (300 μ l) of phenol: chloroform. The upper aqueous layer was collected after centrifuging for 10 min at 12,000g. Aqueous layer was again collected after adding one volume (300 μ l) of chloroform and further centrifugation. The aqueous layer thus obtained was further precipitated with 2.5 volumes (750 μ l) of ice cold 100% ethanol. This was allowed to stand at room temperature for 5 min. The pellet DNA was collected by centrifuging at 12,000g for 15 min at 4^oC. Resuspend the white pellet at the bottom of the tube in 100 μ l TE Buffer pH-7.4 containing 10 μ g/ml RNase A and incubate for 15min at room temperature. The obtained DNA was further precipitated by adding 1/10th volume (10 μ l) of 3M Sodium acetate and 2.5 volumes (250 μ l) of ice cold 100% ethanol. This was placed on ice for 15 min at -20^oC and the pellet was collected by centrifuging at 4^oC for 15 min at 12,000g. The pellet was washed with two volumes (200 μ l) of ice cold ethanol and centrifuged for 2 min at 12,000g. The supernatant was removed with a pipette and the pellet was allowed to dry at room temperature. The DNA pellet was resuspended in 50 μ l of TE (pH 7.4)

4.3.3 Cloning of *TbPAH1*, *AtPAH2* and *DdPAH1*

The full-length coding sequence of PAH from *Trypanosoma brucei* (*TbPAH1*) was amplified using specific primers containing Xho I and BamH I restriction sites (Table 4.1) from genomic DNA. The full-length coding sequence of PAH from *Arabidopsis thaliana* (*AtPAH2*) was amplified using specific primers containing Sal I and BamH I restriction sites (Table 4.1) from genomic DNA. The full-length coding sequence of PAH from *Dictyostelium discoideum* (*DdPAH1*) was amplified using specific primers containing Sal I and BamH I restriction sites (Table 4.1) from genomic DNA. Table 4.2 mentions the PCR reactions and conditions used for amplification. The amplified right sized products of each PAH were cloned into YCplac111 (LEU)(Gietz and Akio, 1988) using SalI and BamHI restriction sites. The constructs were confirmed by release of right sized product by restriction digestion and was further verified by sequencing. These constructs YCplac 111 *TbPAH1*, YCplac 111 *AtPAH2*, YCplac 111 *DdPAH1* were used to complement $\Delta pah1$ yeast strain.

Table 4.1: Oligonucleotides used in chapter 4

No	Oligo Name	Sequence
1	TbPAH1 FP	GCCTCGAGATGATATCTGGTTTTGCAGATTTC
2	TbPAH1 RP	GCGGATCCTCACACAGTGTCACCTTGTTG
3	AtPAH2 FP	GCGTCGACCTCGAGATGAATGCCGTCGGTAGGATC
4	AtPAH2 RP	GCGGATCCGTTTAAACTCACATAAGCGATGGAGGAGG
5	Dd PAH1 FP	GCGTCGACATG AAT TAT GTT GAA AAG TTA TTT G
6	Dd PAH1RP	GCGGATCCCTA AAG AGG ATC TAA TTT ATG AAG

Table 4.2: PCR reaction components and conditions used for amplification of *TbPAH1*, *AtPAH2*, and *DdPAH1* using phusion polymerase

Reaction components	Volume (µl)	Temperature	Time	No. of cycles
Template (100 ng/µl)	1	98°C	1 minute	1
5X Phusion buffer	10	98°C	5 seconds	35
10mM dNTP	1	54, 60,56	30 seconds	
Forward primer	1	72°C	1 minute 30 seconds	
Reverse primer	1	72°C	10 minutes	1
Magnesium chloride	1			
Phusion polymerase	0.5			
Water	34.5			
Total	50			

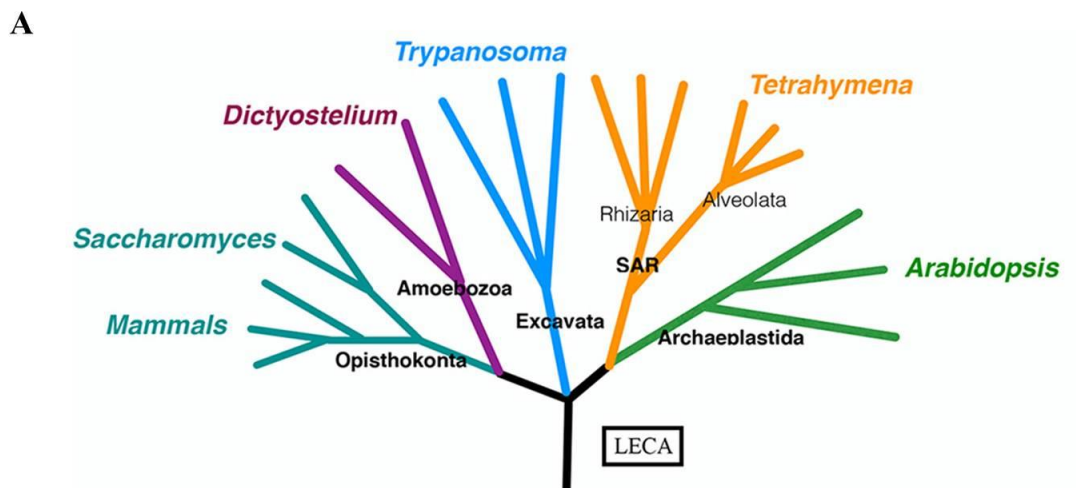
4.3.4 Sequences Used

Sequences of *Tetrahymena PAH* homologs (TTHERM_00189270 and TTHERM_00215970) were retrieved from Tetrahymena Genome Database. Multiple sequence alignment was performed with PRALINE. The sequences of PAH used in this chapter are; S000004775 for *Saccharomyces cerevisiae*, NM_001203528.1 for *Arabidopsis thaliana* (*AtPAH2*) and XM_841075 for *Trypanosoma brucei*, FBgn0263593 for *Drosophila melanogaster*, BC030537.1 for *Homo sapiens* and DDB_G0271730 for *Dictyostelium discoideum*.

4.4 RESULTS

4.4.1 Phosphatidate phosphatase (PAH) has similar domain organization and catalytic motif across eukaryotic lineages

Prior studies on the role of PAH proteins in the regulation of lipid homeostasis and membrane biogenesis have focused mainly on the Opisthokont and Archaeplastid clades. The cellular function of *PAH* is not known in organisms belonging to clades distantly related to Opisthokont. Figure 4.1A represents an evolutionary tree with representative organism for each clade. The sequence analysis of *PAH* homologs from organisms belonging to different clades suggest that it is conserved across eukaryotic lineages (Figure 4.1B). All these protein sequences shared similarity in two conserved regions: the N-LIP region with the conserved Glycine residue and C-LIP region harbouring the HAD like catalytic motif DXDXT/V.



B

<i>Saccharomyces cerevisiae</i>	PSQKKVQVFI	NEKLSNMPMK	LSDSGEAYFV	FEM	N-LIP
<i>Trypanosoma brucei</i>	PGDKVRIEV	NGQMTSAIMK	IGPNGEAFWL	KTT	
<i>Homo sapiens</i>	SREKVVDIEI	NGESVDLHMK	LGDNGEAFFV	QET	
<i>Drosophila melanogaster</i>	SREKVVDIEI	NGVPVDIQMK	LGDSGEAFFV	EEC	
<i>Tetrahymena thermophila</i>	SNEKIVTIKI	NDIIQKVTKM	MDSTGEAYFE	DIR	
<i>Dictyostelium discoideum</i>	SSAKVITIIYV	NGQKTDLQMK	LGQAGEAFFV	EES	
<i>Arabidopsis thaliana</i>	NGRNLIRIDV	NGVDSGFNMY	LAHTGQAYFL	REV	
<i>Caenorhabditis elegans</i>	YSDKYVDIAV	NGVEIDLKMK	LADSGVAFV	EEA	
Consistency	4458594939	*6434553*8	8546*7*886	463	
<i>Saccharomyces cerevisiae</i>	VTSK	LFVWRWDVPI	VISDIDGTIT	KSDALGHVL	
<i>Trypanosoma brucei</i>	VEAN	VYLWDSTDRL	VISDVDGTIT	KSDVLGHIM	
<i>Homo sapiens</i>	CEGT	IYLWNWDDKV	IISDIDGTIT	RSDTLGHIL	
<i>Drosophila melanogaster</i>	CKCY	LFRWKHNDKV	VISDIDGTIT	KSDVLGHIL	
<i>Tetrahymena thermophila</i>	LEGY	IYLWQSNVQI	VISDIDGTIT	KSDVLGQIM	
<i>Dictyostelium discoideum</i>	VSAS	IYYWDNSSKI	VISDIDGTIT	KSDVFGQVL	
<i>Arabidopsis thaliana</i>	VDAR	IYLWKWNSRI	VVSDVDGTIT	RSDVLGQFM	
<i>Caenorhabditis elegans</i>	CSCN	IYLYKWYEQI	VVSDIDGTIT	KSDVLGHVI	
Consistency	5543	8858534458	99**9*****	8**78*677	

Figure 4.1: Phosphatidate phosphatase has similar domain organization across eukaryotic lineages

(A) Eukaryotic evolutionary tree. Five clades with representative organisms from each clade are shown. (B) Multiple sequence alignments showing parts of N-LIP (Top) and C-LIP (Bottom) of PAH proteins from various organisms. Assigned colors of the specific residues are based on alignment consensus. The boxes indicate conserved Glycine at the N-LIP and conserved catalytic motif (DXDXT) at the C-LIP.

4.4.2 Phosphatidate phosphatases (PAH) are conserved across eukaryotic lineages

Putative PAH sequences from divergent species, namely *Dictyostelium discoideum* (representing amoebas), *Arabidopsis thaliana* (representing plants), *Trypanosoma brucei* (representing euglenozoans/excavates) were used for studying the functional conservation of PAH1 across diverse species. PAH from other species like *Caenorhabditis elegans* (representing nematodes), *Mus musculus* (representing mammals), and *Saccharomyces cerevisiae* (representing fungi) which represent Opisthokonts were already shown to exhibit phosphatidic phosphatase activity and complement each other in their cellular functions. This selection covered all major eukaryotic clades except Rhizaria due to non-availability of homologue in Rhizaria.

TbPAH1 rescued growth, respiratory and nuclear defects of *pah1Δ* yeast cells in the complementation assay (Figure 4.2 and 4.3). *PAH1* from *Dictyostelium discoideum* though mitigated nuclear defect and growth defect at 30°C (Figure 4.2 and 4.3); it did not rescue the temperature sensitivity of *pah1Δ* yeast cells. The *Arabidopsis PAH* homologs, *AtPAH1* and *AtPAH2*, have previously been shown to possess some functions of *S. cerevisiae PAH1* based on its ability to rescue the slow growth phenotype of *pah1Δ* yeast. However, it was not reported whether the plant homolog also rescues the nuclear envelope defect (Nakamura et al., 2009; Mietkiewska et al., 2011). We used *AtPAH2* to complement the *pah1Δ* yeast strain. In addition to rescuing the growth phenotype, *AtPAH2* mitigated the aberrant nuclear morphology of *pah1Δ* yeast cells, confirming conservation between Opisthokonta and Archaeplastida (Figure 4.2 and 4.3). Taken together, these results along with results from earlier reports suggest that the *PAH* phosphatase cascade is functionally conserved across

eukaryotic lineages, indicating that it originated before the lineages diverged in eukaryotic evolution.

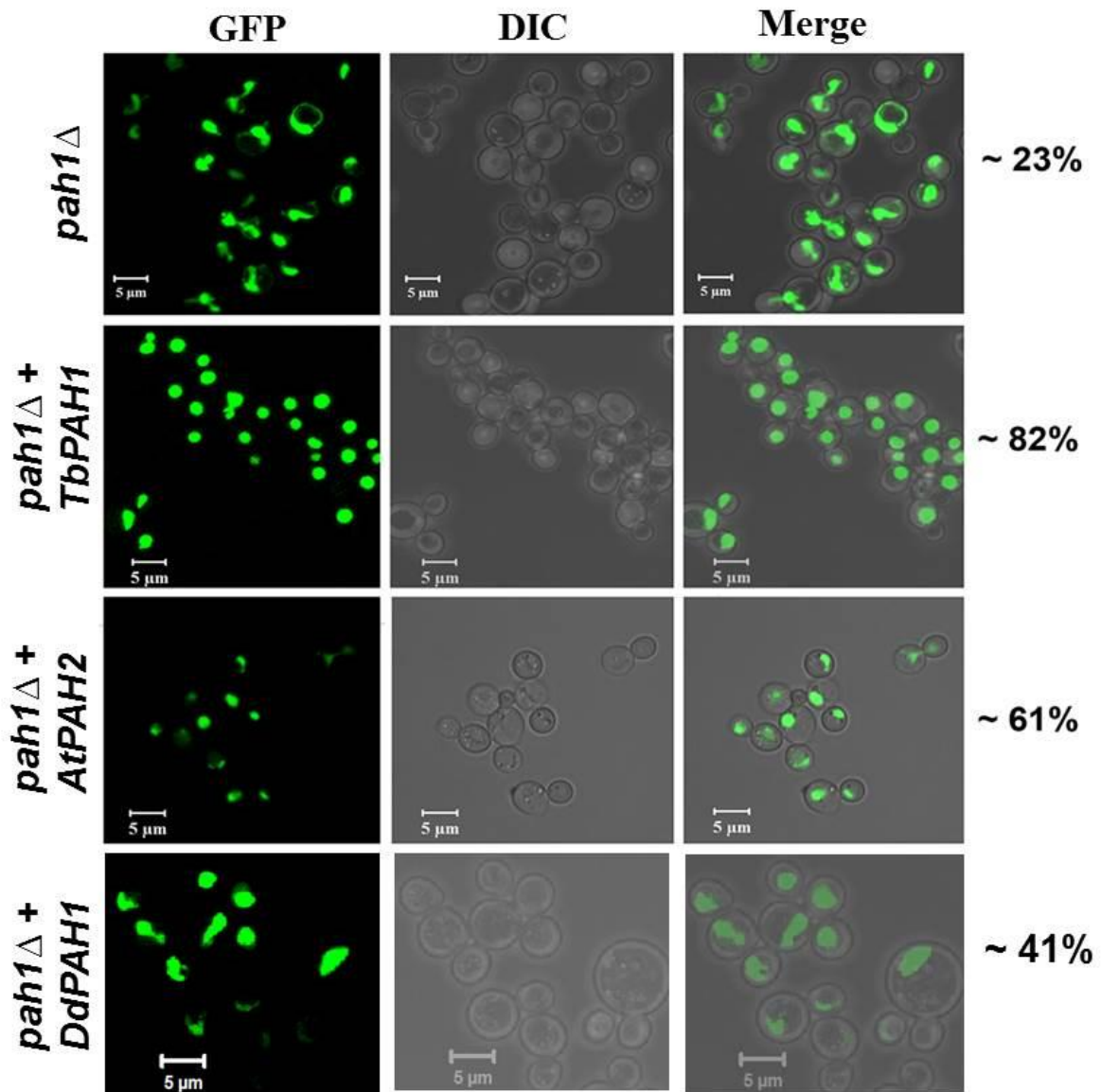


Figure 4.2: Regulation of nuclear envelope expansion function of PAH proteins are conserved across eukaryotic lineages

Confocal images of *pah1*Δ yeast cells complemented either with *Trypanosoma* PAH (*TbPAH1*) with *Arabidopsis* PAH (*AtPAH2*) or with *Dictyostelium discoideum* (*DdPAH1*). The nucleus is visualized by expression of *PUS-GFP*. Two different transformants per strain were analyzed and the number of cells counted for each one was 200 (n=400). The percentage of cells containing round nucleus is indicated on the right.

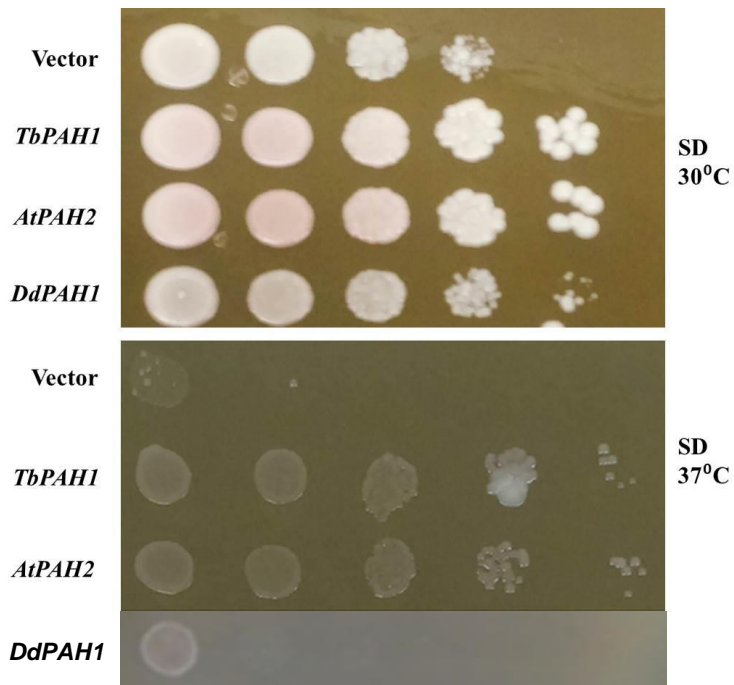


Figure 4.3: PAH proteins from Excavata and Plantae rescued growth phenotypes of yeast *pahl* Δ strains

Rescue of growth defect of *pahl* Δ yeast cells by *TbPAH1*, *AtPAH2* and *DdPAH1* on SD media containing glucose but lacking leucine and uracil at 30°C or 37°C as indicated. Two different transformants per strain were spotted and analyzed.

4.5 DISCUSSION

Regulation of lipid homeostasis and membrane biogenesis is fundamental to all eukaryotes, and the presence of a regulation cascade comprising Pah1 and its phosphatase complex Nem1-Spo7 has been shown in yeast (Siniosoglou et al., 1998; Péterfy et al., 2001; Han et al., 2006; Golden et al., 2009; Nakamura et al., 2009). Similar cascades are also reported in plants (Nakamura et al., 2009; Mietkiewska et al., 2011), mammals (Kim et al., 2007), worms (Golden et al., 2009; Gorjánác and Mattaj, 2009), and flies (Ugrankar et al., 2011). All the studies are restricted to Opisthokonta and Archaeplastida clades. *PAH* homolog is functionally interchangeable between Opisthokonta and Plantae (Nakamura et al., 2009)(Mietkiewska et al., 2011). The presence of such a cascade is not reported in the distantly related lower eukaryotic clades like Amoebozoa, SAR and Excavata.

In the present study *PAH* homologs from organisms representing the clades like Excavata, Amoebozoa and Alveolata are shown to functionally replace yeast *PAH1*. Therefore, this phosphatidic acid phosphatase cascade regulating membrane biogenesis and lipid homeostasis is conserved across the eukaryotic evolutionary tree. Therefore, it can be concluded that cascade comprising *PAH* for regulation of lipid homeostasis and membrane biogenesis was present in common ancestor before the divergence of lineages. *PAH*, in addition to lipid homeostasis and membrane biogenesis, has an additional role such as NEBD (in *C.elegans*) (Golden et al., 2009; Bahmanyar et al., 2014) and nuclear expansion (in yeast) (Santos-Rosa et al., 2005), suggesting that lineage-specific role of *PAH* is adopted after divergence from the common ancestor. Nuclear expansion function of *PAH* is restricted to yeast only. However, *PAH* homologs from all the lineages discussed here rescue abnormal nuclear expansion. Therefore, it can be concluded that though all the known functions of *PAH* were present before lineage divergence, different lineages have adopted these functions to regulate various cellular processes. Overall, the results from this study along with results from previous studies as discussed above clearly demonstrate a common regulatory cascade across eukaryotic lineages and may have appeared before the divergence of lineages. This shows that in the eukaryotic tree of evolution, *PAH* is functionally conserved and was possibly present in the Last Eukaryotic Common ancestor (LECA).

CHAPTER 5

Functional characterisation of Tetrahymena PAH2.

5.1 INTRODUCTION

There are two distinct families of PAP enzymes, magnesium dependent (PAP1) and magnesium independent (PAP2) (Pascual and Carman, 2013). Apart from the distinct cofactor requirement; they vary in their nature of membrane association. PAP1 enzymes are cytosolic or membrane associated proteins whereas PAP2 enzymes are integral membrane proteins (Pascual and Carman, 2013). In yeast PAP2 enzymes are encoded by *DPP* (diacylglycerol pyrophosphate phosphatase) and *LPP* (lipid phosphate phosphatase). These PAP2 enzymes are low molecular proteins with Dpp having 289 amino acids and Lpp with 274 amino acids. The yeast PAP1 enzyme is encoded by *PAH* which has 862 amino acids. *PAH* homologs in other organism including mammals, *C.elegans*, *Arabidopsis thaliana*, *Drosophila melanogaster* are all high molecular weight proteins comparable to yeast.

Tetrahymena possesses two *PAH* homologs, *TtPAH1* and *TtPAH2*. *TtPAH1* encodes a protein of ~ 96kDa, similar in size to PAH proteins of other organisms. *Ttpah2* with length of 335 amino acids is much smaller than known PAH homologs but is similar in size with Dpp and Lpp enzymes which are the magnesium independent PAP2 enzymes. Low molecular weight PA phosphatase exhibiting Mg²⁺-dependent phosphatidate phosphatase activity is not known in any organism. This chapter focuses on functional characterisation of *Tetrahymena PAH2* by

- 1) Amino acid sequence analysis
- 2) Assessing phosphatidic acid phosphatase activity *in vitro*.
- 3) Evaluating whether *Ttpah2* belongs to PAP1 or PAP2 family
- 4) Sub-cellular localization
- 5) Assessing role of *TtPAH2* in maintaining endoplasmic reticulum morphology

5.2 MATERIALS

5.2.1 Plasmids

Tetrahymena specific expression vector pIGF was a gift from Doug Chalker, Washington University. Plasmid vector pET 33b was obtained from Prof. M.S. Shaila, IISc, Bangalore.

5.2.2 *Tetrahymena thermophila* strains and culture media

Tetrahymena strains and culture media used are as described in chapter 2. *TtPAH2* knock out strain ($\Delta Ttpah2$), already available in the laboratory was used.

5.2.3 *E.coli* and culture media

E.coli strain of BL-21(DE3) was obtained from Prof. M.S. Shaila, IISc, Bangalore.

E.coli cells were grown in LB broth at 37⁰C, 220 rpm.

5.2.4 Other reagents:

ER Tracker Green and pENTR/D-TOPO kit were obtained from Invitrogen. Phosphatidic acid was obtained from MP Biomedicals. Protease inhibitor cocktail was obtained from Roche. Other chemicals and media components were from Sigma-Aldrich unless mentioned otherwise.

5.3 METHODS

5.3.1 Cloning:

To generate the *TtPAH2-GFP* construct, full-length *TtPAH2* was amplified from genomic DNA using specific primers (Table 5.1). Table 5.2 mentions the PCR reactions and conditions used for amplification of the gene. The amplified product was cloned into an entry vector using pENTR/D-TOPO kit (Invitrogen). This was further cloned into the destination vector pIGF (an rDNA-based expression vector) using LR clonase (Invitrogen). The construct was screened by mobility shift following PCR checking and finally confirmed by sequencing.

Table 5.1: Oligonucleotides used in chapter 5

No.	Oligo Name	Sequence (5' to 3')
1	<i>TtPAH2</i> -GFP	CACCATGCATCACCATCACCATCACATGATTAACGGAATT AAAAATC
2	<i>TtPAH2</i> -GFP	TCATTTTGGTAATTGCTTATT

Table 5.2: PCR reaction components and conditions used to amplify *TtPAH2* using phusion polymerase

Reaction components	Volume (µl)	Temperature	Time	No. of cycles
Template (100 ng/µl)	1	98°C	1 minute	1
5X Phusion buffer	10	98°C	5 seconds	35
10mM dNTP	1	55	30 seconds	
Forward primer	1	72°C	1 minute 30 seconds	
Reverse primer	1	72°C	10 minutes	1
Magnesium chloride	1			
Phusion polymerase	0.5			
Water	34.5			
Total	50			

5.3.2 Preparation of cell extracts and Western blotting

Wild type cells expressing *TtPAH2* GFP ($4-5 \times 10^5$) was used to prepare cell lysate. Cell lysate preparation, separation into membrane and cytosolic fractions, and detection of *Ttpah2* in the fractions was done as described in chapter 2.

5.3.3 Endoplasmic Reticulum staining

Endoplasmic reticulum of wild type and $\Delta Ttpah2$ were stained with ER-Tracker™ Green dye as described in chapter 2. ER-Tracker Green images were taken at 504 nm excitation /511 nm emissions as described in chapter 2.

5.3.4 Gene synthesis

The coding region of *TtPAH2* was commercially synthesized (Eurofins) after codon optimization and obtained in the pUC57 vector. Codon modification and optimization was done as described in chapter 3 for *TtPAH1*. This commercially synthesized *TtPAH2* cloned in pET33b using BamHI and NdeI restriction sites was used to express *TtPAH2* in bacteria.

5.3.5 Purification of recombinant Ttpah2 in *E.coli*

The *TtPAH2*- pET33b construct was transformed into BL-21(DE3) strains of *E.coli* to express as N-terminal His₆ fusion protein. BL-21(DE3) cells expressing TtPAH2 were cultured in LB broth supplemented with 50µg/ml kanamycin and grown at 37°C with 220 rpm till the OD₆₀₀ reached 0.4. At this density, the culture was induced with 1 mM IPTG and allowed to grow for 5 hours under same conditions. Cells were harvested by centrifugation at 5000 RPM in 4 °C. Cell pellet was resuspended in 50 ml of ice-cold buffer containing 25mM HEPES pH 7.5, 300mM NaCl, 2mM MgCl₂, 2mM β-mercaptoethanol and 10% glycerol (Lysis Buffer) supplemented with EDTA-free protease inhibitor cocktail (Roche) plus 100mM phenylmethane sulfonyl fluoride (Sigma). The cells were lysed by sonication and the crude lysate was centrifuged at 15,000 r.p.m for 45 mins at 4°C. Ni-NTA resins equilibrated with lysis buffer were added to the clarified lysate and incubated for 2 hours. The resin was washed with a 100-bed volume of lysis buffer supplemented with 50mM imidazole and the protein was eluted with 250mM imidazole in the same buffer. The purified protein was checked by coomassie stained SDS-PAGE gel.

5.3.6 Phosphatase Assay

Phosphatase assay was done as mentioned in chapter 2. To check phosphatase activity of recombinant Ttpah2-His6 with increasing protein concentrations phosphatase activity was measured with 0.25 μ M, 0.5 μ M, 1 μ M, 1.5 μ M and 2.0 μ M for 20 minutes.

5.4 RESULTS

5.4.1 Sequence analysis of Ttpah2

Ttpah2 is a small molecular weight protein consisting of 336 amino acids. The amino acid sequence of Ttpah2 was analysed using Interpro: protein sequence analysis & classification (<https://www.ebi.ac.uk/interpro/>). TtPah2 has 34% identity with human lipin and 22% with yeast Pah1. Similar to other phosphatidic acid phosphatases, the amino acids are more conserved in the N-LIP and C-LIP regions of Ttpah2. N-LIP of Ttpah2 has 35% and 30% identity with yeast Pah1 and human lipin1 respectively. C-LIP has 44% identity with both yeast Pah1 and human lipin1. Interpro predicted an N-terminal domain (N-LIP, amino acids 9 to 99), a lipin specific domain (amino acids 142 to 294) and a C-terminal HAD like domains (C-LIP, amino acids 138 to 281) which are characteristic of PAP1 proteins. Moreover, all Magnesium dependent phosphatidic acid phosphatases contain an essential catalytic DXDXT/V motif in the HAD-like domain of the C-LIP region. A similar motif (146 DVDGT 150) was also found within the C-terminal HAD like domain of Ttpah2 suggesting it to be a Mg^{2+} -dependent phosphatidate phosphatase (Figure 5.1 and 5.2). A conserved glycine residue in N-terminal domain is critical for PAH function since its mutation in mammalian lipin1 causes lipodystrophy. Similar conserved Glycine residue was also present at the 79th position of N-LIP region of Ttpah2 (Figure 5.1 and 5.2). These results suggest that Ttpah2 is a potential Mg^{2+} -dependent PAP1 enzyme.

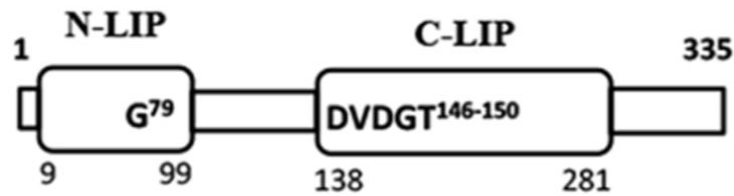


Figure 5.1: Domain organisation of TtPAH2

Predicted N-LIP and C-LIP domains are indicated in the boxes. Also shown are the positions of a conserved glycine residue in N-LIP and the haloacid dehalogenase (HAD) with its conserved DXDXT/V motif in C-LIP.

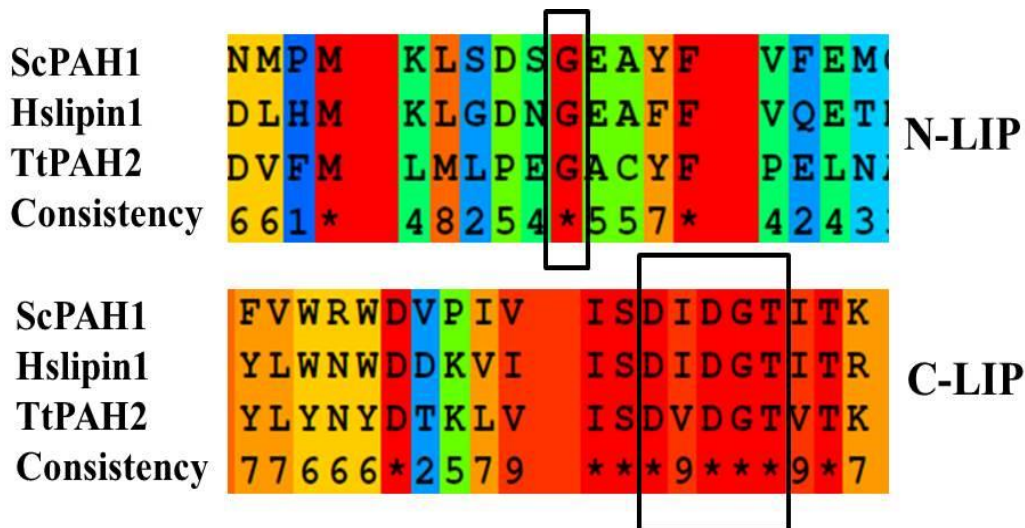


Figure 5.2: Sequence analysis of Ttpah2

Alignments of amino-acid sequences of a part of N-LIP and HAD-like domain in C-LIP of TtPAH2 with yeast PAH1 and human LIPIN1 using PRALINE. Assigned colors of the specific residues are based on alignment consensus. Conserved Glycine residue in N-LIP and catalytic motif (DXDGT/V) in C-LIP are indicated inside the box.

5.4.2 Ttpah2 is a magnesium dependent phosphatidate phosphatase belonging to PAPI family

The enzymatic activity of recombinant Ttpah2 was examined by an *in vitro* phosphatase assay. For this purpose, *TtPAH2* was expressed in bacteria and purified as N-terminal His6 fusion protein. The purity of protein, migrating at ~37 kDa, was confirmed by SDS-PAGE (Figure 5.3A). Phosphatase activity was measured following the release of inorganic phosphate (Pi) from phosphatidic acid. Recombinant Ttpah2 dephosphorylated PA in a concentration and time-dependent manner (Figure 5.3B and 5.3C).

Phosphatidate phosphatase activity of Ttpah2 was checked in the presence and absence of magnesium to find whether Ttpah2 is Mg^{2+} -dependent (PAP1) or Mg^{2+} -independent (PAP2) phosphatidic acid phosphatase. Ttpah2 did not show any detectable phosphatase activity in the absence of magnesium ions (Figure 5.3D). This confirmed that Ttpah2 is a Mg^{2+} -dependent phosphatidic acid phosphatase belonging to PAP1 family.

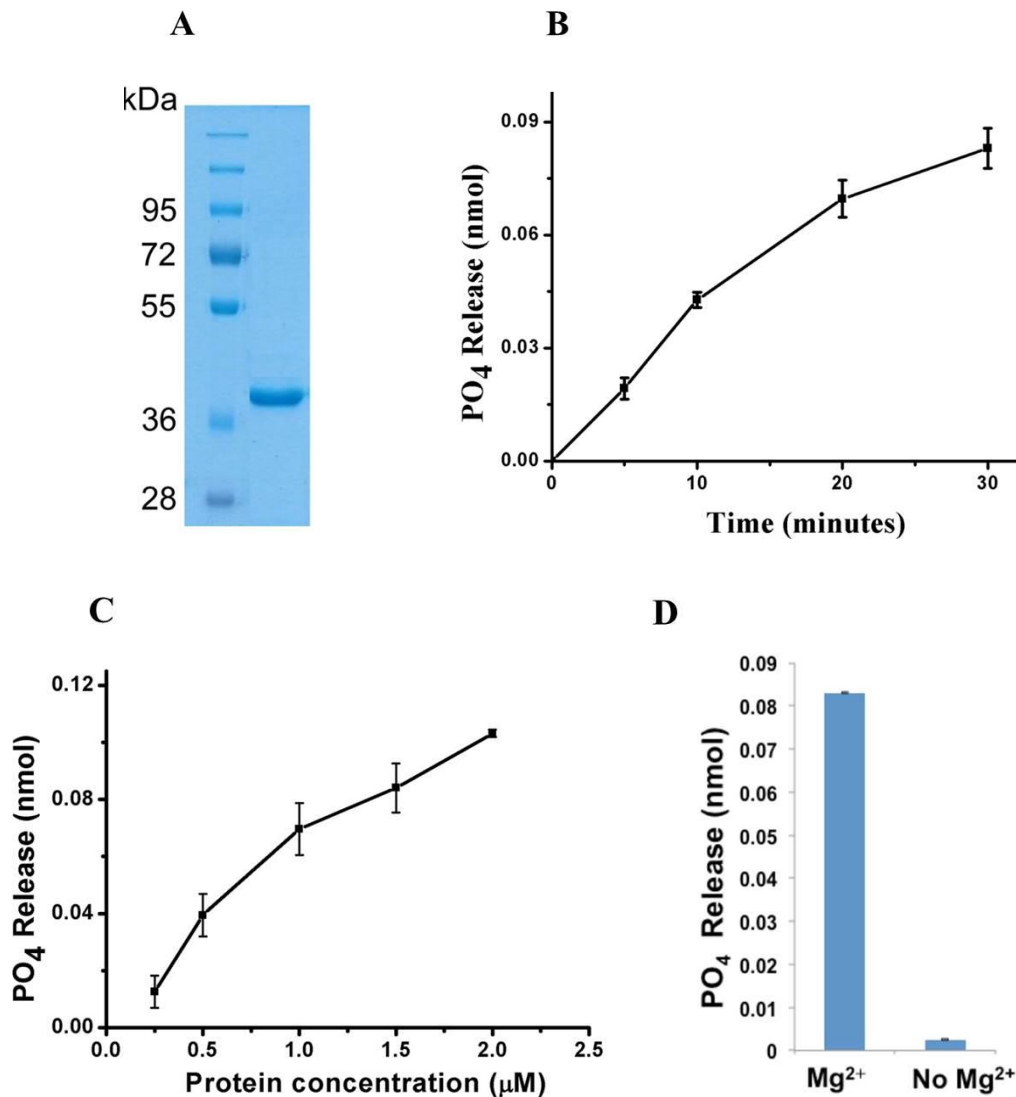


Figure 5.3: TtPah2 encodes a magnesium dependent phosphatidate phosphatase

A) SDS-PAGE gel showing purified Ttpah2-His6 after staining with Coomassie blue. Positions of the molecular weight markers (kDa) are indicated on the left. B) The phosphatidic acid phosphatase activity using $1\mu M$ recombinant TtPah2-His6. C) The phosphatidic acid phosphatase activity of recombinant Ttpah2-His6 was measured with increasing protein concentrations for 20 minutes. D) The phosphatidic acid phosphatase activity of $1\mu M$ recombinant Ttpah2-His6 measured for 20 minutes either in the presence (Mg^{2+}) or in the absence (No Mg^{2+}) of magnesium.

5.4.3 *TtPAH2* localizes to both cytoplasm and membranes

Subcellular localization of Ttpah2 was checked by expressing *TtPAH2-GFP* in *Tetrahymena*. Confocal image analysis showed the distribution of Ttpah2-GFP throughout the cell (Figure 5.4A). Total cell lysate of *Tetrahymena* cells expressing *TtPAH2-GFP* was fractionated into the membrane and cytosolic fractions and Ttpah2 was detected in both fractions using anti-GFP antibody (Figure 5.4B). These results suggest that Ttpah2 shuttles between the cytoplasm and ER similar to other known PAH proteins.

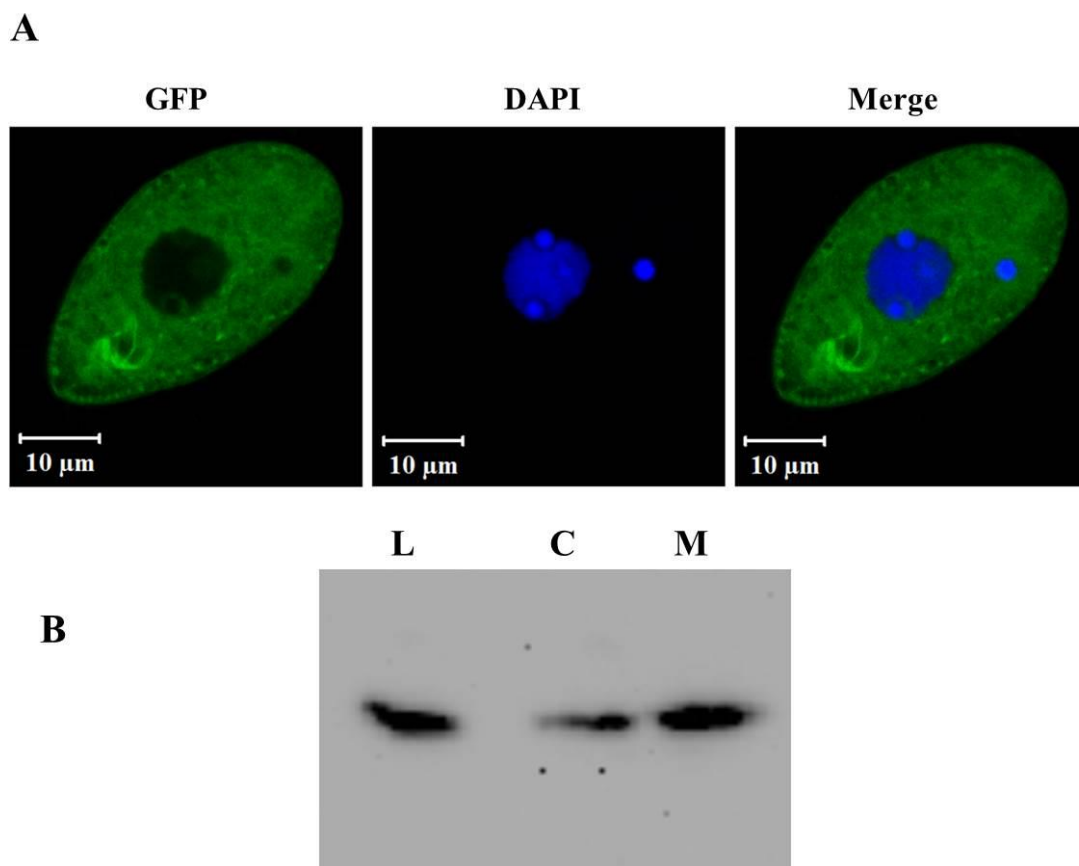


Figure 5.4: TtPAH2 localizes to both cytosol and membranes

A) Sub-cellular localization of Ttpah2 in *Tetrahymena* cells. Fixed *TtPAH2-GFP* expressing *Tetrahymena* cells were imaged after DAPI staining. Ttpah2-GFP (left panel), DAPI stained nuclei (middle panel) and merged image (right panel). (B) Western blot analysis of the total lysate (L), cytosolic fraction (C) and membrane fraction (M) obtained from *Tetrahymena* cells expressing *TtPAH2-GFP* using anti-GFP antibody.

5.4.4 *TtPAH2* does not regulate ER morphology in *Tetrahymena*

PAH regulates ER morphology in organisms like yeast, *C.elegans*, mammals, *Arabidopsis*. Also *TtPAH1*, the large homolog in *Tetrahymena* regulates ER morphology and ER content as mentioned in chapter 2. To find out if *TtPAH2* regulates ER morphology, both $\Delta Ttpah2$ and wild-type cells were stained with ER-Tracker dye and both ER structure and content were evaluated by analyzing confocal images (Figure 5.5 A). The ER morphology of $\Delta Ttpah2$ cells was similar to the wild-type cells. Moreover, total ER content of $\Delta Ttpah2$ cells was comparable to that of wild-type cells as analysed by Image J (Figure 5.5B). These results conclude that *TtPAH2* which encodes a functional phosphatidate phosphatase does not regulate ER morphology.

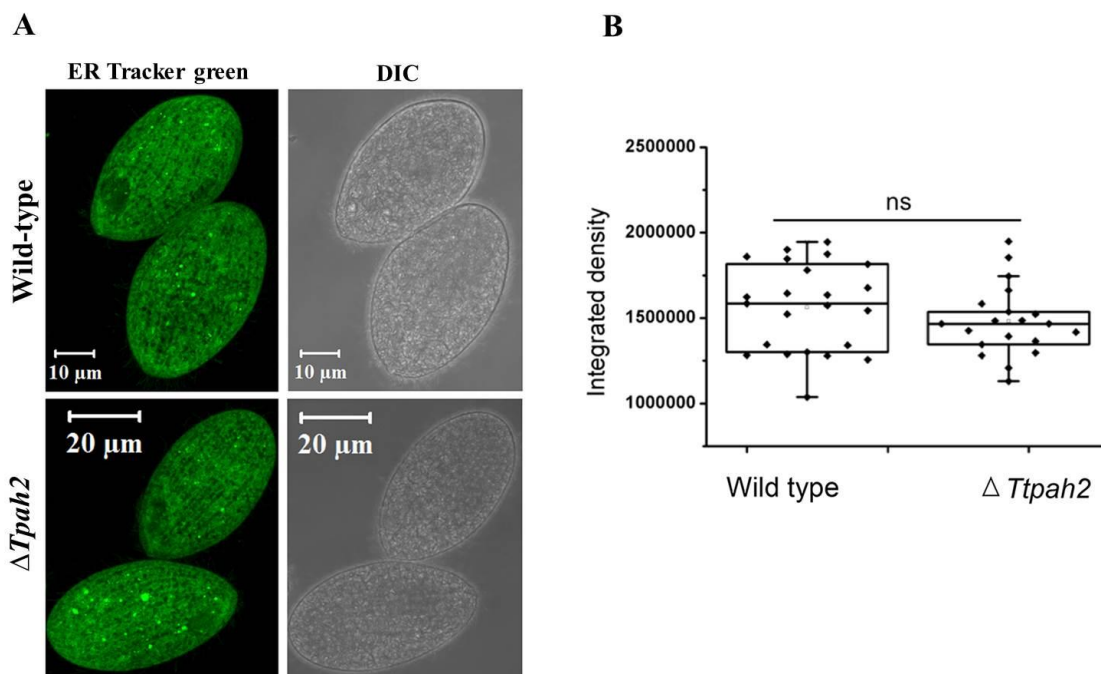


Figure 5.5: *TtPAH2* does not regulate ER morphology

A) Confocal images of wild-type and $\Delta Ttpah2$ cells stained with ER-Tracker Green showing ER morphology. B) Box plot showing the mean density of ER in wild-type and $\Delta Ttpah2$ cells as measured by sum intensity projection of the stacked images. The mean intensity of $\Delta Ttpah2$ (n=20) is similar to that of wild-type (n=23) as analysed by Oneway ANOVA (ns is non significant, $p < 0.051$).

5.5 DISCUSSION

All Mg^{2+} -dependent phosphatidate phosphatases previously characterized are relatively large proteins, close to 100 kDa and low molecular weight proteins showing PA phosphatase activity are usually Mg^{2+} -independent. However, Ttpah2 is a low molecular weight (37 kDa) PAH homolog in *Tetrahymena* exhibiting Mg^{2+} -dependent phosphatidate phosphatase activity. TtPAH2, being the PAP1 enzyme, is anticipated to regulate ER morphology since all the known PAH homologs from other organisms including the large PAH homolog (*TtPAH1*) in *Tetrahymena* regulates ER morphology. Studies in yeast, *C. elegans*, and *Drosophila* show that changes in PA homeostasis are responsible for controlling the morphology of ER, nucleus, and other cell organelles (Carman and Han, 2009; Golden et al., 2009; Ugrankar et al., 2011; Bahmanyar et al., 2014). Even though Ttpah2 dephosphorylated phosphatidic acid *in vitro*, deletion of *TtPAH2* did not affect ER morphology in *Tetrahymena*. This might be due to the presence of the other homolog, *TtPAH1*. However, *TtPAH1* and *TtPAH2* show non-overlapping expression in different cell cycle stages suggesting that *TtPAH2* has a specialized role in *Tetrahymena*. Ttpah2 is the first example of a low molecular weight magnesium dependent phosphatidate phosphatase.

Previous studies show that catalytic activity of PAH proteins is essential for its function in lipid homeostasis and membrane biogenesis (Han et al., 2007). But our results show catalytic activity alone is not sufficient for regulating ER morphology and lipid droplet biogenesis in *Tetrahymena* (Pillai et al., 2017b). These results suggest that the amino acid sequences absent in Ttpah2 but present in other PAH proteins may be critical for performing these cellular functions. The exact role of *TtPAH2* in *Tetrahymena* needs to be investigated.

Summary and Conclusion

Summary

PAP1 enzymes are Mg^{2+} dependent phosphatidate phosphatases catalysing the penultimate step in triglyceride synthesis, the dephosphorylation of phosphatidic acid (PA), to generate diacylglycerol needed for the synthesis of TAG and phospholipids (PE and PC) (Han et al., 2006). PAP1 enzymes in mammals are encoded by *LIPIN* genes whereas *PAH1* is the yeast homolog (Han et al., 2006). PAH proteins reside in the cytoplasm and translocate to the nuclear/ER membrane where it binds its substrate (PA) and catalyzes the enzymatic reaction. Phosphorylation and dephosphorylation at multiple sites regulate the activity and subcellular localization of PAH proteins. In yeast, CDC28 phosphorylation of Pah1p is critical for cell cycle progression while phosphorylation by PHO85 plays other roles; in mammals, mTOR kinases phosphorylate lipins (Laplante and Sabatini, 2009; Peterson et al., 2011; Choi et al., 2012). Dephosphorylation of PAH1 by a nuclear/ER membrane complex consisting of a catalytic phosphatase subunit NEM1, and its regulatory subunit, SPO7, activates its catalytic function and recruit it to the ER membrane where it acts on its substrate PA (Han et al., 2007). Apart from an enzymatic role, yeast PAH1 and mammalian lipin1 also act as transcriptional regulators (Santos-Rosa et al., 2005; Kim et al., 2013). Deletion of *PAH1* leads to reduced lipid droplet number, aberrant nuclear expansion, over developed ER membranes, and slow growth phenotype in yeast (Santos-Rosa et al., 2005; Adeyo et al., 2011). In metazoans, lipin regulates nuclear envelope breakdown, ER homeostasis, organelle morphology, phospholipid levels and lipid storage (Gorjánác and Mattaj, 2009; Golden et al., 2009; Ugrankar et al., 2011; He et al., 2017). Several human metabolic diseases are associated with mutations in genes encoding lipin protein (Müller-felber et al., 2010). Thus, PAH proteins play a crucial role in lipid storage, membrane biogenesis, and organelle morphology and are evolutionarily conserved. Studies of phosphatidic acid phosphatase have focused on Opisthokonta (fungi, nematode, flies, and animals) and Plantae clades. In contrast, these enzymes and the

regulatory cascades in which they participate are not reported in organisms including Amoebozoa, Alveolata, and Excavata.

Tetrahymena which belongs to Alveolata is a single-celled ciliate with two distinct nuclei, a transcriptionally active somatic macronucleus, and a transcriptionally silent germline micronucleus which shows membrane complexity comparable to higher organisms (Rahaman et al., 2008). There are two homologs of phosphatidic acid phosphohydrolase gene (*TtPAH1* and *TtPAH2*) in the genome database of *Tetrahymena thermophila*. The presence of two *PAH* homolog in a lower eukaryote, like *Tetrahymena*, is unusual since multiple homologs are mainly found in higher organisms. The findings from our study show that *TtPAH1* encodes a protein of ~ 96kDa, similar in size to PAH proteins from other organisms. TtPAH1 displayed cytoplasmic as well as membrane localization consistent with previously characterized mammalian and yeast PAH. The deletion of *TtPAH1* in *Tetrahymena* resulted in drastic reduction in lipid droplet number. *TtPAH1* also mitigated reduced TAG levels in yeast, suggesting that the role of *PAH1* in TAG synthesis and lipid droplet biogenesis is also conserved in *Tetrahymena* similar to yeast. PAH proteins are known to regulate ER morphology in yeast and *C.elegans*. Deletion of macronuclear copies of *TtPAH1* in *Tetrahymena* also altered ER morphology resulting in an increased proportion of sheet to tubule structure suggesting their role in regulating ER morphology. In *S. cerevisiae*, where cells lacking *PAH1* showed abnormal expansion of nuclear envelope, but deletion of *TtPAH1* did not cause not visible defect in size or shape of the NE. This suggests that defects in ER morphology in *Tetrahymena* do not necessarily affect nuclear morphology, unlike the coupling in yeast. Mutation of the catalytic motif in TtPAH1 leads to loss of function suggesting that the catalytic activity is necessary for its function. *PAH* homologs from the lineages including Plantae, Amoebozoa and SAR (represented by Alveolata) rescued abnormal nuclear expansion in *pah1Δ* yeast cells.

TtPAH2 encoded a low molecular weight protein (37 kDa) and is the smallest PAH protein belonging to the PAPI class. Even though *TtPAH2* exhibited Mg^{2+} -dependent phosphatidate phosphatase activity, deletion of *TtPAH2* did not alter ER morphology.

Conclusion

TtPAH1 Even though the loss of *TtPAH1* increased the ER sheet structure and altered ER morphology it did not result in any defect in the nuclear envelope morphology. Defects in ER morphology in *Tetrahymena* did not necessarily affect nuclear morphology in *Tetrahymena*. It suggests that in *Tetrahymena*, unlike other organisms, ER content and structure are functionally isolated from mechanisms underlying nuclear expansion. Since *Tetrahymena* shows differential ploidy level in the macronucleus, a different mechanism could be in function to allow plasticity in nuclear expansion to accommodate different nuclear volumes. Rescue of aberrant nuclear morphology with *pah1Δ* yeast cells. Complementation studies with *PAH1* homolog from organisms representing all major eukaryotic lineages rescued aberrant nuclear defect of *pah1Δ* yeast cells. Therefore, it can be concluded that *PAH* is functionally conserved across all eukaryotic lineages. *TtPAH2*, even though catalytically active; did not regulate ER morphology in *Tetrahymena* which shows that catalytic activity alone is not sufficient for performing all the cellular functions. The amino acid sequences absent in *TtPAH2* but present in other *PAH* homologs may be critical for performing these cellular functions which needs to be investigated.

Bibliography

References

- Adeyo, O., Horn, P.J., Lee, S., Binns, D.D., Chandrahas, A., Chapman, K.D., and Goodman, J.M.** (2011). The yeast lipin orthologue Pah1p is important for biogenesis of lipid droplets. *J. Cell Biol.* *192*, 1043–1055.
- Adl, S.M., et.al.** (2013). The revised classification of eukaryotes. *J. Eukaryote Microbiol.* *59*, 1–45.
- Al-Mosawi, Z.S., Al-Saad, K.K., Ijadi-Maghsoodi, R., El-Shanti, H.I., and Ferguson, P.J.** (2007). A splice site mutation confirms the role of LPIN2 in Majeed syndrome. *Arthritis Rheum.* *56*, 960–964.
- Allen, S.L.** (2000). Isolation of micronuclear and macronuclear DNA. In *Methods Cell Biol.* *62*, 241–252.
- Bahmanyar, S.** (2015). Spatial regulation of phospholipid synthesis within the nuclear envelope domain of the endoplasmic reticulum. *Nucleus* *6*, 102–106.
- Bahmanyar, S., Biggs, R., Schuh, A.L., Desai, A., Müller-Reichert, T., Audhya, A., Dixon, J.E., and Oegema, K.** (2014). Spatial control of phospholipid flux restricts endoplasmic reticulum sheet formation to allow nuclear envelope breakdown. *Genes Dev.* *28*, 121–126.
- Beller, M., Thiel, K., Thul, P.J., and Jäckle, H.** (2010). Lipid droplets: A dynamic organelle moves into focus. *FEBS Lett.* *584*, 2176–2182.
- Binns, D., Januszewski, T., Chen, Y., Hill, J., Markin, V.S., Zhao, Y., Gilpin, C., Chapman, K.D., Anderson, R.G.W., and Goodman, J.M.** (2006). An intimate collaboration between peroxisomes and lipid bodies. *J. Cell Biol.* *173*, 719–731.
- Bodenbender J, Prohaska A, Jauker F, Hipke H, C.G.** (1992). DNA elimination and its relation to quantities in the macronucleus of Tetrahymena. *Dev Genet* *13*, 103–110.
- Boettcher, B., and Barral, Y.** (2012). The cell biology of open and closed mitosis. *Nucleus*

4, 160–165.

Botstein, D., and Fink, G.R. (2011). Yeast: An experimental organism for 21st century biology. *Genetics* 189, 695–704.

Briguglio, J.S., and Turkewitz, A.P. (2014). *Tetrahymena thermophila*: A divergent perspective on membrane traffic. *J. Exp. Zool. Part B Mol. Dev. Evol.* 322, 500–516.

Broers, J.L. V. (2006). Nuclear Lamins: Laminopathies and Their Role in Premature Ageing. *Physiol. Rev.* 86, 967–1008.

Bruns, P.J., Smith, H.R., and Cassidy-Hanley, D. (2000). Long-Term Storage. In *Methods in Cell Biology*, pp. 213–218.

Carman, G.M., and Han, G. (2009). Phosphatidic Acid Phosphatase , a Key Enzyme in the Regulation of Lipid Synthesis. *J. Biol. Chem.* 284, 2593–2597.

Carman, G.M., and Han, G.S. (2006). Roles of phosphatidate phosphatase enzymes in lipid metabolism. *Trends Biochem. Sci.* 31, 694–699.

Carman, G.M., and Henry, S.A. (1999). Phospholipid biosynthesis in the yeast *Saccharomyces cerevisiae* and interrelationship with other metabolic processes. *Prog. Lipid Res.* 38, 361–399.

Carman, G.M., and Henry, S.A. (2013). Phosphatidic Acid Plays a Central Role in the Transcriptional Regulation of Glycerophospholipid Synthesis in *Saccharomyces cerevisiae*. *J Biol Chem.* 282, 37293–37297.

Carman, G.M., and Zeimetz, G.M. (1996). Regulation of Phospholipid Biosynthesis in the Yeast *Saccharomyces cerevisiae*. *J. Biol. Chem.* 271, 13293–13296.

Cassidy-Hanley, P.J.B. and D. (2003). Biolistic Transformation of Macro- and Micronuclei. In *Methods in Cell Biology*, 62, 501–512.

Chen, Y., Rui, B.B., Tang, L.Y., and Hu, C.M. (2015). Lipin family proteins - Key regulators in lipid metabolism. *Ann. Nutr. Metab.* 66, 10–18.

- Choi, H.S., Su, W.M., Han, G.S., Plote, D., Xu, Z., and Carman, G.M.** (2012). Pho85p-Pho80p phosphorylation of yeast pah1p phosphatidate phosphatase regulates its activity, location, abundance, and function in lipid metabolism. *J. Biol. Chem.* 287, 11290–11301.
- CLEFFMANN** (1968). Regulierung der DNA-Menge in Makronucleus von Tetrahymena. *Exptl. Cell Res.* 50, 193–207.
- Craddock, C.P., Adams, N., Bryant, F.M., Kurup, S., and Eastmond, P.J.** (2015). Regulation of endomembrane biogenesis in arabidopsis by phosphatidic acid hydrolase. *Plant Signal. Behav.* 10, 1–4.
- Czabany, T., Athenstaedt, K., and Daum, G.** (2007). Synthesis, storage and degradation of neutral lipids in yeast. *Biochim. Biophys. Acta - Mol. Cell Biol. Lipids* 1771, 299–309.
- Doerder FP, Frankel J, Jenkins LM, D.L.** (1975). Form and pattern in ciliated protozoa: analysis of a genic mutant with altered cell shape in Tetrahymena pyriformis, Syngen 1. *J Exp Zool* 192, 237–58.
- Donkor, J., Sariahmetoglu, M., Brindley, D.N., and Reue, K.** (2007). Three Mammalian Lipins Act as Phosphatidate Phosphatases with Distinct Tissue Expression Patterns. *J. Biol. Chem.* 282, 3450-3457
- Donkor, J., Zhang, P., Wong, S., Loughlin, L.O., Dewald, J., Kok, B.P.C., Brindley, D.N., and Reue, K.** (2009). A Conserved Serine Residue Is Required for the Phosphatidate Phosphatase Activity but Not the Transcriptional Coactivator Functions of Lipin-1 and Lipin-2. *J. Biol. Chem.* 284, 29968–29978.
- Ebrahimi, H., and Cooper, J.P.** (2012). Closed mitosis: A timely move before separation. *Curr. Biol.* 22, R880–R882.
- Edurado Orias, M.D.C. and E.H.** (2011). Tetrahymena thermophila, a unicellular eukaryote with separate germline and somatic genomes. *Res Microbiol* 27, 320–331.
- Fagone, P., and Jackowski, S.** (2009). Membrane phospholipid synthesis and endoplasmic

reticulum function. *J. Lipid Res.* 50, S311–S316.

Farese, R. V., and Walther, T.C. (2009). Lipid Droplets Finally Get a Little R-E-S-P-E-C-T. *Cell* 139, 855–860.

Ferguson, P.J.; Chen, S; Tayeh, MK; Ochoa, L, et.al. (2005). Homozygous mutations in LPIN2 are responsible for the syndrome of chronic recurrent multifocal osteomyelitis and congenital dyserythropoietic anaemia (Majeed syndrome). *J. Med. Genet.* 42, 551–557.

Fernández-Murray, J.P., and McMaster, C.R. (2016). Lipid synthesis and membrane contact sites: a crossroads for cellular physiology. *J. Lipid Res.* 57, 1789–1805.

Finck, B.N., Gropler, M.C., Chen, Z., Leone, T.C., Croce, M.A., Harris, T.E., Jr, J.C.L., and Kelly, D.P. (2006). Lipin 1 is an inducible amplifier of the hepatic PGC-1 α / PPAR α regulatory pathway. *Cell Metab.* 4, 199–210.

Flacks, E.Orias.A.M. (1974). Macronuclear genetics of tetrahymena - random distribution of macronuclear gene copies in t. pyriformis, syngen. *Genetics* 79. 187- 206.

Frances, D., and Bryn, R. (1975). Effect of Sterol Replacement Composition of Tetrahymena". *Science* (80). 6998–7005.

Gaertig, J., Gu, L., Hai, B., and Gorovsky, M.A. (1994). High frequency vector-mediated transformation and gene replacement in Tetrahymena. *Nucleic Acids Res.* 22, 5391–5398.

Gaspar, M.L., Chang, Y.F., Jesch, S.A., Aregullin, M., and Henry, S.A. (2017). Interaction between repressor Opi1p and ER membrane protein Scs2p facilitates transit of phosphatidic acid from the ER to mitochondria and is essential for INO1 gene expression in the presence of choline. *J. Biol. Chem.* 292, 1813 –18728.

Gibellini, F., and Smith, T.K. (2010). The Kennedy pathway-de novo synthesis of phosphatidylethanolamine and phosphatidylcholine. *IUBMB Life* 62, 414–428.

Gietz, R.D., and Akio, S. (1988). New yeast-Escherichia coli shuttle vectors constructed with in vitro mutagenized yeast genes lacking six-base pair restriction sites. *Gene* 74, 527–

534.

Gietz, R.D., and Woods, R.A. (2001). Genetic transformation of yeast. *Biotechniques* 30, 816–831.

Gil-Soo Han and George M. Carman (2010). Characterization of the Human LPIN1 - encoded Phosphatidate Phosphatase Isoforms . *J. Biol. Chem.* 285, 14628–14638.

Golden, A., Liu, J., and Cohen-Fix, O. (2009). Inactivation of the *C. elegans* lipin homolog leads to ER disorganization and to defects in the breakdown and reassembly of the nuclear envelope. *J. Cell Sci.* 122, 1970–1978.

Gorjánác, M., and Mattaj, I.W. (2009). Lipin is required for efficient breakdown of the nuclear envelope in *Caenorhabditis elegans*. *J. Cell Sci.* 122, 1963–1969.

Gorovsky MA (1980). Genome organization and reorganization in *Tetrahymena*. *Annu Rev Genet* 14, 203–239.

Greenberg, M.L., and Lopes, J.M. (1996). Genetic Regulation of Phospholipid Biosynthesis in *Saccharomyces cerevisiae*. *Microbiol. Rev.* 60, 1–20.

Han, G.M.C. and G.-S. (2001). Regulation of phospholipid synthesis in yeast. *J. Lipid Res.* 73, 247–260.

Han, G.S., Wu, W.I., and Carman, G.M. (2006). The *Saccharomyces cerevisiae* lipin homolog is a Mg²⁺-dependent phosphatidate phosphatase enzyme. *J. Biol. Chem.* 281, 9210–9218.

Han, G.S., Siniosoglou, S., and Carman, G.M. (2007). The cellular functions of the yeast lipin homolog Pah1p are dependent on its phosphatidate phosphatase activity. *J. Biol. Chem.* 282, 37026–37035.

Han, G.S., O’Hara, L., Carman, G.M., and Siniosoglou, S. (2008b). An unconventional diacylglycerol kinase that regulates phospholipid synthesis and nuclear membrane growth. *J. Biol. Chem.* 283, 20433–20442.

- Han, G.S., O'Hara, L., Siniossoglou, S., and Carman, G.M.** (2008a). Characterization of the yeast DGK1-encoded CTP-dependent diacylglycerol kinase. *J. Biol. Chem.* 283, 20443–20453.
- Han, S., Bahmanyar, S., Zhang, P., Grishin, N., Oegema, K., Crooke, R., Graham, M., Reue, K., Dixon, J.E., and Goodman, J.M.** (2012). Nuclear Envelope Phosphatase 1-Regulatory Subunit 1 (Formerly TMEM188) Is the Metazoan Spo7p Ortholog and Functions in the Lipin Activation Pathway. *J. Biol. Chem.* 287, 3123–3137.
- Harris, T.E., and Finck, B.N.** (2011). Dual function lipin proteins and glycerolipid metabolism. *Trends Endocrinol. Metab.* 22, 226–233.
- He, J., Zhang, F., Tay, L.W.R., Boroda, S., Nian, W., Levental, K.R., Levental, I., Harris, T.E., Chang, J.T., and Du, G.** (2017). Lipin-1 regulation of phospholipid synthesis maintains endoplasmic reticulum homeostasis and is critical for triple-negative breast cancer cell survival. *FASEB J.* 31, 2893–2904.
- Horowitz, S., and Gorovsky, M.** (1985). An unusual genetic code in nuclear genes of *Tetrahymena*. *Proc. Natl. Acad. Sci. U. S. A.* 82, 2452–2455.
- Hsieh, L.S., Su, W.M., Han, G.S., and Carman, G.M.** (2016). Phosphorylation of yeast Pah1 phosphatidate phosphatase by casein kinase II regulates its function in lipid metabolism. *J. Biol. Chem.* 291, 9974–9990.
- Huffman, T.A., Mothe-Satney, I., and Lawrence, J.C.** (2002). Insulin-stimulated phosphorylation of lipin mediated by the mammalian target of rapamycin. *Proc. Natl. Acad. Sci. U. S. A.* 99, 1047–1052.
- Irie, K., Takase, M., Araki, H., and Oshima, Y.** (1993). A gene involved in plasmid maintenance and respiration in *Saccharomyces cerevisiae* encodes a highly charged protein. *Mol Gen Genet*, 236, 283–288.
- Joseph L. Campbell, Alexander Lorenz, Keren L. Witkin, Thomas Hays Josef Loidl,**

and O.C.F. (2006). Yeast Nuclear Envelope Subdomains with Distinct Abilities to Resist Membrane Expansion. *Mol. Biol. Cell* *17*, 1768–1778.

Karanasios, E., Han, G., Xu, Z., Carman, G.M., and Siniossoglou, S. (2010). A phosphorylation-regulated amphipathic helix controls the membrane translocation and function of the yeast phosphatidate phosphatase. *Proc. Natl. Acad. Sci. U. S. A.*, *12*, 17539-17554

Karanasios, E., Barbosa, A.D., Sembongi, H., Mari, M., Han, G.-S., Reggiori, F., Carman, G.M., and Siniossoglou, S. (2013). Regulation of lipid droplet and membrane biogenesis by the acidic tail of the phosphatidate phosphatase Pah1p. *Mol. Biol. Cell* *24*, 2124–2133.

Kim, J.E., and Chen, J. (2004). Regulation of peroxisome proliferator-activated receptor- γ Activity by Mammalian Target of Rapamycin and Amino Acids in Adipogenesis. *53*, 2748-2756.

Kim, H.B., Kumar, A., Wang, L., Liu, G.-H., Keller, S.R., Lawrence, J.C., Finck, B.N., and Harris, T.E. (2010). Lipin 1 represses NFATc4 transcriptional activity in adipocytes to inhibit secretion of inflammatory factors. *Mol. Cell. Biol.* *30*, 3126–3139.

Kim, H.E., Bae, E., Jeong, D.Y., Kim, M.J., Jin, W.J., Park, S.W., Han, G.S., Carman, G.M., Koh, E., and Kim, K.S. (2013). Lipin1 regulates PPAR γ transcriptional activity. *Biochem J* *453*, 49–60.

Kim, Y., Gentry, M.S., Harris, T.E., Wiley, S.E., Lawrence, J.C., and Dixon, J.E. (2007). A conserved phosphatase cascade that regulates nuclear membrane biogenesis. *Proc. Natl. Acad. Sci. U. S. A.* *104*, 6596–6601.

King, M.C., and Lusk, C.P. (2016). A model for coordinating nuclear mechanics and membrane remodeling to support nuclear integrity. *Curr. Opin. Cell Biol.* *41*, 9–17.

Klingenspor, M., Xu, P., Cohen, R.D., Welch, C., and Reue, K. (1999). Altered Gene

Expression Pattern in the Fatty Liver Dystrophy Mouse Reveals Impaired Insulin-mediated Cytoskeleton Dynamics. *274*, 23078–23084.

Koh, Y.K., Lee, M.Y., Kim, J.W., Kim, M., Moon, J.S., Lee, Y.J., Ahn, Y.H., and Kim, K.S. (2008). Lipin1 is a key factor for the maturation and maintenance of adipocytes in the regulatory network with CCAAT/enhancer-binding protein alpha and peroxisome proliferator-activated receptor gamma 2. *J. Biol. Chem.* *283*, 34896–34906.

Kohlwein, S.D. (2010). Triacylglycerol homeostasis: Insights from yeast. *J. Biol. Chem.* *285*, 15663–15667.

Koonin, E. V (2010). The origin and early evolution of eukaryotes in the light of phylogenomics. *Genome Biol.* *11*, 209.

Kurat, C.F., Natter, K., Petschnigg, J., Wolinski, H., Scheuringer, K., Scholz, H., Zimmermann, R., Leber, R., Zechner, R., and Kohlwein, S.D. (2006). Obese yeast: Triglyceride lipolysis is functionally conserved from mammals to yeast. *J. Biol. Chem.* *281*, 491–500.

Lagace, T.A., and Ridgway, N.D. (2013). The role of phospholipids in the biological activity and structure of the endoplasmic reticulum. *Biochim. Biophys. Acta* *1833*, 2499–2510.

Laplante, M., and Sabatini, D.M. (2009). An Emerging Role of mTOR in Lipid Biosynthesis Minireview. *Curr. Biol.* *19*, R1046–R1052.

Laura O'Hara, Gil-Soo Han, Sew Peak-Chew, Neil Grimsey, George M. Carman, and S.S. (2006). Control of Phospholipid Synthesis by Phosphorylation of the Yeast Lipin Pah1p/Smp2p Mg²⁺-dependent Phosphatidate Phosphatase. *J. Biol. Chem.* *281*, 34537–34548.

Leitch, A.R. (2000). Higher Levels of Organization in the Interphase Nucleus of Cycling and Differentiated Cells. *Microbiol. Mol. Biol. Rev.* *64*, 138–152.

- Lin, Y., and Carman, G.M.** (1989). Purification and Characterization of Phosphatidate Phosphatase from *Saccharomyces cerevisiae*. *264*, 8641–8645.
- Liu, G., Qu, J., Carmack, A.E., Kim, H.B., Chen, C., Ren, H., Morris, A.J., Finck, B.N., and Harris, T.E.** (2010). Lipin proteins form homo- and hetero-oligomers. *Biochem.J.* *76*, 65–76.
- Loewen, C.J.R., Gaspar, M.L., Jesch, S. a, Delon, C., Ktistakis, N.T., Henry, S. a, and Levine, T.P.** (2004). Phospholipid metabolism regulated by a transcription factor sensing phosphatidic acid. *Science* *304*, 1644–1647.
- Mah, A.S., Elia, A.E.H., Devgan, G., Ptacek, J., Schutkowski, M., Snyder, M., Yaffe, M.B., and Deshaies, R.J.** (2005). Substrate specificity analysis of protein kinase complex Dbf2-Mob1 by peptide library and proteome array screening. *BMC Biochem.* *6*, 22.
- Mall, M., Walter, T., Gorjánác, M., Davidson, I.F., Ly-Hartig, T.B.N., Ellenberg, J., and Mattaj, I.W.** (2012). Mitotic lamin disassembly is triggered by lipid-mediated signaling. *J. Cell Biol.* *198*, 981–990.
- McMahon, H.T., and Gallop, J.L.** (2005). Membrane curvature and mechanisms of dynamic cell membrane remodelling. *Nature* *438*, 590–596.
- Mietkiewska, E., Siloto, R.M.P., Dewald, J., Shah, S., Brindley, D.N., and Weselake, R.J.** (2011). Lipins from plants are phosphatidate phosphatases that restore lipid synthesis in a *pah1* Δ mutant strain of *Saccharomyces cerevisiae*. *FEBS J.* *278*, 764–775.
- Mobberley, P.S., Sullivan, J.L., Angus, S.P., Kong, X., and Pennock, D.G.** (1999). *Tetrahymena thermophila*. *Curr. Biol.* *46*, 147–154.
- Morlock, K.R., Mclaughlin, J.J., Lin, Y., and Carman, G.M.** (1991). Phosphatidate phosphatase from *Saccharomyces cerevisiae*. *J. Biol. Chem.* *266*, 3586–3593.
- Müller-felber, W., Venkateswaran, R., Ogier, H., Desguerre, I., and Altuzarra, C.** (2010). LPIN1 Gene Mutations: A Major Cause of Severe Rhabdomyolysis in Early

Childhood. *Hum Mutat*, *31*, 1564–1573.

Murphy, D.J. (2001). The biogenesis and functions of lipid bodies in animals, plants and microorganisms. *Prog. Lipid Res.* *40*, 325–438.

Nakamura, Y., Koizumi, R., Shui, G., Shimojima, M., Wenk, M.R., and Ito, T. (2009). Arabidopsis lipins mediate eukaryotic pathway of lipid metabolism and cope critically. *Proc. Natl. Acad. Sci. U. S. A.*, *106*, 20978-20983

Natter, K., and Kohlwein, S.D. (2013). Yeast and cancer cells - Common principles in lipid metabolism. *Biochim. Biophys. Acta - Mol. Cell Biol. Lipids* *1831*, 314–326.

Orias, E., Hamilton, E.P., and Orias, J.D. (2000). Tetrahymena as a laboratory organism: useful strains, cell culture, and cell line maintenance. *Methods Cell Biol.* *62*, 189–211.

Osellame, L.D., Blacker, T.S., and Duchen, M.R. (2012). Cellular and molecular mechanisms of mitochondrial function. *Best Pract. Res. Clin. Endocrinol. Metab.* *26*, 711–723.

Parfrey, L.W., Barbero, E., Lasser, E., Dunthorn, M., Bhattacharya, D., Patterson, D.J., and Katz, L.A. (2006). Evaluating support for the current classification of eukaryotic diversity. *PLoS Genet.* *2*, 2062–2073.

Park, Y., Han, G., Mileykovskaya, E., Garrett, T.A., and Carman, G.M. (2015). Altered Lipid Synthesis by Lack of Yeast Pah1 Phosphatidate Phosphatase Reduces Chronological Life Span. *J. Biol. Chem.* *290*, 25382–25394.

Park, Y., Han, G.-S., and Carman, G.M. (2017). A conserved tryptophan within the WRDPLVDID domain of yeast Pah1 phosphatidate phosphatase is required for its *in vivo* function in lipid metabolism. *J. Biol. Chem.* *292*, 19580-19589.

Pascual, F., and Carman, G.M. (2013). Phosphatidate phosphatase, a key regulator of lipid homeostasis. *Biochim. Biophys. Acta - Mol. Cell Biol. Lipids* *1831*, 514–522.

Péterfy, M., Phan, J., Xu, P., and Reue, K. (2001). Lipodystrophy in the fld mouse results

from mutation of a new gene encoding a nuclear protein, lipin. *Nat. Genet.* 27, 121–124.

Péterfy, M., Phan, J., and Reue, K. (2005). Alternatively spliced lipin isoforms exhibit distinct expression pattern, subcellular localization, and role in adipogenesis. *J. Biol. Chem.* 280, 32883–32889.

Peterson, T.R., Sengupta, S.S., Harris, T.E., Carmack, A.E., Kang, S.A., Balderas, E., Guertin, D.A., Madden, K.L., Carpenter, A.E., Finck, B.N., et al. (2011). MTOR complex 1 regulates lipin 1 localization to control the srebp pathway. *Cell* 146, 408–420.

Phan, J., and Reue, K. (2004). Lipin Expression Preceding Peroxisome Proliferator-activated Receptor- γ Is Critical for Adipogenesis in Vivo and in Vitro. *J. Biol. Chem.* 279, 29558–29564.

Pillai, A.N., Shukla, S., and Rahaman, A. (2017a). An evolutionarily conserved phosphatidate phosphatase maintains lipid droplet number and endoplasmic reticulum morphology but not nuclear morphology. *Biol. Open* 6, 1629–1643.

Pillai, A.N., Shukla, S., Gautam, S., and Rahaman, A. (2017b). Small phosphatidate phosphatase (TtPAH2) of *Tetrahymena* complements respiratory function and not membrane biogenesis function of yeast PAH1. *J. Biosci.* 42, 613–621.

Radulovic, M., Knittelfelder, O., Cristobal-Sarramian, A., Kolb, D., Wolinski, H., and Kohlwein, S.D. (2013). The emergence of lipid droplets in yeast: Current status and experimental approaches. *Curr. Genet.* 59, 231–242.

Rahaman, A., Elde, N.C., and Turkewitz, A.P. (2008). A Dynamin-Related Protein Required for Nuclear Remodeling in *Tetrahymena*. *Curr Biol.* 18, 1227–1233.

Raikov IB (1976). Evolution of macronuclear organization. *Annu Rev Genet* 10, 413–440.

Reue, K., and Brindley, D.N. (2008). Multiple roles for lipins / phosphatidate phosphatase enzymes in lipid metabolism. *J. Lipid Res.* 49, 2493–2503.

Reue, K., and Zhang, P. (2008). The lipin protein family: Dual roles in lipid biosynthesis

and gene expression. *FEBS Lett.* 582, 90–96.

Santos-Rosa, H., Leung, J., Grimsey, N., Peak-Chew, S., and Siniossoglou, S. (2005). The yeast lipin Smp2 couples phospholipid biosynthesis to nuclear membrane growth. *EMBO J.* 24, 1931–1941.

Sasser, T., Qiu, Q.S., Karunakaran, S., Padolina, M., Reyes, A., Flood, B., Smith, S., Gonzales, C., and Fratti, R.A. (2012). Yeast lipin 1 orthologue Pah1p regulates vacuole homeostasis and membrane fusion. *J. Biol. Chem.* 287, 2221–2236.

Sazer, S., Lynch, M., and Needleman, D. (2014). Deciphering the evolutionary history of open and closed mitosis. *Curr. Biol.* 24, R1099–R1103.

Schmitt, S., Ugrankar, R., Greene, S.E., Prajapati, M., and Lehmann, M. (2015). *Drosophila* Lipin interacts with insulin and TOR signaling pathways in the control of growth and lipid metabolism. *J Cell Sci* 128, 4395–4406.

Sciorra, V.A., and Morris, A.J. (2002). Roles for lipid phosphate phosphatases in regulation of cellular signaling. *Biochim Biophys Acta.* 1582, 45–51.

Sherman, F. (2002). Getting Started with Yeast Contents. In *Methods in Enzymology*, 350. 3–41.

Shetty, A., and Lopes, J.M. (2010). Derepression of INO1 transcription requires cooperation between the Ino2p-Ino4p heterodimer and Cbf1p and recruitment of the ISW2 chromatin-remodeling complex. *Eukaryot. Cell* 9, 1845–1855.

Siniossoglou, S. (2009). Lipins, lipids and nuclear envelope structure. *Traffic* 10, 1181–1187.

Siniossoglou, S., Santos-rosa, H., Rappsilber, J., Mann, M., and Hurt, E. (1998). A novel complex of membrane proteins required for formation of a spherical nucleus. *EMBO J.* 17, 6449–6464.

Soliman, G.A., Acosta-Jaquez, H.A., and Fingar, D.C. (2010). mTORC1 inhibition via rapamycin promotes triacylglycerol lipolysis and release of free fatty acids in 3T3-L1

adipocytes. *Lipids* 45, 1089–1100.

Soto-Cardalda, A., Fakas, S., Pascual, F., Choi, H.S., and Carman, G.M. (2012). Phosphatidate phosphatase plays role in zinc-mediated regulation of phospholipid synthesis in yeast. *J. Biol. Chem.* 287, 968–977.

Stukey, J., and Carman, G.M. (2008). Identification of a novel phosphatase sequence motif. *Protein Sci.* 6, 469–472.

Su, W.M., Han, G.S., Casciano, J., and Carman, G.M. (2012). Protein kinase A-mediated phosphorylation of Pah1p phosphatidate phosphatase functions in conjunction with the Pho85p-Pho80p and Cdc28p-Cyclin B kinases to regulate lipid synthesis in yeast. *J. Biol. Chem.* 287, 33364–33376.

Su, W.M., Han, G.S., and Carman, G.M. (2014). Cross-talk phosphorylations by protein kinase C and Pho85p-Pho80p protein kinase regulate pah1p phosphatidate phosphatase abundance in *saccharomyces cerevisiae*. *J. Biol. Chem.* 289, 18818–18830.

Talamas, J.A., and Capelson, M. (2015). Nuclear envelope and genome interactions in cell fate. *Front. Genet.* 5, 1–16.

Tange, Y; Hirata, A; Niwa, O. (2002). An evolutionarily conserved fission yeast protein, Ned1, implicated in normal nuclear morphology and chromosome stability, interacts with Dis3, Pim1/RCC1 and an essential nucleoporin. *J. Cell Sci.* 115, 4375–4385.

Tauchi-Sato, K., Ozeki, S., Houjou, T., Taguchi, R., and Fujimoto, T. (2002). The surface of lipid droplets is a phospholipid monolayer with a unique fatty acid composition. *J. Biol. Chem.* 277, 44507–44512.

Thiele, C., and Spandl, J. (2008). Cell biology of lipid droplets. *Curr. Opin. Cell Biol.* 20, 378–385.

Turkewitz, A.P., Orias, E., and Kapler, G. (2002). Functional genomics: the coming of age for *Tetrahymena thermophila*. *Trends Genet.* 18, 35–40.

- Ugrankar, R., Liu, Y., Provaznik, J., Schmitt, S., and Lehmann, M.** (2011). Lipin Is a Central Regulator of Adipose Tissue Development and Function in *Drosophila melanogaster*. *Mol. Cell. Bio.* *31*, 1646–1656.
- Ungrecht, R., and Kutay, U.** (2017). Mechanisms and functions of nuclear envelope remodelling. *Nat. Rev. Mol. Cell Biol.* *18*, 229–245.
- Van Meer, G., Voelker, D.R., and Feigenson, G.W.** (2008). Membrane lipids: where they are and how they behave. *Nat. Rev. Mol. Cell Biol.* *9*, 112–124.
- Voeltz, G.K., and Prinz, W.A.** (2007). Sheets, ribbons and tubules - How organelles get their shape. *Nat. Rev. Mol. Cell Biol.* *8*, 258–264.
- Webster, M., Witkin, K.L., and Cohen-Fix, O.** (2009). Sizing up the nucleus: nuclear shape, size and nuclear-envelope assembly. *J. Cell Sci.* *122*, 1477–1486.
- Witkin, K.L., and Collins, K.** (2004). Holoenzyme proteins required for the physiological assembly and activity of telomerase. *Genes Dev.* *18*, 1107–1118.
- Wolins, N.E., Brasaemle, D.L., and Bickel, P.E.** (2006). A proposed model of fat packaging by exchangeable lipid droplet proteins. *FEBS Lett.* *580*, 5484–5491.
- Wu, W.I., Liu, Y., Riedel, B., Wissing, J.B., Fischl, A.S., and Carman, G.M.** (1996). Purification and characterization of diacylglycerol pyrophosphate phosphatase from *Saccharomyces cerevisiae*. *J. Biol. Chem.* *271*, 1868–1876.
- Zhang, P., and Reue, K.** (2017). Lipin proteins and glycerolipid metabolism: Roles at the ER membrane and beyond. *Biochim. Biophys. Acta - Biomembr.* *1859*, 1583–1595.
- Zhang, P., Takeuchi, K., Csaki, L.S., and Reue, K.** (2012). Lipin-1 Phosphatidic Phosphatase Activity Modulates Phosphatidate Levels to Promote Peroxisome Proliferator-activated Receptor γ (PPAR γ) Gene Expression during adipogenesis. *J. Biol. Chem.* *287*, 3485–3494.